

Robust Detection of Watermarks for Large Language Models Under Human Edits

Xiang Li* Feng Ruan† Huiyuan Wang‡ Qi Long§ Weijie J. Su¶

November 21, 2024

Abstract

Watermarking has offered an effective approach to distinguishing text generated by large language models (LLMs) from human-written text. However, the pervasive presence of human edits on LLM-generated text dilutes watermark signals, thereby significantly degrading detection performance of existing methods. In this paper, by modeling human edits through mixture model detection, we introduce a new method in the form of a truncated goodness-of-fit test for detecting watermarked text under human edits, which we refer to as Tr-GoF. We prove that the Tr-GoF test achieves optimality in robust detection of the Gumbel-max watermark in a certain asymptotic regime of substantial text modifications and vanishing watermark signals. Importantly, Tr-GoF achieves this optimality *adaptively* as it does not require precise knowledge of human edit levels or probabilistic specifications of the LLMs, in contrast to the optimal but impractical (Neyman–Pearson) likelihood ratio test. Moreover, we establish that the Tr-GoF test attains the highest detection efficiency rate in a certain regime of moderate text modifications. In stark contrast, we show that sum-based detection rules, as employed by existing methods, fail to achieve optimal robustness in both regimes because the additive nature of their statistics is less resilient to edit-induced noise. Finally, we demonstrate the competitive and sometimes superior empirical performance of the Tr-GoF test on both synthetic data and open-source LLMs in the OPT and LLaMA families.

1 Introduction

Large language models (LLMs) have recently emerged as a transformative technique for generating human-like text and other media [72, 58, 2]. While this advancement boosts productivity across various industries, it also introduces risks related to the ownership and creation of content. These risks include the spread of misinformation [80, 74, 70], challenges to education and academic integrity [71, 53], and issues concerning data authenticity [64, 69, 15]. These problems highlight the urgent need for methodologies to authenticate and verify the origin of text, specifically, determining whether it is generated by LLMs or humans.

Watermarking text during generation by LLMs has offered a principled and viable approach to resolving these issues [44, 1, 13]. Since 2023, a variety of watermarking schemes have been introduced

*University of Pennsylvania; Email: lx10077@upenn.edu.

†Northwestern University; Email: fengruan@northwestern.edu.

‡University of Pennsylvania; Email: huiyuanw@upenn.edu.

§University of Pennsylvania; Email: qlong@upenn.edu.

¶University of Pennsylvania; Email: suw@wharton.upenn.edu.

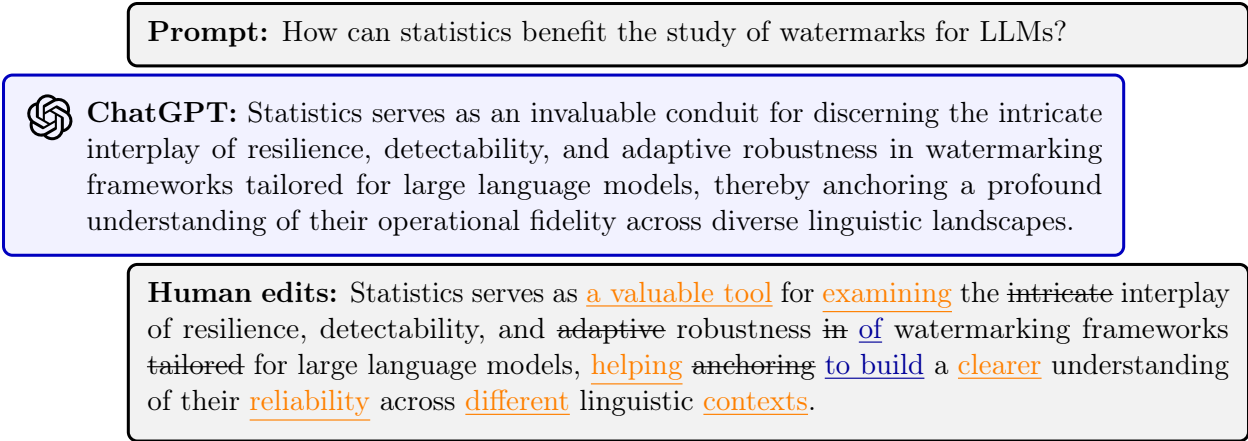


Figure 1: How users modify ChatGPT’s response through edits such as substitution, deletion, and insertion. Orange underline marks substitutions, ~~black strikethrough~~ indicates deletions, and blue underline highlights insertions.

[23, 46, 33, 76, 83, 82, 50, 25, 24, 16, 78]. Loosely speaking, a watermarking scheme embeds signals into the process of generating text by using controlled pseudorandomness. This is made possible by the probabilistic nature of LLMs through next-token prediction (NTP) for sequentially generating text. The watermark signals are nearly unnoticeable, if possible, to human readers but are provably detectable once a verifier has knowledge of how the pseudorandomness is constructed [13].

In real-world scenarios, however, text generated from LLMs often undergoes various forms of human edits before its use (see Figure 1 for an illustration), which presents perhaps the most significant challenge for applying watermarks [45, 21]. In the simplest case, a user of LLMs might replace several words of the generated text, either to improve the text from the user’s perspective or make it less LLM-sounding. This simple editing process would weaken the watermark since the signals from the modified tokens—the smallest unit in text generation, which can be a word or a sub-word—turn to noise. Worse, how the editing process proceeds is unknown to the verifier. For example, it is not clear if a token in the text is generated by the LLM or has been modified by a human. In light of this, a watermark detection rule should not only be efficient in the edit-free scenario but also, perhaps more importantly, its detection power should not be unduly affected by various forms of human edits. Equally important is adaptivity: the rule should perform well without prior knowledge of how or to what extent the text has been edited, ensuring practical applicability in handling diverse and unpredictable editing behaviors.

To get a handle on how robust and adaptive existing watermark detection rules are against human edits, we conduct a numerical experiment and present the results in Figure 2. The experiment is concerned with the Gumbel-max watermark [1], which has been implemented internally at OpenAI and is the first unbiased¹ watermark. With 5% of the tokens modified by humans, the detection power when text length is 400 drops from 87.8% in the edit-free case to 64.7% with paraphrase edits and further to 30.2% with adversarial edits. While this significant performance degradation is concerning, it is not surprising as these detection rules [48, 1] are developed without any robustness

¹A watermarking scheme is (approximately) unbiased if the watermarked LLM generates each token with (approximately) the same probability distribution as the unwatermarked counterpart.

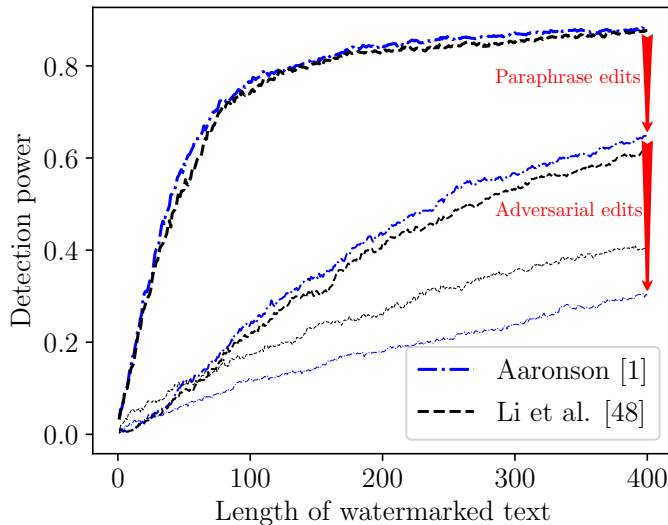


Figure 2: Empirical study of detection methods for the Gumbel-max watermark. Statistical power is evaluated at a 0.01 significance level using 1,000 prompts from the C4 dataset [65] and 400 generated tokens per prompt with the OPT-1.3B model [81] (temperature 0.3). Paraphrase edits randomly replace 5% of tokens with WordNet synonyms [54], while adversarial edits replace the 5% with the strongest watermark signals. Thinner curves indicate higher levels of human edits. See Appendix C.1 for details.

consideration, in particular, assuming there is no signal corruption due to human edits. More critically, the editing process would render the computation of pseudorandomness, which takes as input the before-edited tokens [44, 1], impossible for detecting watermarks.

Thus, there is a pressing need to develop robust and adaptive methods for detecting watermarks in LLM-generated text that may undergo human edits. Existing work on watermark detection typically assumes a scenario where each token contributes a signal to the watermark. For example, Li et al. [48] introduced a statistical framework for evaluating detection efficiency based on sum-based statistics that measure the cumulative watermark strength across all tokens. However, this framework operates under the ideal assumption that tokens are either fully human-written or entirely generated by an LLM. When applied to human-edited text—a combination of human- and LLM-generated tokens—sum-based statistics may be easily corrupted by noise, leading to substantial degradation in efficiency, as illustrated in Figure 2.

1.1 Our Contributions

In this paper, we address the robustness of detecting LLM watermarks from a statistical viewpoint, providing both a rigorous framework and methodologies with theoretical guarantees alongside empirical validation.

A primary challenge lies in formally modeling how humans edit LLM-generated text—a necessary step for analyzing the efficiency of robust watermark detection. Recognizing the complexity of human editing processes, we consider three editing operations: substitution, insertion, and deletion, which humans apply sequentially while reviewing LLM-generated text. While the specifics of the editing process cannot be inferred from the modified text alone, a crucial observation we make is

that, due to the indistinguishability between pseudorandomness and true randomness, each token in the text under scrutiny contributes either noise or signal, depending on whether it has been affected by human edits. Moreover, the noise follows a fixed and known distribution under the framework of Li et al. [48], while the signal distribution depends on the probability distribution of the token predicted by the LLM. We call this multinomial distribution the NTP distribution and denote it by $\mathbf{P}_t = (P_{t,w})_{w \in \text{Voc}}$ for predicting the t -th token, where Voc denotes the token vocabulary. For example, the vocabulary size $|\text{Voc}|$ is 50,257 for GPT-2/3.5 series models [63, 8] and 32,000 for the LLaMA-2 series models [72].

Under this human editing model, we introduce a binary process $\{\eta_t\}_{t=1}^n$ to indicate whether the watermark signal remains at the position of the t -th token in a text of length n . This allows us to model the watermark signal across all tokens as a mixture distribution, with one component being a signal distribution when $\eta_t = 1$ and the other component being the noise distribution when $\eta_t = 0$. First and foremost, a key question is when it is statistically possible to distinguish this mixture as the alternative hypothesis (indicating watermarked text under human editing) from the pure noise distribution as the null hypothesis (indicating human-written text), for example, in the case of the Gumbel-max watermark. This is addressed in the following finding of our paper (we write $a_n \asymp b_n$ if there exist constants C_1 and C_2 such that $C_1 a_n \leq b_n \leq C_2 a_n$ for all n):

Phase transition for watermark detection. We consider an asymptotic regime where the text length n tends to infinity, but individual tokens contain less watermark signal. Specifically, we assume $\mathbb{P}(\eta_t = 1) = \mathbb{E}[\eta_t] \asymp n^{-p}$ and $1 - \max_{w \in \text{Voc}} P_{t,w} \asymp n^{-q}$ for constants $0 < p, q < 1$, inspired by the sparse mixture detection problem [19]. Detection becomes more challenging as either p or q increases. A larger value of p means fewer tokens contribute to the watermark after human editing, resulting in a diluted watermark; similarly, a larger value of q indicates that the NTP distributions are less regular due to being approximately degenerate, which weakens watermark signals (see elaboration in Section 4.3). Our finding is that the optimal detection region in the (p, q) plane has boundary $q + 2p = 1$. Explicitly, when $q + 2p > 1$, no test can asymptotically achieve zero Type I and Type II errors for the Gumbel-max watermark; when $q + 2p < 1$, in stark contrast, both Type I and Type II errors approach zero using the likelihood-ratio test.

While the likelihood-ratio test achieves theoretical optimality, it requires knowledge of the watermark fraction $\mathbb{E}[\eta_t]$ and all NTP distributions \mathbf{P}_t for $t = 1, \dots, n$. To make this boundary practically relevant, it is essential to develop a practical method that can reliably separate the null and alternative distributions as $n \rightarrow \infty$. For this purpose, it is instructive to examine the statistical limits of sum-based test statistics as employed in [48, 46, 23]. We prove that these sum-based detection rules fail to achieve the optimal boundary $q + 2p = 1$ in general, and more precisely, the best possible detection boundary these methods can achieve is $q + p = 1/2$.

This analysis offers insights into the causes of this suboptimality, which we leverage to develop a new, practically adaptive method that achieves the optimal boundary:

An adaptively optimal method. Our approach utilizes the empirical cumulative distribution function of p-values from the text under detection, comparing it with the null counterpart through a form of divergence [38]. Unlike sum-based approaches [48, 46, 23], this goodness-of-fit test adaptively identifies areas of significant departure between null and alternative distributions without requiring prior knowledge of the watermark fraction or NTP regularity. Moreover, a crucial innovation is to truncate the search for the location to filter out extreme scores for stability. This gives a family of truncated goodness-of-fit tests, which we refer to as Tr-GoF for short (details in Algorithm 1). We show that Tr-GoF achieves the robust detection boundary $q + 2p = 1$ without relying on any tuning

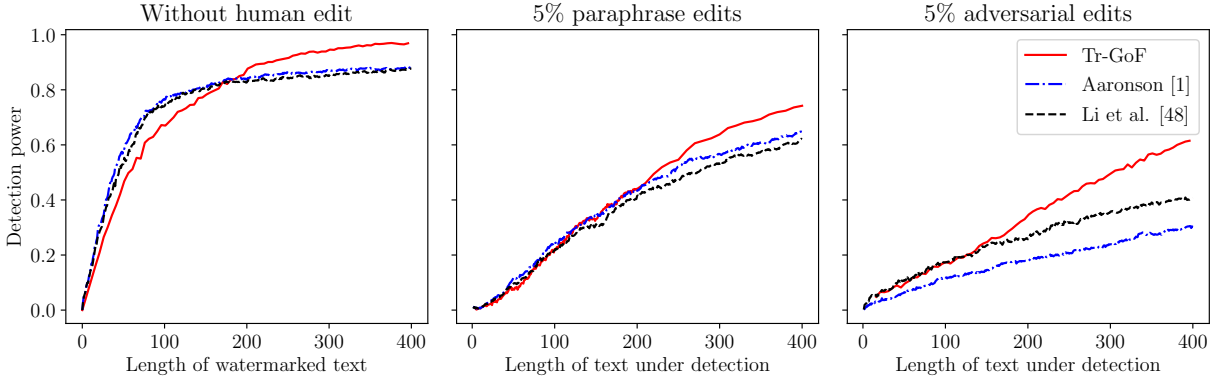


Figure 3: Tr-GoF shows improved detection efficiency under the same setup as Figure 2, with a more pronounced performance advantage in adversarial edits compared to paraphrase edits.

parameters, thereby possessing adaptive optimality [19, 20]. Figure 3 demonstrates the robustness of Tr-GoF in detecting the Gumbel-max watermark in human-edited text.

Having established the optimality of Tr-GoF for sparse watermark detection, we further examine its performance in a regime of “dense” watermark signals. More precisely, we consider the setting where the watermark fraction $\mathbb{E}[\eta_i] \equiv \varepsilon$ remains constant, and the regularity level of the NTP distribution satisfies $1 - \max_{w \in \text{Voc}} P_{t,w} \geq \Delta$ for some constant $0 < \Delta < 1$. Below is our third main result in this paper:

Tr-GoF attains optimal efficiency rate. We show that the Tr-GoF test achieves the highest class-dependent efficiency under the framework of watermarks for LLMs proposed by Li et al. [48]. This optimality is adaptive in that it does not rely on any prior knowledge of Δ or ε , whereas existing sum-based detection rules fail to achieve the same level of efficiency due to their lack of adaptivity for dense watermark detection (see Figure 6 for illustration). This finding is unexpected as the Tr-GoF test was originally motivated by sparse watermark detection. Taken together, our results show that the Tr-GoF test achieves optimality in both sparse and dense regimes of watermark detection.

1.2 Related Work

Most robust watermarking methods focus on algorithmic or cryptographic approaches. Algorithmic methods emphasize resilient watermarking designs [79, 46, 84, 32, 67, 25], while cryptographic approaches protect watermark signals through robust pseudorandom codes [26, 12]. However, rigorous statistical analysis of robustness in watermark detection remains limited, largely due to the absence of a cohesive statistical framework. Definitions of robustness also vary widely across studies.

Our approach introduces a statistical perspective by modeling human edits as a mixture distribution, enabling the establishment of detection boundaries and class-dependent efficiency rates. Another statistical approach to robustness is the edit tolerance limit, which quantifies the maximum proportion of edits a detection method can withstand while remaining effective. Studies often apply this perspective to the green-red list watermark, initially proposed by Kirchenbauer et al. [44, 45] and valued for its simplicity [23, 33, 76, 84, 49]. Zhao et al. [82] further improved its tolerance by

introducing a fixed pseudorandom code, enhancing resilience against text modifications. Additional refinements of this approach are discussed in [46, 11, 34].

Other forms of robustness include decoder-focused and cryptographic approaches. Zhao et al. [83] examines decoder functions that map logit vectors to token probabilities, proposing a provably robust decoder for enhanced resilience. In cryptographic studies, robustness is designed to make pseudorandom codes resistant to a fixed proportion of human edits [26, 12]. Our statistical viewpoint complements these approaches, providing an orthogonal framework for assessing robustness.

Robust statistics, which traditionally addresses resilience to outliers and perturbations, provides a relevant foundation for our study [35, 36, 17]. Our mixture formulation connects with Huber’s contamination model [35]; however, unlike in Huber’s model where the contaminated distribution is typically unknown, in watermark detection, this distribution is known. Additionally, our work is related to sparse mixture detection, first introduced by Dobrusin [18] to identify sparse signals, with further developments in mixtures model [37, 19, 10, 9, 4] and rare-signal models [40, 42, 41]. Robust watermark detection also diverges from traditional sparse detection due to the autoregressive nature of text generation, which results in time-varying signal (or NTP) distributions. While some methods address inhomogeneity using stationary Gaussian processes [29] or temporal correlations [30], they are inapplicable to text generation. Our theoretical analysis directly leverages the autoregressive nature to analyze inhomogeneity in watermark detection, as detailed in Section 4.

1.3 Organization of the Paper

The remainder of the paper is organized as follows. In Section 2, we introduce basics of LLMs and the statistical framework of LLM watermarks [48]. In Section 3, we develop the Tr-GoF test and establish its theoretical guarantees for robust detection in Section 4. We evaluate the empirical performance of the Tr-GoF test in Sections 5 and 6. We conclude in Section 7 with a discussion of future research directions. Most technical proofs are provided in the appendix.

2 Preliminaries

Watermark embedding. LLMs, like GPT models [63, 8], generate text by sampling tokens autoregressively. Given an existing sequence $w_{1:(t-1)} := w_1 w_2 \cdots w_{t-1}$, the LLM computes the NTP distribution $\mathbf{P}_t := (P_{t,w})_{w \in \text{Voc}}$ and samples the next token w_t . The NTP distribution \mathbf{P}_t is unknown to the verifier since it depends on all prior generated tokens, the user-supplied prompt, as well as system prompts that are hidden from users [73]. We denote this dependence explicitly as $\mathbf{P}_t = \text{LLM}(w_{1:(t-1)})$. A watermarked LLM embeds watermarks during next-token sampling by generating a pseudorandom variable ζ_t via $\zeta_t = \mathcal{A}(w_{(t-m):(t-1)}, \text{Key})$ where \mathcal{A} is a (deterministic) hash function, m is the context window, and Key is a secret key. The next token w_t is then computed as: $w_t := \mathcal{S}(\mathbf{P}_t, \zeta_t)$, where \mathcal{S} is a deterministic decoder function. The pseudorandom variables $\zeta_{1:n}$ can be recovered with the sequence $w_{1:n}$, \mathcal{A} , and Key . Without the key, ζ_t behaves like a random variable due to the cryptographic properties of hash functions [5, 68]. We assume ζ_t are i.i.d. with distribution π for analysis, representing perfect pseudorandomness [76, 83]. The decoder \mathcal{S} is *unbiased* if it follows the NTP distribution \mathbf{P} , meaning $\mathbb{P}_{\zeta \sim \pi}(\mathcal{S}(\mathbf{P}, \zeta) = w) = P_w$ for any \mathbf{P} and token w . An unbiased decoder corresponds to standard multinomial sampling methods.

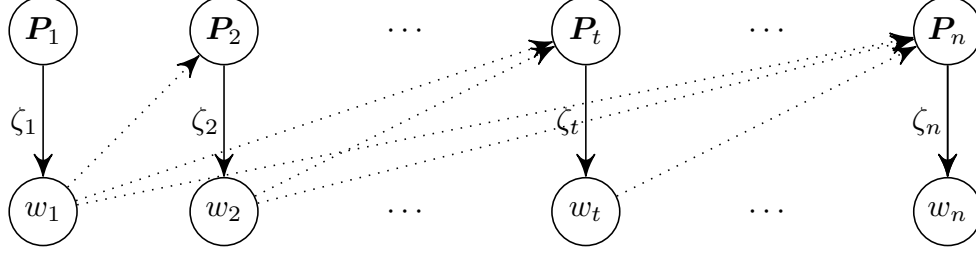


Figure 4: An illustrative diagram showcasing the autoregressive generation of LLMs. The solid line represents the decoder function \mathcal{S} , and the dotted line represents the dependence on the NTP distributions of history tokens.

Watermark detection. Li et al. [48] formulated watermark detection as a hypothesis testing problem and analyzed the effectiveness of existing detection methods. In this framework, determining whether a watermark is embedded is reduced to testing for the statistical dependence between the text $w_{1:n}$ and the corresponding pseudorandom numbers $\zeta_{1:n}$. The two hypotheses are as follows:

- The null hypothesis H_0 asserts that no watermark is present and that $w_{1:n}$ is human-written. Since the NTP distributions of human writing are generally unknown, a pivotal statistic $Y_t = Y(w_t, \zeta_t)$ is introduced. The pivotal function $Y(\cdot, \cdot)$ ensures that Y_t has a known distribution under H_0 , as long as w_t is independent of ζ_t , regardless of w_t 's distribution. Working Hypothesis 2.2 in Li et al. [48] posits that human writing should always be treated as independent of watermarked generation due to the undisclosed watermarking process. Consequently, Y_t are i.i.d. samples from a known distribution under H_0 , denoted by μ_0 .
- The alternative hypothesis H_1 asserts that $w_{1:n}$ is generated by a watermarked LLM. The watermarking process introduces a dependence between w_t and ζ_t through the decoder: $w_t = \mathcal{S}(\mathbf{P}_t, \zeta_t)$. As a result, under H_1 , the distribution of Y_t for a given \mathbf{P}_t differs from its null distribution μ_0 . Working Hypothesis 2.1 in [48] assumes that $\zeta_{1:n}$ are i.i.d. samples from a known distribution, and each ζ_t is independent of \mathbf{P}_t . In this setup, $Y_t | \mathbf{P}_t$ follows a distribution that depends only on \mathbf{P}_t , which we denote by μ_{1, \mathbf{P}_t} .

Therefore, watermark detection is equivalent to the following hypothesis testing problem:

$$H_0 : Y_t \sim \mu_0 \text{ i.i.d. for } 1 \leq t \leq n \quad \text{versus} \quad H_1 : Y_t | \mathbf{P}_t \sim \mu_{1, \mathbf{P}_t} \text{ for } 1 \leq t \leq n. \quad (1)$$

The Gumbel-max watermark: Decoder and detection. Our paper focuses on the Gumbel-max watermark, one of the most influential and the first unbiased watermark [1], which has been implemented internally at OpenAI [59] and serves as a baseline in many studies. This watermark utilizes the Gumbel-max trick, a sampling technique for multinomial distributions [28, 60, 51, 39]. The trick ensures that $\arg \max_{w \in \text{Voc}} P_w^{-1} \log U_w$ follows the distribution $\mathbf{P} = (P_w)_{w \in \text{Voc}}$, where $\zeta = (U_w)_{w \in \text{Voc}}$ consists of $|\text{Voc}|$ i.i.d. $U(0, 1)$ random variables. Scott Aaronson proposed the following unbiased decoder [1]:

$$\mathcal{S}^{\text{gum}}(\mathbf{P}, \zeta) := \arg \max_{w \in \text{Voc}} \frac{\log U_w}{P_w}. \quad (2)$$

The pivotal statistic is $Y_t = Y(w_t, \zeta_t) = U_{t, w_t}$, where $\zeta_t = (U_{t, w})_{w \in \text{Voc}}$ represents the pseudorandom numbers. The watermark is detected when the sum-based statistic $T_n^{\text{ars}} = \sum_{t=1}^n h_{\text{ars}}(Y_t)$, with

$h_{\text{ars}}(y) = -\log(1 - y)$, exceeds a set threshold. The method works because, without a watermark, the U_{t,w_t} 's are i.i.d. $U(0, 1)$, so $Y_t \sim \mu_0 = U(0, 1)$. In contrast, if the watermark is present, (2) makes tokens with a larger pseudorandom number more likely to be selected. Indeed, we have $Y_t | \mathbf{P}_t \sim \mu_{1,\mathbf{P}_t}$, where $\mu_{1,\mathbf{P}}(Y \leq r) = \sum_{w \in \text{Voc}} P_w r^{1/P_w}$ for $r \in [0, 1]$ [48]. The alternative distribution $\mu_{1,\mathbf{P}}$ is distinct from μ_0 unless \mathbf{P} equals $(1, 0, \dots, 0)$, up to a permutation.

The Gumbel-max watermark can be detected with provable guarantees by examining the distributional differences between μ_0 and $\mu_{1,\mathbf{P}}$. In addition to the h_{ars} function, other scoring functions have been proposed to detect watermarks. Examples include the log function $h_{\log}(y) = \log y$ [46, 23] and the optimal least-favorable function [48]:

$$h_{\text{opt},\Delta}(y) = \log\left(\left\lfloor \frac{1}{1-\Delta} \right\rfloor y^{\frac{\Delta}{1-\Delta}} + y^{\frac{\tilde{\Delta}}{1-\tilde{\Delta}}}\right) \quad \text{with} \quad \tilde{\Delta} = (1-\Delta)\left\lfloor \frac{1}{1-\Delta} \right\rfloor, \quad (3)$$

where Δ is a user-specified parameter representing the belief about regularity. An important belief class, which we believe each \mathbf{P}_t might fall into (that is, $\mathbf{P}_{1:n} \subset \mathcal{P}_\Delta$ where $\mathbf{P}_{1:n} := \{\mathbf{P}_t\}_{t=1}^n$ is the collection of all NTP distributions) in some theoretical analysis, is the Δ -regular class, denoted by \mathcal{P}_Δ and defined as:

$$\mathcal{P}_\Delta = \{\mathbf{P} : \max_{w \in \text{Voc}} P_w \leq 1 - \Delta\}. \quad (4)$$

Li et al. [48] shows that $h_{\text{opt},\Delta}$ leads to the optimal sum-based test, achieving the fastest exponential rate of decrease in Type II errors at a given significance level α , under the least favorable (or worst-case) NTP distribution within the class \mathcal{P}_Δ (see Definition 4.1 for the formal definition).

3 Method

In this section, we first formally formulate the robust detection problem in Section 3.1 and then introduce Tr-GoF in Section 3.2.

3.1 Problem Formulation

Human edits are common following text generation by LLMs. We conceptualize this as a two-step process:

1. **Initial watermarked generation:** In the first step, the LLM generates tokens with embedded watermarks as usual. Let $\tilde{w}_{1:n_0}$ represent the (unedited) watermarked text, with associated pseudorandom variables $\tilde{\zeta}_{1:n_0}$, where n_0 is the original text length, potentially unknown to the verifier. Each $\tilde{w}_t = \mathcal{S}(\tilde{\mathbf{P}}_t, \tilde{\zeta}_t)$, where $\tilde{\mathbf{P}}_t = \text{LLM}(\tilde{w}_{1:(t-1)})$ is the NTP distribution of the LLM, and $\tilde{\zeta}_t$ is the pseudorandom variable computed by $\mathcal{A}(\tilde{w}_{(t-m):(t-1)}, \text{Key})$.
2. **Human editing:** In the second step, a human user edits the watermarked text $\tilde{w}_{1:n_0}$ by (i) retaining, (ii) replacing, or (iii) deleting tokens, and potentially (iv) inserting new tokens. This process yields a modified text $w_{1:n}$, where n may differ from n_0 .

In the detection phase, the verifier only has access to the edited text $w_{1:n}$, with no information on $\tilde{\mathbf{P}}_{1:n_0}$, $\tilde{w}_{1:n_0}$, or the specifics of the human edits. A pseudorandom variable can still be computed for each token w_t via $\zeta_t = \mathcal{A}(w_{(t-m):(t-1)}, \text{Key})$; however, the resulting sequence $\zeta_{1:n}$ may not align with the original $\tilde{\zeta}_{1:n_0}$. Indeed, the sequence lengths may even differ.

However, given that each pseudorandom variable $\tilde{\zeta}_t$ depends only on the preceding m tokens $\tilde{w}_{(t-m):(t-1)}$, watermark detection remains feasible as long as this local dependency is preserved. We represent this dependency through pivotal statistics. Within the framework of [48], watermark detection aims to identify distributional shifts in the pivotal statistic $Y_t := Y(w_t, \zeta_t)$. This statistic is a deterministic function of each (edited) token w_t and its associated pseudorandom variable ζ_t . If human edits maintain a continuous sequence of $(m + 1)$ tokens—such that $w_{(t-m):t} = \tilde{w}_{(\tilde{t}-m):\tilde{t}}$ for some t and \tilde{t} —then $\tilde{Y}_{\tilde{t}} := Y(\tilde{w}_{\tilde{t}}, \tilde{\zeta}_{\tilde{t}})$ will also appear within the sequence $Y_{1:n}$ as $Y_t = \tilde{Y}_{\tilde{t}}$. In this case, there exists an NTP distribution \mathbf{P}_t such that $Y_t := Y(w_t, \zeta_t)$ follows the original alternative distribution μ_{1, \mathbf{P}_t} . A closer examination reveals that \mathbf{P}_t must be the NTP distribution of w_t . Conversely, if an edit disrupts the dependency between w_t and ζ_t so that ζ_t no longer serves as the correct pseudorandom variable for generating w_t , w_t and ζ_t become statistically independent due to the high statistical specificity of hash functions to input changes. A detailed explanation is provided in Appendix A.1. Based on the definition of pivotal statistics (see Section 2), in this case, Y_t follows the original null distribution μ_0 .

From the preceding analysis, the distribution of Y_t is either μ_0 or μ_{1, \mathbf{P}_t} , depending on whether the watermark signal—the statistical dependence between w_t and ζ_t —is intact. Motivated by this, we introduce a binary random process $\{\eta_t\}_{t=1}^n \subset \{0, 1\}$, where η_t indicates if Y_t has shifted from the null distribution μ_0 . Specifically, we model $Y_t \mid (\mathbf{P}_t, \eta_t)$ as following the mixture distribution $(1 - \eta_t)\mu_0 + \eta_t\mu_{1, \mathbf{P}_t}$, combining the null μ_0 and alternative μ_{1, \mathbf{P}_t} distributions. Therefore, the robust watermark detection can be cast as the following hypothesis testing problem:

$$H_0 : Y_t \sim \mu_0, \text{ i.i.d. } \forall 1 \leq t \leq n \quad \text{versus} \quad H_1^{\text{mix}} : Y_t \mid (\mathbf{P}_t, \eta_t) \sim (1 - \eta_t)\mu_0 + \eta_t\mu_{1, \mathbf{P}_t}, \forall 1 \leq t \leq n. \quad (5)$$

Given our focus on the Gumbel-max watermark [1], we have $\mu_0 = U(0, 1)$ and $\mu_{1, \mathbf{P}}(Y \leq r) = \sum_{w \in \text{Voc}} P_w r^{1/P_w}$ for any $r \in [0, 1]$. If attention shifts to other watermarking methods, it is necessary and feasible to identify the corresponding distributions μ_0 and μ_{1, \mathbf{P}_t} similarly as in [48].

3.2 The Tr-GoF Detection Method

In this section, we introduce our detection method, Tr-GoF (Algorithm 1), which we apply to the robust watermark detection problem (5). To begin, we explain the rationale behind this approach. The null hypothesis H_0 in (5) assumes that all pivotal statistics $Y_{1:n}$ are drawn from the same distribution μ_0 . This indicates that the testing problem in (5) essentially assesses how well the entire data set $Y_{1:n}$ conforms to the null distribution μ_0 . Roughly speaking, Tr-GoF rejects the null hypothesis H_0 when the deviation between the empirical distribution of $Y_{1:n}$ and the null distribution μ_0 is sufficiently large.

We now introduce the deviation measure which is based on a specific ϕ -divergence [38]. Without loss of generality, we assume the data used in Tr-GoF are all p-values, which is always feasible by transforming observations using the CDF of μ_0 . In the Gumbel-max watermark, the p-values are linear transformations of $Y_{1:n}$. Given that $\mu_0 = U(0, 1)$, the p-value for each observation is defined as:

$$p_t := \mathbb{P}_0(Y \geq Y_t | Y_t) = 1 - Y_t.$$

Let $\mathbb{F}_n(r)$ denote the empirical distribution of the p-values,

$$\mathbb{F}_n(r) = \frac{1}{n} \sum_{t=1}^n \mathbf{1}_{p_t \leq r} \quad \text{for } r \in [0, 1],$$

and its expected distribution under H_0 is always the uniform $U(0, 1)$, with CDF $\mathbb{F}_0(r) = r$ for $r \in [0, 1]$. Tr-GoF utilizes the following test statistic to measure the deviation between the empirical CDF \mathbb{F}_n and the expected CDF \mathbb{F}_0 :

$$S_n^+(s) = \sup_{r \in [p^+, 1]} K_s^+(\mathbb{F}_n(r), \mathbb{F}_0(r)). \quad (6)$$

In the above, there are two truncations: the first is on the r -domain, where $p^+ = \sup\{p(t) : p(t) \leq c_n^+\}$ with $c_n^+ \in [0, 1]$ introduced for stability. The second is the truncation of K_s to K_s^+ , which is defined as a truncated version of K_s defined by

$$K_s^+(u, v) = \begin{cases} K_s(u, v), & \text{if } 0 < v < u < 1, \\ 0, & \text{if } 0 \leq u \leq v < 1, \end{cases} \quad (7)$$

where $K_s(u, v)$ represents the ϕ_s -divergence between $\text{Ber}(u)$ and $\text{Ber}(v)$:²

$$K_s(u, v) = D_{\phi_s}(\text{Ber}(u) \parallel \text{Ber}(v)) = v\phi_s\left(\frac{u}{v}\right) + (1-v)\phi_s\left(\frac{1-u}{1-v}\right).$$

Here the scalar function $\phi_s(x)$, indexed by $s \in \mathbb{R}$, is convex in x and is defined as follows [38]:

$$\phi_s(x) = \begin{cases} x \log x - x + 1, & \text{if } s = 1, \\ \frac{1-s+sx-x^s}{s(1-s)}, & \text{if } s \neq 0, 1, \\ -\log x + x - 1, & \text{if } s = 0. \end{cases} \quad (8)$$

In this family, ϕ_s provides a range of examples depending on the value of s . For $s = 1$, $\phi_1(x) = x \log x - x + 1$, which reduces K_1 to the KL divergence: $K_1(u, v) = v \log \frac{u}{v} + (1-u) \log \frac{1-u}{1-v}$. When $s = 2$, $\phi_2(x) = \frac{1}{2}(x^2 - x - 1)$, yielding $K_2(u, v) = \frac{(u-v)^2}{2v(1-v)}$, a form associated with Higher Criticism [19, 20], as discussed in Remark 3.4. For $s \neq 0, 1$, we have $K_s(u, v) = \frac{1}{s(1-s)} [1 - u^s v^{1-s} - (1-u)^s (1-v)^{1-s}]$. This definition of ϕ_s ensures continuity in s for all $x \in (0, 1)$.

Tr-GoF is based on the test statistic $S_n^+(s)$, which is introduced in (6) and can be straightforwardly computed using (9). This statistic is expected to be small under the null hypothesis H_0 and large under the alternative hypothesis H_1^{mix} . We define the detection method as follows: for a small $\delta > 0$, we reject H_0 in favor of H_1^{mix} if

$$n \cdot S_n^+(s) \geq (1 + \delta) \log \log n. \quad (10)$$

In other words, if our measure $S_n^+(s)$ of deviance from \mathbb{F}_n to \mathbb{F}_0 is sufficiently large—satisfying the condition in (10)—then the detection method will conclude that the observed text was (partially) generated by a watermarked LLM rather than being human-written.

Remark 3.1 (Selection of the critical value). We discuss the selection of the critical value $(1 + \delta) \log \log n$. Given the setup in (5), where $Y_{1:n}$ are i.i.d. samples from μ_0 , the Type I error can be controlled by carefully choosing this critical value. Notably, this control is independent of any human edits. In our experiments, we determine the critical value using Monte Carlo simulations, a method that is both computationally efficient and effective in controlling the Type I error even with finite sample sizes.

² $\text{Ber}(u)$ denotes a Bernoulli distribution with parameter (or head probability) u .

Algorithm 1 Truncated GoF detection method (Tr-GoF)

- 1: **Input:** Edited text $w_{1:n}$, hash function \mathcal{A} , secret key \mathbf{Key} , pivot statistic function Y , stability parameter c_n^+ , and critical value δ .
- 2: For $t = 1, 2, \dots, n$, compute the pseudorandomness number $\zeta_t = \mathcal{A}(w_{(t-m):(t-1)}, \mathbf{Key})$.
- 3: For $t = 1, 2, \dots, n$, compute the pivot statistic $Y_t = Y(w_t, \zeta_t)$.
- 4: For $t = 1, 2, \dots, n$, calculate the p-value as $p_t = 1 - Y_t$.
- 5: Sort the p-values in the ascending order $p_{(1)} < p_{(2)} < \dots < p_{(n)}$ and set $p_{(n+1)} = 1$.
- 6: Define the function K_s^+ as in (7) and compute the test statistic by

$$S_n^+(s) = \sup_{t: p_{(t+1)} \geq c_n^+} K_s^+(t/n, p_{(t)}). \quad (9)$$

- 7: **Claim:** Text $w_{1:n}$ is partially LLM-generated if (10) holds; otherwise, it is human-written.
-

Remark 3.2 (Differences from previous work). Our Tr-GoF test departs from the GoF test in [38] by incorporating two key truncations. First, we truncate K_s to K_s^+ to facilitate theoretical analysis, leveraging the property that $\lim_{n \rightarrow \infty} \mathbb{P}_0(p_{(t)} \leq t/n + \delta, \forall t \in [n]) = 1$ for any $\delta > 0$. Second, we restrict the domain of r to $[p^+, 1)$ instead of $(0, 1)$ to exclude small p-values, such as $p_{(1)}$ and $p_{(2)}$, in defining $S_n^+(s)$. In summary, Jager and Wellner [38] focus on the untruncated statistic $S_n(s) := \sup_{r \in (0,1)} K_s(\mathbb{F}_n(r), \mathbb{F}_0(r))$ and its theoretical properties under i.i.d. data. In contrast, we propose a truncated $S_n^+(s)$ for watermark detection in settings where the data is not i.i.d.

Remark 3.3 (Drawbacks of an untruncated r -domain). As introduced in Remark 3.2, the untruncated $S_n(s)$ has two main drawbacks. First, its weak convergence is slow: Jager and Wellner [38] show that $n \cdot S_n(s)$ converges weakly to a random variable under H_0 (see their Theorem 3.1), but Gontscharuk et al. [27] indicate that this convergence rate is extremely slow, suggesting r -domain truncation as a remedy. This observation also motivates our use of Monte Carlo simulations for determining critical values, despite the exact computation available in [47, 55]. Second, without removing extreme values from small p-values like $p_{(1)}$ or $p_{(2)}$, $S_n(s)$ is prone to a heavy-tail issue. In fact, it holds that $\mathbb{P}_0(n \cdot S_n(s) \geq z) \geq \frac{1}{2z}$ for large $z > 0$ over certain s values. Test statistics with heavy tails are generally undesirable, as they reduce power at stringent significance levels in small samples. Removing these small p-values mitigates the heavy-tail effect significantly in numerical experiments. See Appendix A.5 for more detailed discussion.

Remark 3.4 (Relationship to Higher Criticism). The celebrated Higher Criticism (HC) is a special instance of the above Tr-GoF. HC rejects H_0 if a test statistic, denoted by HC_n^+ , exceeds $\sqrt{2(1 + \delta) \log \log n}$ for a small value $\delta > 0$. This test statistic is related to our $S_n^+(2)$ as follows:

$$n \cdot S_n^+(2) = \sup_{r \in [p^+, 1)} \frac{n(\mathbb{F}_n(r) - r)^2}{2r(1-r)} \mathbf{1}_{\mathbb{F}_n(r) \geq r} = \frac{1}{2}(\text{HC}_n^+)^2. \quad (11)$$

Our rejection rule aligns perfectly with HC as described in the literature [19, 10, 9]. See Appendix A.4 for further introduction and its theoretical property. Since HC using HC_n^+ can be viewed as a special case of Tr-GoF involving $nS_n^+(2)$, our primary analysis focuses on $nS_n^+(s)$ to cover a wide range of s . For completeness, we perform a simulation study on HC in Appendix B.2 and B.3.

Procedure 1 Statistical modeling for human edits

- 1: **Input:** The watermarked text $\tilde{w}_{1:n_0}$ generated by $\tilde{w}_t = \mathcal{S}(\tilde{P}_t, \tilde{\zeta}_t)$ and $\tilde{P}_t = \text{LLM}(\tilde{w}_{1:(t-1)})$.
 - 2: **Initialize:** $w_{1:0} = \emptyset$ and $t = t_0 = 1$.
 - 3: **while** the edit is not complete **do**
 - 4: Try to determine w_t by inspecting the referenced token \tilde{w}_{t_0} .
 - 5: **if** the user approves \tilde{w}_{t_0} **then**
 - 6: **No edit:** Set $w_t = \tilde{w}_{t_0}$ and update $(t, t_0) \leftarrow (t + 1, t_0 + 1)$.
 - 7: **else if** the user prefers to generate w_t themselves **then**
 - 8: Generate $w_t \sim P_t^h$ where P_t^h depends on $w_{1:(t-1)}$ and $\tilde{w}_{1:(t_0-1)}$.
 - 9: **Substitution:** Update $(t, t_0) \leftarrow (t + 1, t_0 + 1)$.
 - 10: **Insertion:** Update $(t, t_0) \leftarrow (t + 1, t_0)$.
 - 11: **else if** the user searches for a better alternative in the watermarked text **then**
 - 12: **Deletion:** Update $(t, t_0) \leftarrow (t, t_0 + 1)$. Note that w_t remains undetermined at this stage.
 - 13: **end if**
 - 14: **end while**
 - 15: **Return:** The edited text $w_{1:t}$.
-

4 Theoretical Guarantees

In this section, we present the theoretical properties of Tr-GoF. We begin with a statistical model for human edits, followed by several distributional assumptions on the LLM watermarks and human edits.

4.1 Modeling the Process of Human Edits

For the sake of theoretical analysis, we should model the way humans edit. In the two-step process described in Section 3.1, we assume the human edits the watermarked text $\tilde{w}_{1:n_0}$ following Procedure 1. This procedure simplifies and standardizes how humans modify LLM outputs, but it is still fairly general. The only requirement is that the human edits tokens in an autoregressive manner, meaning they cannot change tokens that have already been edited.

We briefly describe Procedure 1 as follows. This procedure constructs an edited text $w_{1:n}$ by alternatively scanning each token in the original text $\tilde{w}_{1:n_0}$ and deciding whether and how to edit it. Let t denote the target position in the edited text, and t_0 represent the current position in the watermarked text being scanned. To model this process, we assume that, if a user wishes to replace or insert a new token, they generate it according to a multinomial distribution P_t^h , which depends on both the existing edited text $w_{1:(t-1)}$ and the watermarked subtext $\tilde{w}_{1:(t_0-1)}$ up to the current step. At each iteration, the length of the edited text increases by either copying the watermarked token \tilde{w}_{t_0} to position t (without edits) or by generating a new token (for substitution or insertion). Once w_t is determined, t always increments by one, extending the edited text. However, t_0 remains unchanged in the case of insertion, allowing \tilde{w}_{t_0} to be revisited in the next iteration. For all other operations, t_0 also increments by one, advancing to the next token in the watermarked text.

Examples of the binary process $\{\eta_t\}_{t=1}^n$. We now show how different token modifications lead to various η_t processes. For each iteration t , we define \tilde{t} as the longest length of the original text the user has scanned before w_t is finalized. Technically, it is the largest value of t_0 before Procedure 1

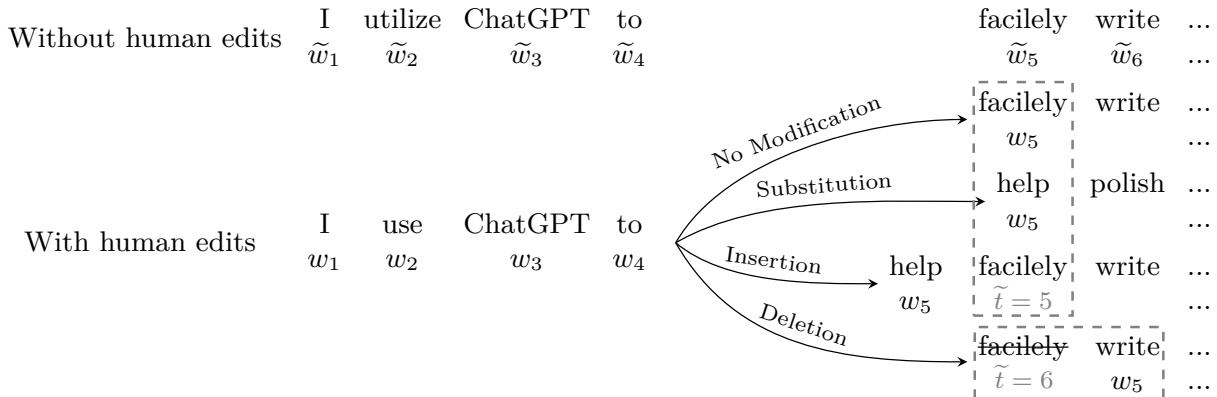


Figure 5: Illustration of Procedure 1 when $t = 5$. For each t , before w_t is finalized, the human has scanned the watermarked (or original) text up to $\tilde{w}_{1:\tilde{t}}$.

determines the value of w_t .³ According to Procedure 1, if no edit is performed, w_t will be equal to $\tilde{w}_{\tilde{t}}$; otherwise, w_t will be human-written. We define $X_t := \mathbf{1}_{w_t = \tilde{w}_{\tilde{t}}}$ as the indicator of whether the user keeps the watermarked token $\tilde{w}_{\tilde{t}}$ for the position w_t . From the above analysis, we have that⁴

$$\eta_t = \mathbf{1}_{w_{(t-m):t} = \tilde{w}_{(\tilde{t}-m):\tilde{t}}} = \prod_{j=(t-m)}^t X_j.$$

By the last equation, we connect the token modification (that is, X_t) with watermark signal modification (that is, η_t). Here are two examples.

Example 4.1 (I.i.d. edit). *If each token in $\tilde{w}_{1:n_0}$ is edited (that is, substituted, deleted, or inserted by a new token) independently with probability $a \in [0, 1]$ —that is, X_1, \dots, X_n are i.i.d. copies of $\text{Ber}(1 - a)$ —and otherwise kept unchanged, then*

$$\mathbb{P}(\eta_t = 1) = \mathbb{P}(\tilde{w}_{(t-m):t} = w_{(t-m):t}) = (1 - a)^{m+1}.$$

This result implies that as the context window m increases, the likelihood of maintaining the watermark signal decreases. Therefore, a larger context window is more susceptible to human edits, which is why in practice, m is often set to a relatively small value, such as 4 or 5. This relationship also suggests that the fraction of watermark signal retained is generally lower than the fraction of unedited tokens. For example, a 5% random paraphrasing removes about 22.6% of watermark signals when $m = 5$.

Example 4.2 (Markov edit). *A more practical example assumes that the human edits each token based on whether they edit the previous tokens. If many preceding tokens have been altered, it is more likely that the next token will also be changed. Conversely, if most preceding tokens are untouched, the user may leave the following token unchanged. In this case, we could model the user’s behavior $\{X_t\}_{t=1}^n$ as an M -order Markov process [52], where the edit state of the current token*

³The reason \tilde{t} may differ from t_0 is that, during a deletion, only t_0 is incremented while t remains unchanged, allowing the user to skip multiple watermarked tokens before finalizing w_t . In cases of no edit, substitution, or insertion, \tilde{t} equals the value of t_0 at the beginning of iteration t .

⁴This equation holds because $\{w_{(t-m):t} = \tilde{w}_{(\tilde{t}-m):\tilde{t}}\}$ is equivalent to $\{X_{j-m} = \dots = X_t = 1\}$, which can be shown by noting that if $X_t = X_{t+1} = 1$ (that is, no edit at iteration t and $t + 1$), then $\widetilde{t+1} = \tilde{t} + 1$.

X_t depends only on the previous M states X_{t-1}, \dots, X_{t-M} and is independent of earlier states. If $\{X_t\}_{t \geq 1}$ forms a stationary sequence, meaning that $(X_1, \dots, X_m) \stackrel{d}{=} (X_{t-m+1}, \dots, X_t)$ for any t , then the sequence $\{\eta_t\}_{t \geq 1}$ is also stationary. By the ergodic theorem, we have $\frac{1}{n} \sum_{t=1}^n X_t \xrightarrow{a.s.} \mathbb{E} X_1$ and $\frac{1}{n} \sum_{t=1}^n \eta_t \xrightarrow{a.s.} \mathbb{E}[\eta_1]$ as $n \rightarrow \infty$. A careful examination shows that $\mathbb{E}[\eta_1] = \mathbb{E}[X_1 \cdots X_m] \leq \mathbb{E} X_1$, indicating that the expected fraction of preserved watermark signals is still no larger than the fraction of unedited tokens.

4.2 Assumptions

For theoretical purposes, we assume that humans generate tokens using the same decoder \mathcal{S} . Specifically, each new token is generated as $w_t = \mathcal{S}(\mathbf{P}_t^h, \zeta_t^h)$, where \mathbf{P}_t^h represents the user’s NTP distribution, and ζ_t^h denotes the human internal randomness in the generation process. Importantly, we assume ζ_t^h follows the same distribution as $\tilde{\zeta}_t$ (the randomness governing watermarked tokens) and is independent of other sources of non-human randomness, such as $\tilde{w}_{1:n_0}$. With this conceptual equivalence in mind, we now introduce the following assumptions.

Assumption 4.1. *Assume the human edits the watermarked text according to Procedure 1. For each t , let \tilde{t} be the length of the original text reviewed before determining w_t . Let $\mathcal{F}_{t-1} = \sigma(\{w_j, \zeta_j, \zeta_j^h\}_{j=1}^{t-1} \cup \{\tilde{\zeta}_j\}_{j=1}^{\tilde{t}-1})$ be the σ -field generated by all text-generating randomness immediately after w_{t-1} is determined. We introduce the following assumptions:*

- (i) *Time-homogeneous edit:* $\mathbb{E}[\eta_1] = \dots = \mathbb{E}[\eta_n] = \varepsilon_n \asymp n^{-p}$ where $p \in [0, 1]$ is unknown.
- (ii) *Perfect (pseudo)randomness:* The elements in the set $\{\tilde{\zeta}_{\tilde{t}}, \zeta_t^h, \zeta_t\}$ are i.i.d. conditional on $(\mathcal{F}_{t-1}, \eta_t)$ for any t .⁵
- (iii) *Generation-unaware edit:* $\eta_t \perp \mathcal{F}_{t-1}$ and $\eta_t \perp \{\tilde{\zeta}_{\tilde{t}}, \zeta_t^h, \zeta_t\} \mid \mathcal{F}_{t-1}$ for any t .

A direct result of Assumption 4.1 is that the mixture formulation in (5) is statistically valid, that is, $Y_t \mid (\mathbf{P}_t, \eta_t) \sim (1 - \eta_t)\mu_0 + \eta_t\mu_{1, \mathbf{P}_t}$ for any t if Procedure 1 produces $w_{1:n}$. We briefly comment on this assumption. Condition (i) models varying edit levels using different values of $p \in [0, 1]$. We consider the time-homogeneous editing where $\mathbb{E}[\eta_t]$ remains constant for simplicity.

When the user is about to determine w_t (but has not yet), they observe the original text up to $\tilde{w}_{1:(\tilde{t}-1)}$. Therefore, \mathcal{F}_{t-1} collects all the information from the random variables used to generate $w_{1:(t-1)}$ but none about w_t . Condition (ii) requires that, conditioned on the history \mathcal{F}_{t-1} , the randomness involved in generating or detecting w_t —including the pseudorandom $\tilde{\zeta}_{\tilde{t}}$ and ζ_t , and the human-endogenous ζ_t^h —remains truly i.i.d., regardless of whether the watermark signal has been removed or not (that is, $\eta_t = 0$). This assumption is mainly for theoretical purposes. In fact, treating pseudorandom values as true random is standard practice in the literature, whether stated explicitly [76, 83, 61, 48] or implicitly [44, 45, 23]. Additionally, considering the human randomness as true random is conceptually valid since human edits are essentially unbiased samples from the human NTP distribution \mathbf{P}_t^h . As a note, Condition (ii) aligns with the spirit of the Working Hypothesis presented in our companion paper [48].

Condition (iii) assumes that the indicator of watermark signals η_t is independent of any prior text-generating history (that is, \mathcal{F}_{t-1}) and does not affect the randomness used to determine w_t (namely,

⁵When $\eta_t = 0$, the set $\{\tilde{\zeta}_{\tilde{t}}, \zeta_t^h, \zeta_t\}$ contains three distinct random variables; however, when $\eta_t = 1$, there are only two, as $\zeta_t = \tilde{\zeta}_{\tilde{t}}$ always in this case.

$\tilde{\zeta}_t^h, \zeta_t^h, \zeta_t$), given that history. The rationale is threefold. First, η_t is independent of $\{\zeta_j\}_{j=1}^{t-1} \cup \{\tilde{\zeta}_j\}_{j=1}^{t-1}$ because the human lacks access to the secret key **Key**. Second, η_t is independent of $\{w_j, \zeta_j^h\}_{j=1}^{t-1}$ due to the statistical model on human behavior which requires that the decision to edit is decoupled from the method of editing. For example, a human may decide to edit the text based on prior actions rather than the edited text (see Example 4.2). Third, the conditional independence between η_t and $\{\tilde{\zeta}_t, \zeta_t^h, \zeta_t\}$ ensures that, given the history, the decision to edit does not affect the distribution of potential outcomes.

4.3 Detectability

We begin by focusing on the challenging scenario where the watermark signal diminishes asymptotically. Specifically, with Assumption 4.1 and the following Assumption 4.2, we assume that both the non-null fraction, $\varepsilon_n \asymp n^{-p}$, and the distribution singularity, $\Delta_n \asymp n^{-q}$, decrease with the text length n . This setup draws inspiration from the classic framework of sparse detection problems [19, 20], where the signal strength of non-null effects also declines at a polynomial rate in sparse Gaussian mixture detection. Additionally, Assumption 4.2 can be relaxed to a weaker condition, which we discuss in Remark 4.2.

Assumption 4.2. Define $\Delta(\mathbf{P}) := 1 - \max_{w \in \text{Voc}} P_w$ as the distribution singularity of \mathbf{P} . For any positive integer $t \leq n$, we assume $\Delta(P_t) = \Delta_n \asymp n^{-q}$ with $q \in [0, 1]$.

Remark 4.1. The distribution singularity $\Delta(\mathbf{P})$ is equivalent to the entropy, defined as $\text{Ent}(\mathbf{P}) := \sum_{w \in \text{Voc}} P_w \log \frac{1}{P_w}$ (up to constant factors) via the relation $\text{Ent}(\mathbf{P}) = \Theta(\Delta(\mathbf{P}) \log \frac{1}{\Delta(\mathbf{P})})$. The proof is provided in Proposition A.2 in the appendix.

The first question to address is whether there exists a statistical algorithm that can reliably detect the embedded watermark based on the pivotal statistics $Y_{1:n}$ we compute. As an extreme example, if $\varepsilon_n = 0$ or $\Delta_n = 0$, we would have $H_1^{\text{mix}} = H_0$ and thus no test could differentiate H_1^{mix} from H_0 . In general, the detectability depends on the difference between the joint distributions of $Y_{1:n}$ under H_0 and H_1^{mix} . In the terminology of Donoho and Jin [19], we say that H_0 and H_1^{mix} merge asymptotically if the total variation distance between the joint distribution of $Y_{1:n}$ under H_0 and that under H_1^{mix} tends to zero as the sequence length n goes to infinity. Otherwise, we say they separate asymptotically. The detection problem is detectable if and only if H_0 and H_1^{mix} separate asymptotically.

The detectability behaves very differently in two regimes: the heavy edit regime where $\frac{1}{2} < p \leq 1$ and the light edit regime where $0 < p \leq \frac{1}{2}$. We begin by considering the heavy edit regime where $p \in (1/2, 1]$. Theorem 4.1 proves that no statistical test based on the observed pivotal statistics $Y_{1:n}$ can reliably detect the embedded watermark. Notably, this impossibility result holds irrespective of the underlying NTP distribution \mathbf{P}_t 's. Therefore, in the heavy edit regime, detection of embedded watermarks is impossible, regardless of the NTP distribution \mathbf{P}_t 's.

Theorem 4.1 (Heavy edits case). *Under Assumption 4.1, if $\frac{1}{2} < p \leq 1$, H_0 and H_1^{mix} merge asymptotically. For any test, the sum of Type I and Type II errors is 1 as $n \rightarrow \infty$.*

The situation is much more involved when the edit is light where $p \in (0, 1/2]$. It turns out that the detectability of the embedded watermark further depends on the NTP distribution \mathbf{P}_t 's. To account for this, we introduce Assumption 4.2 which assumes the largest probability in all NTP distributions share the same value $1 - \Delta_n$ and $\Delta_n \asymp n^{-q}$.

Theorem 4.2 (Light edits case). *Under Assumptions 4.1 and 4.2, let $0 \leq p \leq \frac{1}{2}$ and $0 \leq q \leq 1$.*

- *If $q + 2p > 1$, H_0 and H_1^{mix} merge asymptotically. Hence, for any test, the sum of Type I and Type II errors tends to 1 as $n \rightarrow \infty$.*
- *If $q + 2p < 1$, H_0 and H_1^{mix} separate asymptotically. For the likelihood-ratio test that rejects H_0 if the log-likelihood ratio is positive, the sum of Type I and Type II errors tends to 0 as $n \rightarrow \infty$.*

Remark 4.2 (A weaker assumption for Theorem 4.2). For simplicity of presentation, we adopt Assumption 4.2, though the proof relies on a weaker condition: we assume that all NTP distributions \mathbf{P}_t are either uniformly $\mathbf{P}_{1:n} \subset \mathcal{P}_{\Delta_n}$ or $\mathbf{P}_{1:n} \subset \mathcal{P}_{\Delta_n}^c$ according to (4). In our appendix, we show that Theorem 4.2 holds under Assumption 4.1 and this weaker condition. Specifically, we prove that under Assumption 4.1, if $q + 2p > 1$ and $\mathbf{P}_{1:n} \subset \mathcal{P}_{\Delta_n}$, H_0 and H_1^{mix} merge asymptotically; conversely, if $q + 2p < 1$ and $\mathbf{P}_{1:n} \subset \mathcal{P}_{\Delta_n}^c$, H_0 and H_1^{mix} separate asymptotically. The same reasoning applies to the subsequent Theorem 4.3 and 4.4.

Theorem 4.2 demonstrates that given $q + 2p < 1$, it is possible to distinguish between H_0 and H_1^{mix} asymptotically, using the likelihood-ratio test as an effective detection method. Conversely, if $q + 2p > 1$, H_0 and H_1^{mix} become indistinguishable asymptotically. Hence, $q + 2p = 1$ represents the theoretical boundary distinguishing detectable from undetectable regions across the entire $[0, 1]^2$ plane. Unfortunately, the likelihood-ratio test is impractical cause it relies on the unknown token distribution \mathbf{P}_t and non-null fraction ε_n .

Corollary 4.1 (Detection boundary). *Under Assumptions 4.1 and 4.2, the hypothesis testing problem (5) is detectable if and only if $q + 2p < 1$.*

4.4 Adaptive Optimality

An ideal optimal method should achieve the detection boundary $q + 2p = 1$ automatically in the previous difficult case, without requiring any problem-dependent knowledge such as p , q , or \mathbf{P}_t 's. This property is known as ‘‘adaptive optimality’’ in the literature [19, 20], as it consistently works regardless of the underlying parameters and does not require this information. In the following theorem, we show that Tr-GoF achieves adaptive optimality.

Theorem 4.3 (Optimal adaptivity of Tr-GoF). *Under Assumptions 4.1 and 4.2, if $q + 2p < 1$, for Tr-GoF with any $0 \leq c_n^+ \leq 1/n$ and $s \in [-1, 2]$, the sum of Type I and Type II errors tends to 0 as $n \rightarrow \infty$.*

Remark 4.3 (Proof sketch of Theorem 4.3). We provide the intuition behind Theorem 4.3 which focuses on the different behaviors of $S_n^+(s)$ under H_0 and H_1^{mix} . By Theorem 3.1 in [38], under H_0 ,

$$\lim_{n \rightarrow \infty} \mathbb{P}_0(n \cdot S_n^+(s) \leq \log \log n) = 1.$$

This means that $nS_n^+(s)$ increases towards infinity at an exceptionally slow rate under H_0 . In Appendix A.6, we show that under H_1^{mix} ,

$$\lim_{n \rightarrow \infty} \mathbb{P}_1(n \cdot S_n^+(s) \geq n^{\frac{1}{2} - \frac{q}{2} - p}) = 1.$$

This implies that $nS_n^+(s)$ grows faster than $\log \log n$ as long as $p + \frac{q}{2} < \frac{1}{2}$. These results imply that by rejecting H_0 whenever $nS_n^+(s) \geq (1 + \delta) \log \log n$ for any given $\delta > 0$, both Type I and Type II

errors converge to zero asymptotically. As a result, Tr-GoF can asymptotically distinguish between H_0 and H_1^{mix} .

Due to the prevalence of sum-based detection rules in the literature [1, 23, 48], we next examine whether these tests can achieve the same optimal adaptivity. We say a score function h is parameter-free if for any $y \in [0, 1]$, $h(y)$ does not depend on Δ and ε .

Theorem 4.4 (Suboptimality of parameter-free sum-based detection rules). *Let Assumptions 4.1 and 4.2 hold. Consider the detection rule specified by h : $T_h(Y_{1:n}) = 1$ if $\sum_{t=1}^n h(Y_t) \geq n \cdot \mathbb{E}_0 h(Y) + \Theta(1) \cdot n^{\frac{1}{2}} a_n$, otherwise it equals 0, where $a_n \rightarrow \infty$ and $\frac{a_n}{n^\gamma} \rightarrow 0$ for any $\gamma > 0$.⁶ For any score function that is (i) non-decreasing, (ii) non-constant, (iii) parameter-free, and (iv) does not have discontinuities at both 0 and 1, the following results hold for T_h :*

- If $q + p < \frac{1}{2}$, the sum of Type I and Type II errors tends to 0.
- If $q + p > \frac{1}{2}$, the sum of Type I and Type II errors tends to 1.

As shown in Theorem 4.4, for nearly any non-decreasing and parameter-free score function h , the sum-based detection rule it introduces is strictly suboptimal. Specifically, Theorem 4.4 shows that the detection boundary for these rules is $q + p = \frac{1}{2}$, rather than the optimal $q + 2p = 1$. Consequently, all existing sum-based detection rules fail to achieve the optimal detection boundary.

Corollary 4.2. *Under Assumptions 4.1 and 4.2, the detection boundary for the existing score function $h \in \{h_{\text{ars}}, h_{\text{log}}, h_{\text{ind},\delta}, h_{\text{opt},\Delta_0}\}$ with both $\delta, \Delta_0 \in (0, 1)$ is $q + p = \frac{1}{2}$.*

4.5 Optimal Efficiency Rate

We now turn to the constant edit region, where $\Delta_n = \Delta \in (0, 1)$ and $\varepsilon_n \equiv \varepsilon \in (0, 1]$. In this scenario, $p = q = 0$ according to the notation $\Delta_n \asymp n^{-p}$ and $\varepsilon_n \asymp n^{-q}$. Theorem 4.1 implies that detection is always possible, as H_0 and H_1^{mix} asymptotically separate. Furthermore, Theorems 4.3 and 4.4 suggest that both Tr-GoF and sum-based detection rules are viable detection methods. Unlike the detection boundary, which assesses adaptivity to varying problem difficulties, we employ a different criterion to evaluate feasible detection methods.

Li et al. [48] introduces a notion of test efficiency for watermark detection. The key idea is to define efficiency as the rate of exponential decrease in Type II errors for a fixed significance level α , considering the least-favorable NTP distribution within a belief class \mathcal{P} . The formal definition is provided in Definition 4.1.

Definition 4.1 (\mathcal{P} -dependent efficiency or \mathcal{P} -efficiency [48]). *Consider the detection rule that rejects H_0 if $S(Y_{1:n})$ is larger than a critical value. Let $\gamma_{n,\alpha}$ be the critical value that ensures a Type I error of α for the problem (5), that is, $\mathbb{P}_0(S(Y_{1:n}) \geq \gamma_{n,\alpha}) = \alpha$ for all $n \geq 1$. For a given belief class \mathcal{P} , we define the following limit as the \mathcal{P} -efficiency rate of S and denote it by $R_{\mathcal{P}}(S)$:*

$$\lim_{n \rightarrow \infty} \sup_{\mathbf{P}_t \in \mathcal{P}} \frac{1}{n} \log \mathbb{P}_1(S_n \leq \gamma_{n,\alpha}) = -R_{\mathcal{P}}(S).$$

⁶The choice of a_n ensures that T_h has a vanishing Type I error. Examples include any polynomial function of $\log n$ or $\log \log n$ with positive coefficients.

This efficiency notion is referred to as class-dependent efficiency, as it depends on a given class \mathcal{P} , which characterizes the prior belief about the underlying NTP distributions \mathbf{P}_t 's. In their study, they set the prior class as the Δ -regular set \mathcal{P}_Δ (defined in (4)) and identify the optimal score function $h_{\text{opt},\Delta}$ for sum-based detection rules. It is natural to compute the \mathcal{P}_Δ -efficiency rate for Tr-GoF, which provides a quantitative measure of their detection efficiency in the constant parameter region. We present the results in the following theorem.

Theorem 4.5 (Optimal \mathcal{P}_Δ -efficiency). *Assume Assumption 4.1 hold. Let $s \in (0, 1)$, $c_n^+ = 0$, $\varepsilon_n \equiv \varepsilon \in (0, 1]$ and $\Delta_n \equiv \Delta \in (0, 1)$. Given a dataset of pivotal statistics $Y_{1:n}$, for any measurable function S of $Y_{1:n}$, it follows that*

$$\sup_{\text{measurable } S} R_{\mathcal{P}_\Delta}(S) = D_{\text{KL}}(\mu_0, (1 - \varepsilon)\mu_0 + \varepsilon\mu_{1, \mathbf{P}_\Delta^*}) = R_{\mathcal{P}_\Delta}(S_n^+(s))$$

where \mathbf{P}_Δ^* is the least-favorable NTP distribution defined by

$$\mathbf{P}_\Delta^* = \left(\underbrace{1 - \Delta, \dots, 1 - \Delta}_{\lfloor \frac{1}{1-\Delta} \rfloor \text{ times}}, 1 - (1 - \Delta) \cdot \left\lfloor \frac{1}{1 - \Delta} \right\rfloor, 0, \dots \right). \quad (12)$$

Remark 4.4 (Proof sketch of Theorem 4.5). If all the underlying NTP distributions \mathbf{P}_t 's are identical (e.g., by setting \mathcal{P} as a singleton class), the \mathcal{P} -efficiency reduces to the Hodges-Lehmann asymptotic efficiency. When $s \in (0, 1)$ and $c_n^+ = 0$, the asymptotic behavior of $S_n^+(s)$ closely resembles that of the Kolmogorov–Smirnov test. Since the Hodges-Lehmann asymptotic efficiency of the Kolmogorov–Smirnov test is well-established in the literature [57], in our proof, we address the heterogeneity of the NTP distributions \mathbf{P}_t 's by reducing them to the least-favorable NTP distribution, \mathbf{P}_Δ^* , and apply this established result [57] to analyze $R_{\mathcal{P}_\Delta}(S_n^+(s))$. It is also worth noting that the conditions $s \in (0, 1)$ and $c_n^+ = 0$ are also required by the conventional analysis of Bahadur efficiency for $S_n^+(s)$ (see Theorem 4.4 in [38]). Whether and how to relax these conditions is still open even in the original line of research.

Theorem 4.5 establishes both upper and lower bounds in terms of \mathcal{P}_Δ -efficiency for the robust detection problem (5) under the constant parameter region. On one hand, it implies that the \mathcal{P}_Δ -efficiency rate of any measurable function is upper-bounded by $D_{\text{KL}}(\mu_0, (1 - \varepsilon)\mu_0 + \varepsilon\mu_{1, \mathbf{P}_\Delta^*})$. On the other hand, it shows that Tr-GoF achieves this optimal \mathcal{P}_Δ -efficiency rate without any prior knowledge of ε and Δ . When $\varepsilon = 1$, this optimality is also achieved by the sum-based detection rule introduced by $h_{\text{opt},\Delta}$ in [48]. However, as can easily be seen, computing $h_{\text{opt},\Delta}$ requires knowledge or correct belief about the value of Δ , which limits its practical applicability. Furthermore, when $\varepsilon < 1$, $h_{\text{opt},\Delta}$ is no longer optimal because it does not consider the factor ε .

To illustrate this optimal efficiency further, Figure 6 presents the \mathcal{P}_Δ -efficiency rates of different detection methods across various values of Δ , with the left panel showing the case $\varepsilon = 1$ and the right panel showing $\varepsilon = 0.5$. Here, h_{ars} , h_{log} , $h_{\text{ind},\delta}$, and h_{opt,Δ_0} represent commonly used sum-based detection rules, with $\delta = 0.5$ and $\Delta_0 = 0.1$ set for illustration purposes. In both cases, it is clear that Tr-GoF consistently achieves the optimal \mathcal{P}_Δ -efficiency rate for all $\Delta \in [0.001, 1]$. In contrast, sum-based detection rules generally fail to reach the optimal efficiency rate across most values of Δ due to their lack of adaptivity. For example, when $\varepsilon = 1$, h_{opt,Δ_0} attains the optimal \mathcal{P}_Δ -efficiency rate if $\Delta = \Delta_0$. However, once $\varepsilon < 1$, h_{opt,Δ_0} loses this optimality, as it does not incorporate any information about ε .

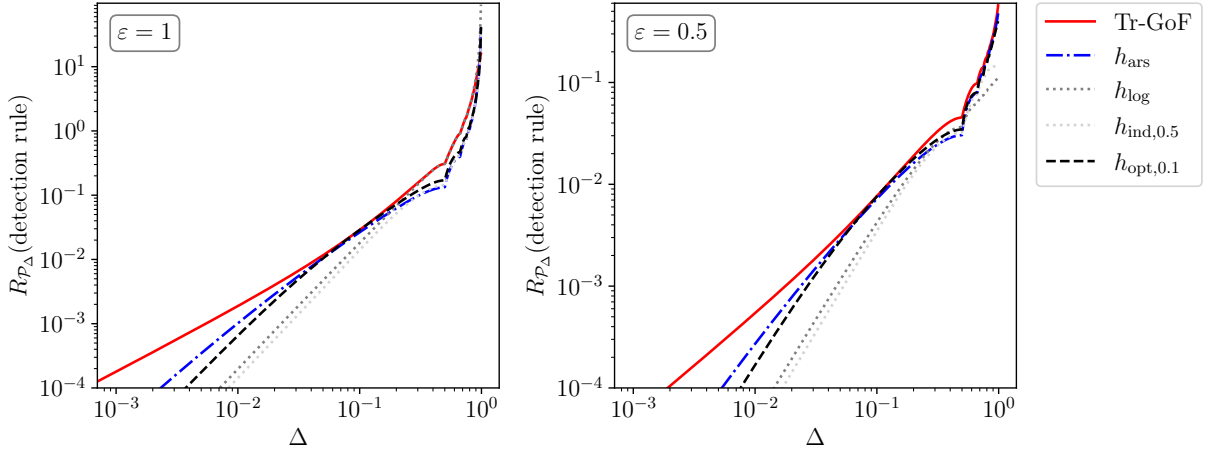


Figure 6: \mathcal{P}_Δ -efficiency rates of different detection methods for the Gumbel-max watermarks. $R_{\mathcal{P}_\Delta}$ has non-smooth points when $\Delta = \frac{1}{2}, \frac{2}{3}, \frac{3}{4}, \dots$ [48].

5 Simulations

In this section, our simulation studies first visualize the null and alternative distributions of the GoF statistic $S_n^+(s)$ and then identify the empirical transition boundaries for different detection methods.

5.1 Experimental Setup

We use a vocabulary of size $|\text{Voc}|$ and model the pseudorandom variables $\zeta_{t,w}$ as true i.i.d. samples from $U(0, 1)$. We will explore the practical setting where ζ_t is computed via a hash function later. For given $p, q \in (0, 1]$, we set $\varepsilon_n = n^{-p}$ and $\Delta_n = n^{-q}$ where n is the text length. We use the following procedure to obtain samples of $\log(nS_n^+(s))$ under different settings:

1. Draw n i.i.d. samples from $U(0, 1)$ to represent $Y_{1:n}$ in H_0 and calculate $\log(nS_n^+(s))$.
2. Replace $\lceil n\varepsilon_n \rceil$ of the previous samples by the same number of samples from F_{1, \mathbf{P}_t} where the NTP distributions \mathbf{P}_t are i.i.d. generated. Then, calculate $\log(nS_n^+(s))$.
3. Repeat Steps 1 and 2 N times. Obtain N independent samples of $\log(nS_n^+(s))$ under H_0 and H_1^{mix} respectively and create histograms of the simulated statistics.

In all subsequent experiments, we fix $N = 10^3$ while varying the values of $|\text{Voc}|$, n , and the pair (p, q) , which will be specified accordingly. We explore two methods for generating \mathbf{P}_t , denoted by M1 and M2. In particular,

M1 randomly generates \mathbf{P}_t by first setting its largest probability to $1 - \Delta_n$, and then configuring the remaining probabilities in \mathbf{P}_t to adhere to Zipf's law [85]. In particular, we first i.i.d. sample $a_t \sim U(0.95, 1.5)$ and $b_t \sim U(0.01, 0.1)$, and then define $P_{t,w} = \Delta_n \cdot (w - 1 + b_t)^{-a_t} / C$, where $C = \sum_{w=2}^{|\text{Voc}|} (w - 1 + b_t)^{-a_t}$ serves as the normalizing constant.

M2 straightforwardly sets \mathbf{P}_t to be equivalent to $\left(1 - \Delta_n, \frac{\Delta_n}{|\text{Voc}|-1}, \dots, \frac{\Delta_n}{|\text{Voc}|-1}\right)$.

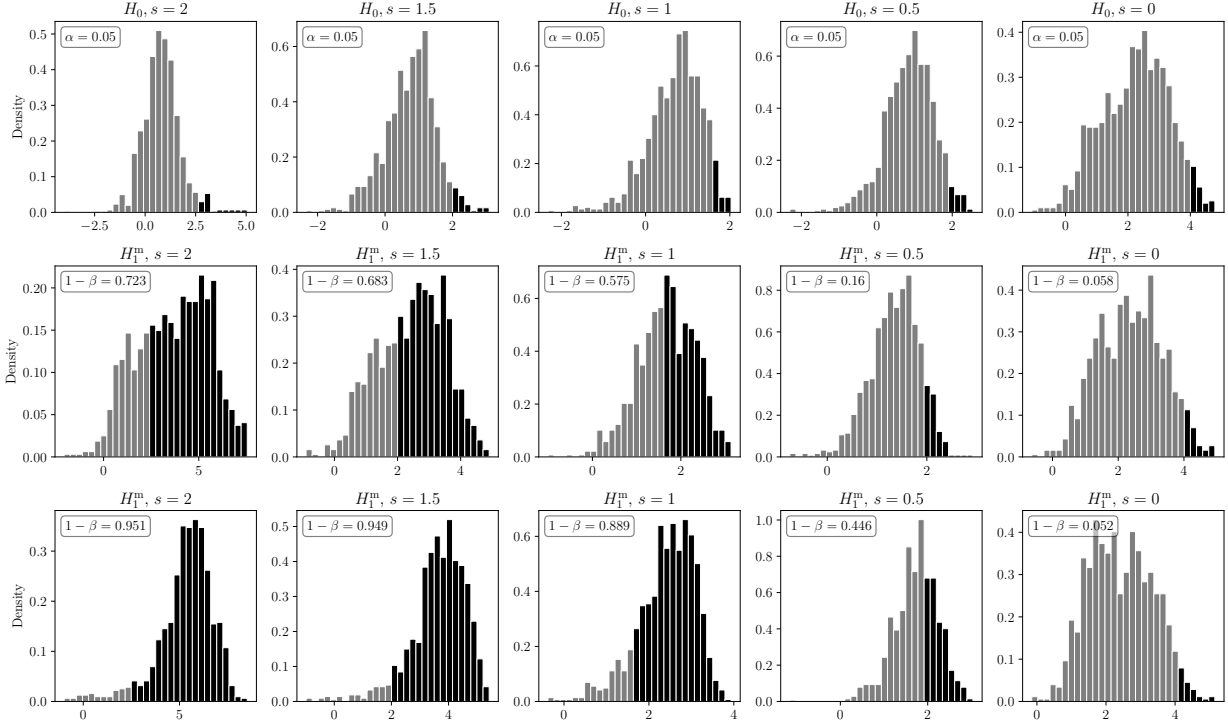


Figure 7: Density histograms and powers of $\log(nS_n^+(s))$ for different values of s with $c_n^+ = \frac{1}{n^2}$ and $(p, q) = (0.2, 0.5)$. The first row presents results under H_0 , while the second and third rows display results under H_1^{mix} , corresponding to the M1 and M2 settings. The dark area indicates the portion of the distribution that rejects H_0 which is the the Type I error α under the null hypothesis H_0 and the power $1 - \beta$ under the alternative hypothesis H_1^{mix} .

5.2 Histograms of Tr-GoF Statistics

To begin with, we investigate the empirical distribution of $\log(nS_n^+(s))$ under H_0 and H_1^{mix} . We set $|\text{Voc}| = n = 10^3$ in this investigation and collect $N = 10^3$ samples of $\log(nS_n^+(s))$ for different settings. In Figure 7, we visualize the empirical density histograms of $\log(nS_n^+(s))$ for five values of $s \in \{2, 1.5, 1, 0.5, 0\}$ and three settings. We shade the rejection regions and mark the corresponding statistical powers as $1 - \beta$. We observe that

- For $0.5 \leq s \leq 1.5$, the null distributions of $\log(nS_n^+(s))$ exhibit similar shapes and supports. However, for $s \in \{0, 2\}$, there are noticeable changes in shape and support. Remarkably, the maximum value that $\log(nS_n^+(s))$ could take increases dramatically from 2 (at $s = 1$) to 4 or even 5 (when $s = 0$ or 2).
- For the majority of the s values, the empirical distribution of $\log(nS_n^+(s))$ under H_1^{mix} resembles its counterpart under H_0 , albeit with a notable shift to the right. This shift can range from moderate (for $s \in \{0, 0.5\}$) to quite significant (for $s \in \{1, 1.5, 2\}$). It is this shift that enables the statistics $nS_n^+(s)$ to detect the distributional differences caused by embedded watermarks.
- The critical value is determined using the $(1 - \alpha)$ -quantile of the empirical null distribution, and we display the statistical power (denoted by $1 - \beta$) in the top-left corner of figures for

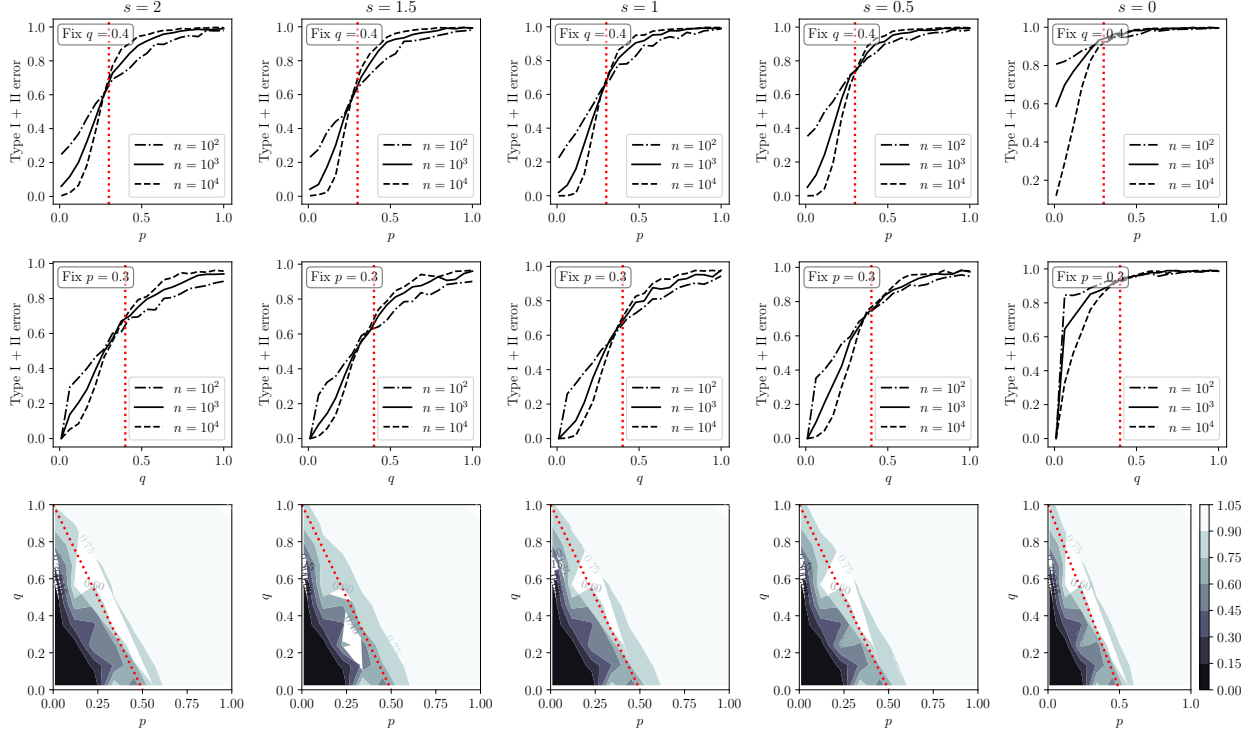


Figure 8: Empirical detection boundaries of Tr-GoF for different values of s . Each column corresponds to results for a specific value of s . The first two rows display the sum of Type I and II errors, with q fixed at 0.4 and p at 0.3, respectively. The last row features the contour plot which illustrates the sum of errors across the domain $[0, 1]^2$, with $n = 10^4$. Red dotted lines present the theoretical detection boundaries. All the results are averaged over $N = 10^3$ independent trials.

results under H_1^{mix} . Note that \mathbf{P}_t generated by M2 exhibits higher entropy than that generated by M1. Consequently, detection under the setup M2 would be easier, resulting in a larger statistical power.

Even if we set $c_n^+ = 0$, the observed patterns remain consistent, except that the support under H_1^{mix} would be considerably larger due to the heavy-tailed behavior of $p_{(1)}$. See Appendix B.1 for additional histogram results of $c_n^+ = 0$. We also tested negative values of s within the range of $[-1, 0)$, but found their histograms and statistical powers to be nearly identical to those when $s = 0$. Consequently, these results are not included in the section.

5.3 Detection Boundary and Optimal Adaptivity

We then study the detection boundary of Tr-GoF. They reject H_0 when $\log(nS_n^+(s)) \geq C_{\text{GoF}}$ for a predetermined critical value C_{GoF} and a given value $s \in \{2, 1.5, 1, 0.5, 0\}$. We use the same setup introduced in Section 5.1 but with $|\text{Voc}| = 5$ and focus on the M2 construction for each NTP distribution \mathbf{P}_t . We aim to check how the smallest sum of Type I and Type II errors changes as we vary the other parameters such as (p, q) , and n . Following the approach used in [10], we compute the smallest sum errors by tuning the critical value C_{GoF} from a predetermined set. Here, we use the set $\mathcal{R}(0, 30, 10^3)$ where $\mathcal{R}(a, b, K)$ consist of K equally spaced points starting from a to b over an interval defined by $(K - 1)$ divisions, that is, $\mathcal{R}(a, b, K) = \{a + \frac{k}{K-1} \cdot (b - a) : k = 0, 1, \dots, K - 1\}$.

Phase transition for a fixed p or q . We first fix either $q = 0.4$ or $p = 0.3$ and select a sample size n from $\{10^2, 10^3, 10^4\}$. According to Theorem 4.2, the detection boundary is given by $q + 2p = 1$, which suggests a transition at either $p = 0.3$ or $q = 0.4$. This prediction is validated by the first and second rows of Figure 8. For instance, when q is fixed at 0.4, the error sum $\alpha + \beta$ initially increases from zero and stabilizes at one as we increase p from zero to one. The transition point occurs around $p = 0.3$ and aligns well with the red dashed line. Furthermore, larger sample sizes make the alignment with the theoretical prediction more pronounced.

Adaptive optimality of Tr-GoF. To accurately capture the empirical detection boundary, we use $n = 10^4$ independent samples to calculate $\log(nS_n^+(s))$. For any $p \in \mathcal{R}(0.01, 1, 20)$ and $q \in \mathcal{R}\left(\log_n \frac{|\text{Voc}|}{|\text{Voc}|-1}, 1, 20\right)$,⁷ we compute the smallest sum of Type I and Type II errors by tuning the critical value as mentioned earlier. These results are displayed in the bottom row of Figure 8. Here, darker areas indicate lower error sums, while lighter regions present higher error sums. A red dashed line represents the theoretical detection boundary $q + 2p = 1$. Most darker regions are below this boundary, while lighter regions are above it. This empirical boundary aligns well with the theoretical prediction in Theorem 4.3, no matter what the value of s we choose.

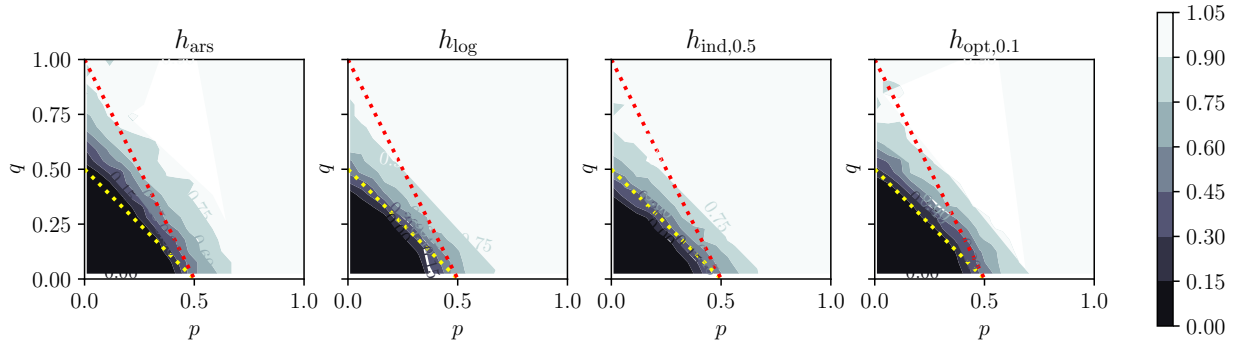


Figure 9: Empirical detection boundaries for different sum-based detection rules T_h 's.

Suboptimality of existing detection methods. For any function $h \in \{h_{\text{ars}}, h_{\text{log}}, h_{\text{ind},\delta}, h_{\text{opt},\Delta_0}\}$, we consider the following sum-based detection rule specified by h :

$$T_h(Y_{1:n}) = \begin{cases} 1 & \text{if } \sum_{t=1}^n h(Y_t) \geq n \cdot \mathbb{E}_0 h(Y) + C_{\text{sum}} \cdot n^{\frac{1}{2}} \log n, \\ 0 & \text{if } \sum_{t=1}^n h(Y_t) < n \cdot \mathbb{E}_0 h(Y) + C_{\text{sum}} \cdot n^{\frac{1}{2}} \log n. \end{cases}$$

The expectation $\mathbb{E}_0 h(Y)$ for different h 's has been listed in Table 1 in [48]. Mirroring our approach with Tr-GoF, for each detection rule T_h , we tune the parameter C_{sum} from a given set to obtain the smallest sum of Type I and Type II errors. This set for h_{ars} is $\mathcal{R}(8, 60, 10^3)$, for h_{log} is $\mathcal{R}(-20, 0, 10^3)$, and for $h_{\text{ind},0.5}, h_{\text{opt},0.1}$ is $\mathcal{R}(-10, 10, 10^3)$. The findings are presented in Figure 9, which was created using the same procedure as the contour plot in Figure 8. Observations reveal that the empirical boundaries closely match the theoretical prediction of $p + q = \frac{1}{2}$, represented by yellow dotted lines. This alignment corroborates our Theorem 4.4. In contrast, the red dotted line represents the optimal detection boundary $q + 2p = 1$. The discrepancy between the yellow and red dotted lines shows the suboptimality of sum-based tests.

⁷ $\log_n \frac{|\text{Voc}|}{|\text{Voc}|-1} \leq q$ is solved from the fact $1 - n^{-q} \geq \frac{1}{|\text{Voc}|}$ which always holds due to the pigeonhole principle.

6 Experiments on Open-Source LLMs

6.1 Experiment Setup

We follow the experimental setup from [46, 48]. We begin by sampling 1,000 documents from the news-like C4 dataset [65], which serve as the initial prompts. Using these prompts, we then ask two language models, the OPT-1.3B model [81] and Sheared-LLaMA-2.7B [77], to generate an additional $n = 400$ tokens for each document. Our evaluation focuses on two key aspects:

1. **Statistical power:** To evaluate the statistical power of different detection methods, we set the theoretical Type I error at $\alpha = 0.01$ by tuning the critical values, either using central limit theorem predictions or Monte Carlo simulations. We then assess the actual Type I errors using unwatermarked texts and Type II errors using watermarked texts.
2. **Robustness to edits:** Almost any editing method tends to weaken watermark signals. We focus on three representative types of edits [46]: random edits (including substitution, insertion, and deletion), adversarial edits, and roundtrip translation. In random edits, a random fraction of the watermarked tokens is replaced, inserted, or deleted, with substitutions and insertions involving tokens uniformly selected from the vocabulary Voc . Adversarial edits, by contrast, are more targeted, selectively modifying watermarked tokens to maximize the removal of watermark signals within a given edit budget. Finally, roundtrip translation involves translating the text from English to French and back to English using another language model. Random and adversarial edits enable systematic control over the level of edits, while roundtrip translation reflects a more realistic scenario likely to be encountered in practice.

We compare the Tr-GoF test across three different values of s from the set $\{1, 1.5, 2\}$ alongside three sum-based detection rules, each specified by a particular score function h . These include: (i) Aaronson’s function $h_{\text{ars}}(y) = -\log(1 - y)$ [1], (ii) the logarithmic function $h_{\log}(y) = \log y$ [46, 23], and (iii) the optimal least-favorable function [48], which is defined in (3) with Δ a user-specified parameter representing the prior belief for the level of regularity. We test Δ from the set $\{0.1, 0.2, 0.3\}$ and find that $\Delta = 0.1$ performs best; therefore, we use this value in the subsequent experiments. In all experiments, we use 1-sequence repeated context masking [16]. This approach watermarks a token only when the current text window is unique within the generation history, aiming to preserve text quality. In the following, we present our numerical results on the OPT-1.3B model for illustrative purposes, as the results for Sheared-LLaMA-2.7B are similar and are provided in the appendix. Additional experimental details are also deferred to the appendix.

6.2 Statistical Power

We first evaluate the statistical power of considered detection methods using unmodified texts. Unlike in simulation studies, we cannot manipulate each NTP distribution \mathbf{P}_t in language model experiments to ensure they are Δ -regular. However, Δ -regularity correlates closely with the temperature parameter in LLMs [3]. The temperature parameter modulates the raw outputs of the model’s final layer (also known as the logit layer) before the softmax function is applied. Typically, a high temperature yields more uniform probabilities, encouraging diverse generations, while a low temperature sharpens the distribution, emphasizing the most probable prediction and thus favoring the greedy generation. As an approximation, we use four temperatures $\{0.1, 0.3, 0.5, 0.7\}$ to check the effect of Δ -regularity on

statistical power. The evaluation results are displayed in Figures 10 and 11. Similar results on the Sheared-LLaMA-2.7B model are documented in Appendix C.2.

Type I error control. We begin by examining Type I error control, using 5000 unwatermarked texts sampled from the C4 dataset as human-written data and evaluating Type I error at the significance level $\alpha = 0.01$. Figure 10 shows how the empirical Type I error varies with increasing text lengths, revealing a consistent pattern: across all detection methods, empirical Type I errors remain well-controlled within the interval $[0.006, 0.014]$. This suggests that the pseudorandom variables effectively mimic the behavior of true random variables, enabling their empirical performance to closely align with theoretical expectations.

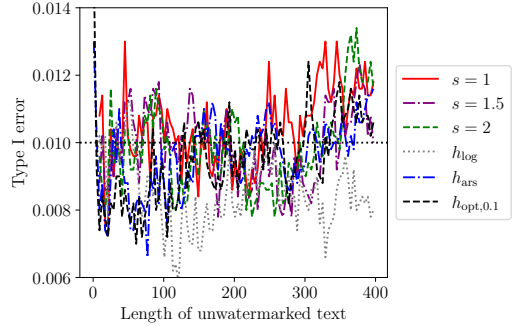


Figure 10: Empirical Type I errors.

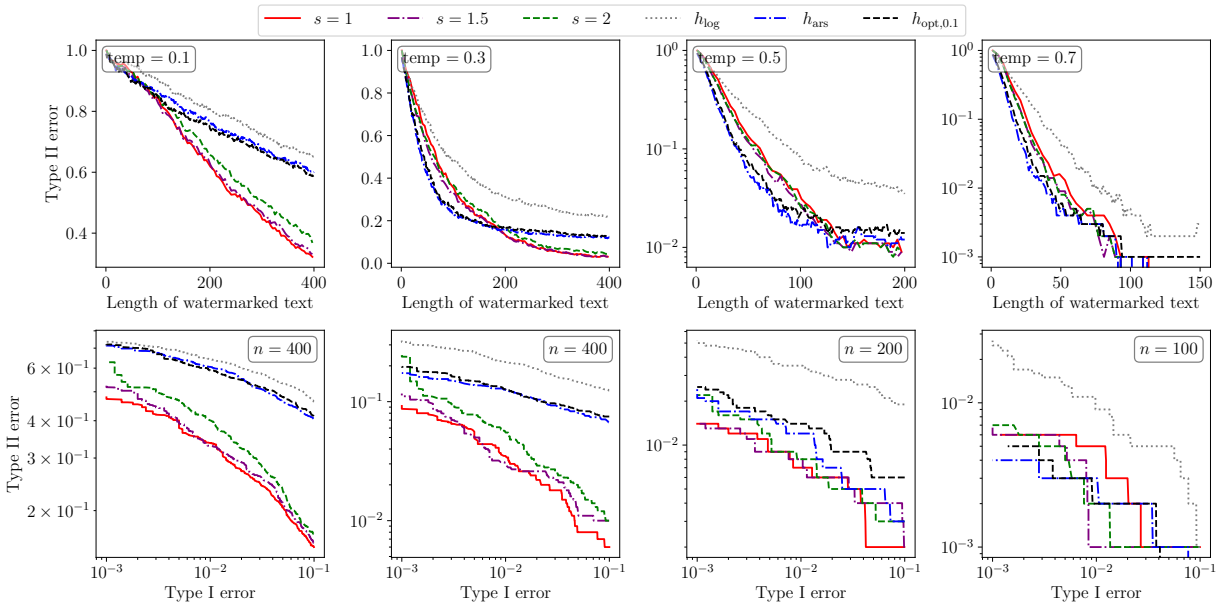


Figure 11: Empirical Type II errors (top row) across different detection rules applied to the Gumbel-max watermark. The bottom row illustrates the trade-off function in the log-log scale for a specific length n . The temperatures used, from left to right columns, are 0.1, 0.3, 0.5, and 0.7, respectively.

Type II error decay. We then examine the decay of Type II errors at a significance level of $\alpha = 0.01$, shown in the top row of Figure 11. The bottom row displays a trade-off function illustrating detection performance across all critical values, extending beyond the fixed $\alpha = 0.01$ case. From left to right, the columns show increasing temperatures from 0.1 to 0.7. We observe that:

- *Tr-GoF excels in the low-temperature region.* When the temperature is relatively low (that is, 0.1, 0.3), the Type II errors for the Tr-GoF test decrease more rapidly and eventually fall below those of all baseline detection rules (when $s \in \{1, 1.5\}$). For instance, at a temperature of 0.1 and using 400 watermarked tokens, the baseline detection methods obtain a Type II

error of approximately 0.6, whereas the best Tr-GoF test exhibits Type II errors around 0.3. Interestingly, although the optimal least-favorable function $h_{\text{opt},0.1}$ performs (slightly) better than h_{ars} , it is still inferior to the Tr-GoF test. The superior performance of the Tr-GoF test is further evidenced by the trade-off functions, where the Tr-GoF test consistently outperforms other methods for nearly all given Type I errors. However, this does not contradict the claimed optimality of h_{opt,Δ_0} in [48]. The reason is that this optimality is defined for the least-favorable case; however, in practice, conditions are not challenging enough for this optimality to play a role.

- *Tr-GoF performs comparably in the high-temperature region.* At relatively high temperatures (that is, 0.5 and 0.7), the Tr-GoF test achieves Type II error decay comparable to the baseline h_{ars} . At a temperature of 0.5, most detection methods reach a Type II error of 0.01 with only 100 watermarked tokens. The trade-off function indicates that the Tr-GoF test maintains a slightly lower trade-off for small Type I errors (>0.001). At a temperature of 0.7, nearly all Type II errors decay to 0.01 with approximately 50 watermarked tokens. This improved detection effectiveness at higher temperatures is due to the increased variability introduced during token generation, which strengthens statistical signals and facilitates watermark detection.

6.3 Robustness Evaluation

Robustness to random edits. We examine three types of edits: random substitution, insertion, and deletion. For each specified edit method and a given fraction, we randomly modify the corresponding fraction of tokens in the watermarked text. We set the Type I error to $\alpha = 0.01$ and investigate how the Type II error changes with the edit fraction across four different temperatures: $\{0.1, 0.3, 0.7, 1\}$. This approach allows us to assess the robustness of watermark detection methods under various text edit conditions and temperature settings. Generally, with a text window of size m , modifying a single token can affect the computation of up to m pseudorandom numbers. Therefore, a window size of m can always withstand an edit fraction of up to $1/m$, as not all watermarked signals are removed. In our experiments, we set $m = 5$.

The results of random edits are shown in Figure 12, with the top, middle, and bottom rows corresponding to random substitution, insertion, and deletion, respectively. Across all edit types, we observe a consistent pattern: any edit increases the Type II error for all detection methods. At lower temperatures, the error rate increases sharply with rising edit fractions, while at higher temperatures, the increase is more gradual, indicating reduced sensitivity to edits.

- *Tr-GoF demonstrates better robustness at lower temperatures.* The Tr-GoF test consistently achieves the lowest Type II error rates across all three edit types at lower temperatures (that is, 0.1, 0.3), outperforming other methods such as $h_{\text{opt},0.1}$ and h_{ars} . This makes it particularly effective when the LLM outputs are more deterministic.
- *Tr-GoF maintains comparable robustness at higher temperatures.* While the Tr-GoF test slightly trails behind h_{ars} at a temperature of 0.7, it remains competitive, with an average difference in Type II error of only 0.02 compared to h_{ars} across different edit fractions. At a temperature of 0.7, $s = 2$ slightly outperforms the others. This suggests that, even in high-temperature scenarios, the Tr-GoF test maintains robust performance and adapts effectively to the impact of temperature on detection difficulty.

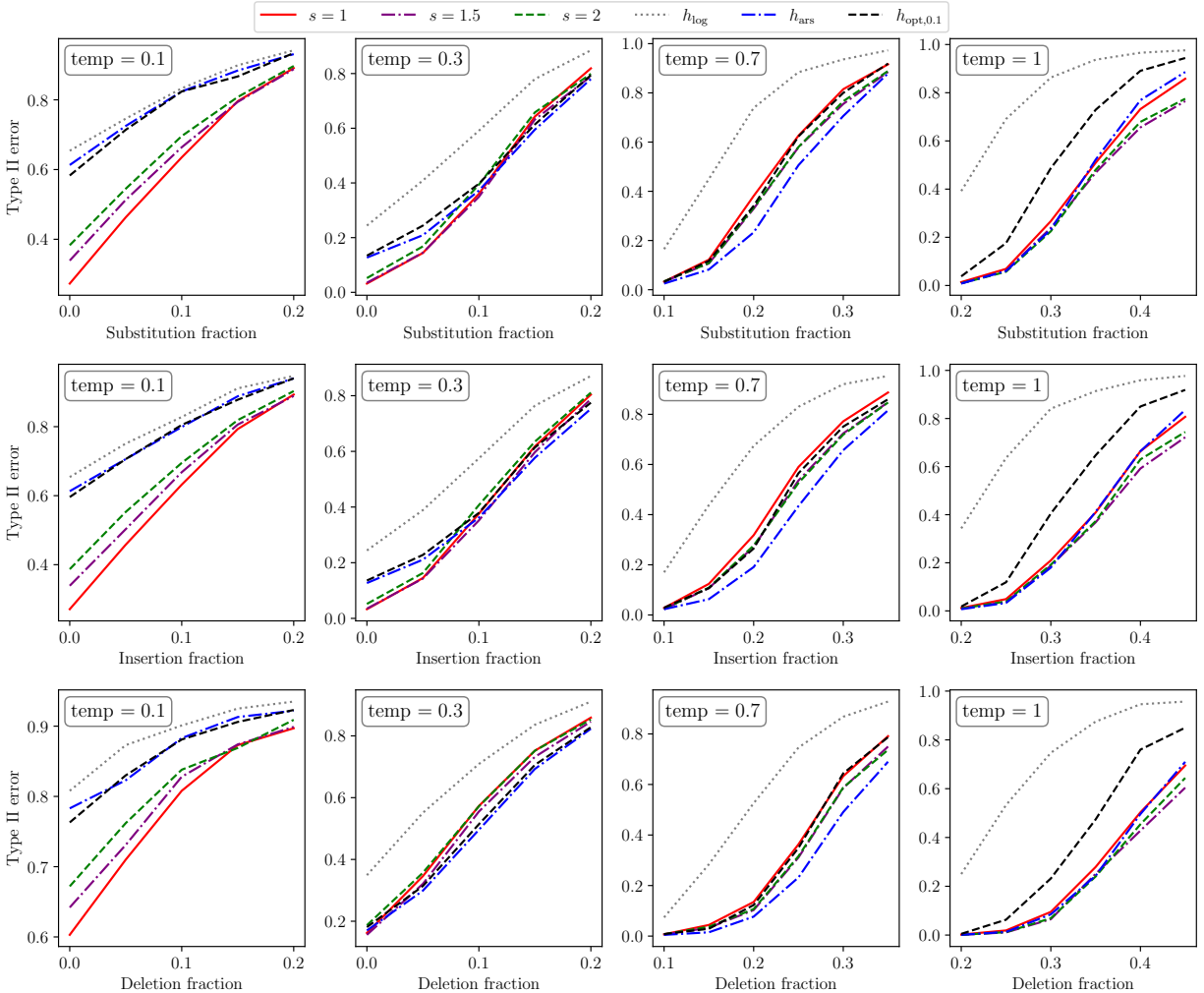


Figure 12: Effect of three random edits on Type II error across different temperatures at a fixed Type I error of $\alpha = 0.01$. The top, middle, and bottom plots correspond to random substitution, insertion, and deletion, respectively.

Edit tolerance limit. We define the edit tolerance limit as the largest fraction of edits that can be applied to a watermarked text with the detection method still rejecting the null hypothesis H_0 . In general, the higher the edit tolerance limit, the more robust the detection method, as it is more sensitive to the weak watermark signal.

We compute the edit tolerance limits for different detection methods across two tasks: (i) poem recitation, where the LLM is asked to recite an existing poem, and (ii) poem generation, where the LLM generates a new poem in the style of a given one. The latter task is more open-ended, leading to more stochastic and regular generation. The results, averaged over 100 popular poems, are reported in Table 1, with the highest values (in percentage) highlighted in bold. Notably, the Tr-GoF test with $s = 2$ consistently achieves the highest edit tolerance across all three edit types and both tasks. These findings align with the results shown in Figure 12. Similar results for the Sheared-LLaMA-2.7B model are provided in Appendix C.3.

Task	Edit types	$s = 1$	$s = 1.5$	$s = 2$	h_{\log}	h_{ars}	$h_{\text{opt},0.3}$	$h_{\text{opt},0.2}$	$h_{\text{opt},0.1}$
Poem Recitation	Substitution	37.16	38.8	39.49	25.04	37.96	27.83	30.04	33.87
	Insertion	42.15	45.25	45.64	26.46	44.12	30.38	33.32	37.78
	Deletion	39.78	41.85	42.67	23.21	41.92	27.08	30.12	33.76
Poem Generation	Substitution	36.89	38.72	38.9	24.71	38.64	27.47	30.04	33.49
	Insertion	40.08	42.52	43.09	25.54	41.65	29.49	32.75	36.28
	Deletion	39.79	41.83	42.42	26.38	40.99	29.59	32.3	35.15

Table 1: The edit tolerance limits (%) for detection methods on the OPT-1.3B model.

Robustness to adversarial edits. In adversarial edits, we assume the human user knows the hash function \mathcal{A} and the secret key Key , allowing them to selectively replace tokens with the strongest watermark signals to evade detection. To approximate this behavior, we use the following procedure: for the LLM-generated response, the user first computes all corresponding pivotal statistics, identifies a given fraction of tokens with the highest pivotal statistics, and replaces them with randomly selected tokens. This targeted replacement is more disruptive than random edits. Results for a 5% replacement are shown in Figure 13, with results for other fractions provided in Appendix C.3.

In this adversarial setting, the Tr-GoF test demonstrates steady robustness, consistently achieving a lower Type II error across most temperature settings. Notably, h_{ars} is less resilient under adversarial edits, while $h_{\text{opt},0.1}$ performs better. This increased robustness in $h_{\text{opt},0.1}$ likely stems from its design through minimax optimization, which enhances its ability to withstand adversarial edits.

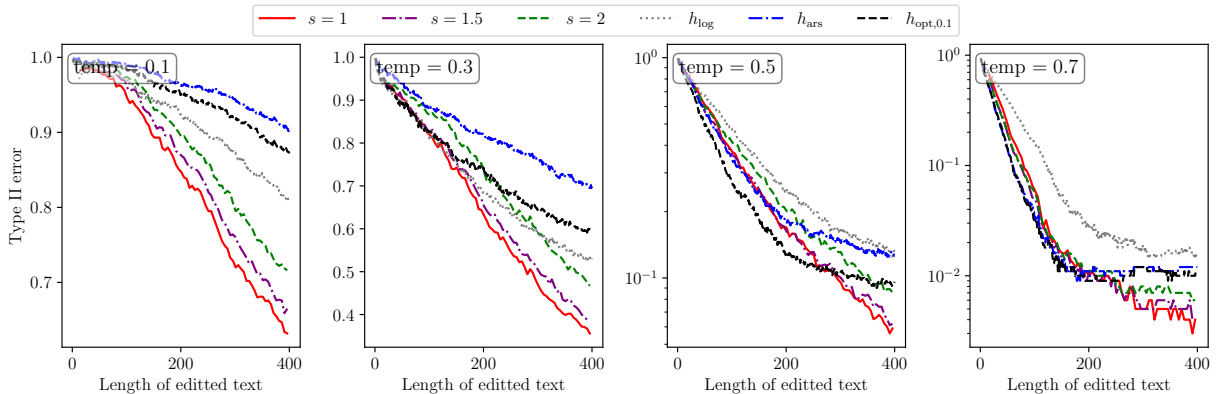


Figure 13: Effect of adversarial edits on Type II error across different temperatures.

Robustness to roundtrip translation. In the roundtrip translation, we cannot control the edit level. By maintaining a fixed significance level of $\alpha = 0.01$, we examine how the Type II error varies with the modified text length and different temperatures. The results are present in Figure 14. Using $n = 200$ tokens, we observe that the final Type II errors decrease as the temperature increases, suggesting that higher temperatures facilitate easier detection. In the low-temperature range, the Tr-GoF test with $s = 1$ consistently outperforms all other detection methods. Conversely, in the high-temperature range, Tr-GoF tests with $s \in \{1, 1.5\}$ achieve comparable or occasionally

superior performance to the previous h_{ars} . These experiments underscore the robust performance and detection efficiency of Tr-GoF for Gumbel-max watermarks.

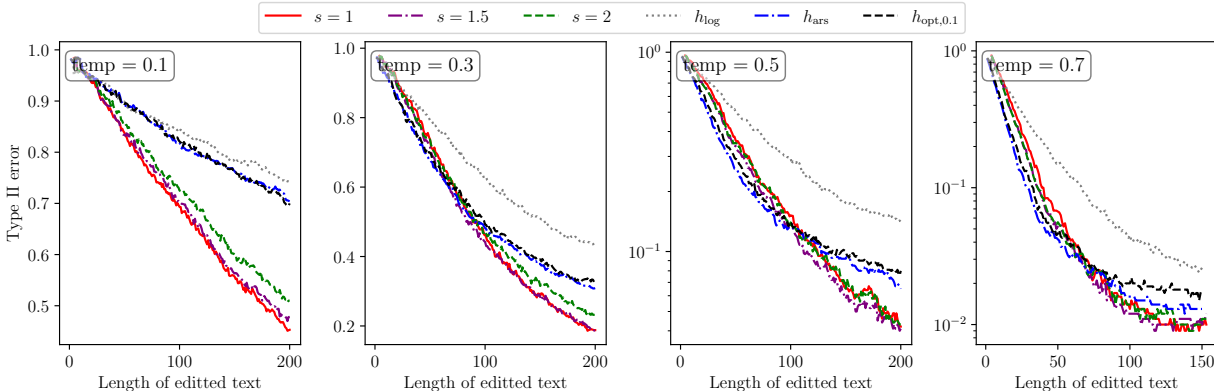


Figure 14: Effect of roundtrip translation on Type II error across different temperatures.

7 Discussion

In this paper, we have developed an adaptive and robust method for detecting watermarks in text generated by LLMs but subsequently edited by humans, along with theoretical guarantees corroborated by numerical experiments. We start by proposing a procedure for modeling the human editing process, which prompts us to formulate this problem as sparse mixture detection. Our method, which we call the Tr-GoF test, is shown to achieve the optimal detection boundary in the regime of increasing edit level and vanishing regularity of NTP distributions under the framework of [48]. In contrast, we show that sum-based detection rules are provably suboptimal in the sense that the detection region is strictly smaller than that of the Tr-GoF test. Additionally, we show that the Tr-GoF test continues to provide high detection efficiency when the edit level and regularity of NTP distributions remain constant. In contrast, sum-based detection rules fail to achieve robustness in either regime due to their inability to adapt to unknown specifics of problem instances.

Our findings open new avenues for the robust detection of LLM watermarks. First, although we focus on the Gumbel-max watermark, which is perhaps the most influential, it would be valuable to investigate robust detection for other watermarking schemes [78], such as the inverse transform watermark [46] and the green-red list watermark [44]. In these cases, the truncation technique underlying Tr-GoF could offer useful insights. More broadly, future research might consider alternative nonparametric testing approaches [56, 14], such as the Kolmogorov–Smirnov test, Pearson’s Chi-square test, and the Khmaladze–Aki statistic [43, 62], which may offer adaptivity comparable to or even surpassing goodness-of-fit tests in certain parameter regimes. Empirical evaluation of these classical nonparametric methods could motivate the development of new procedures tailored to specific challenges, such as high-temperature regimes, where Tr-GoF may undergo a decline in detection power. Additionally, detection power could be enhanced by incorporating spatial information from watermark signals, as human edits often form clusters within text. From a theoretical standpoint, it is noteworthy that the optimal detection boundary $q + 2p = 1$ is achieved through pivotal statistics, suggesting that investigating an information-theoretic detection boundary could yield interesting insights. Lastly, for interpretive purposes, estimating the watermark fraction may offer insights into

the degree of human contribution in content generated collaboratively by LLMs and humans.

Acknowledgments

This work was supported in part by NIH grants, RF1AG063481 and U01CA274576, NSF DMS-2310679, a Meta Faculty Research Award, and Wharton AI for Business. The content is solely the responsibility of the authors and does not necessarily represent the official views of the NIH.

References

- [1] Scott Aaronson. Watermarking of large language models, August 2023. URL <https://simons.berkeley.edu/talks/scott-aaronson-ut-austin-openai-2023-08-17>.
- [2] Josh Achiam, Steven Adler, Sandhini Agarwal, Lama Ahmad, Ilge Akkaya, Florencia Leoni Aleman, Diogo Almeida, Janko Altschmidt, Sam Altman, Shyamal Anadkat, et al. GPT-4 technical report. *arXiv preprint arXiv:2303.08774*, 2023.
- [3] David H Ackley, Geoffrey E Hinton, and Terrence J Sejnowski. A learning algorithm for Boltzmann machines. *Cognitive science*, 9(1):147–169, 1985.
- [4] Ery Arias-Castro and Meng Wang. Distribution-free tests for sparse heterogeneous mixtures. *Test*, 26:71–94, 2017.
- [5] Boaz Barak. An intensive introduction to cryptography, lectures notes for Harvard CS 127. <https://intensecrypto.org/public/index.html>, Fall 2021.
- [6] AA Borokov and NM Sycheva. On asymptotically optimal non-parametric criteria. *Theory of Probability & Its Applications*, 13(3):359–393, 1968.
- [7] Aleksandr A Borovkov. Boundary-value problems for random walks and large deviations in function spaces. *Theory of Probability & Its Applications*, 12(4):575–595, 1967.
- [8] Tom Brown, Benjamin Mann, Nick Ryder, Melanie Subbiah, Jared D Kaplan, Prafulla Dhariwal, Arvind Neelakantan, Pranav Shyam, Girish Sastry, Amanda Askell, et al. Language models are few-shot learners. In *Advances in Neural Information Processing Systems*, volume 33, pages 1877–1901, 2020.
- [9] T Tony Cai and Yihong Wu. Optimal detection of sparse mixtures against a given null distribution. *IEEE Transactions on Information Theory*, 60(4):2217–2232, 2014.
- [10] T Tony Cai, X Jessie Jeng, and Jiashun Jin. Optimal detection of heterogeneous and heteroscedastic mixtures. *Journal of the Royal Statistical Society Series B: Statistical Methodology*, 73(5):629–662, 2011.
- [11] Zhongze Cai, Shang Liu, Hanzhao Wang, Huaiyang Zhong, and Xiaocheng Li. Towards better statistical understanding of watermarking LLMs. *arXiv preprint arXiv:2403.13027*, 2024.
- [12] Miranda Christ and Sam Gunn. Pseudorandom error-correcting codes. In *Annual International Cryptology Conference*, pages 325–347. Springer, 2024.

- [13] Miranda Christ, Sam Gunn, and Or Zamir. Undetectable watermarks for language models. In *Conference on Learning Theory*, pages 1125–1139. PMLR, 2024.
- [14] Ralph B D’Agostino. *Goodness-of-fit-techniques*. Routledge, 2017.
- [15] Debarati Das, Karin De Langis, Anna Martin, Jaehyung Kim, Minhwa Lee, Zae Myung Kim, Shirley Hayati, Risako Owan, Bin Hu, Ritik Parkar, et al. Under the surface: Tracking the artifactuality of LLM-generated data. *arXiv preprint arXiv:2401.14698*, 2024.
- [16] Sumanth Dathathri, Abigail See, Sumedh Ghaisas, Po-Sen Huang, Rob McAdam, Johannes Welbl, Vandana Bachani, Alex Kaskasoli, Robert Stanforth, Tatiana Matejovicova, Jamie Hayes, Nidhi Vyas, Majd Al Merey, Jonah Brown-Cohen, Rudy Bunel, Borja Balle, Taylan Cemgil, Zahra Ahmed, Kitty Stacpoole, Ilia Shumailov, Ciprian Baetu, Sven Gowal, Demis Hassabis, and Pushmeet Kohli. Scalable watermarking for identifying large language model outputs. *Nature*, 634(8035):818–823, Oct 2024. URL <https://doi.org/10.1038/s41586-024-08025-4>.
- [17] Ilias Diakonikolas and Daniel M Kane. *Algorithmic high-dimensional robust statistics*. Cambridge university press, 2023.
- [18] RL Dobrusin. A statistical problem arising in the theory of detection of signals in the presence of noise in a multi-channel system and leading to stable distribution laws. *Theory of Probability & Its Applications*, 3(2):161–173, 1958.
- [19] David Donoho and Jiashun Jin. Higher criticism for detecting sparse heterogeneous mixtures. *The Annals of Statistics*, 32(3):962–994, 2004.
- [20] David Donoho and Jiashun Jin. Higher criticism for large-scale inference, especially for rare and weak effects. *Statistical science*, 30(1):1–25, 2015.
- [21] Nature editorial. AI watermarking must be watertight to be effective. *Nature*, 634:753, 2024. URL <https://www.nature.com/articles/d41586-024-03418-x>.
- [22] M. R. Farhangdoost and M. Kargar Dolatabadi. New inequalities for Gamma and Digamma functions. *Journal of Applied Mathematics*, 2014, 2014.
- [23] Pierre Fernandez, Antoine Chaffin, Karim Tit, Vivien Chappelier, and Teddy Furon. Three bricks to consolidate watermarks for large language models. *arXiv preprint arXiv:2308.00113*, 2023.
- [24] Jiayi Fu, Xuandong Zhao, Ruihan Yang, Yuansen Zhang, Jiangjie Chen, and Yanghua Xiao. GumbelSoft: Diversified language model watermarking via the GumbelMax-trick. *arXiv preprint arXiv:2402.12948*, 2024.
- [25] Eva Giboulot and Furon Teddy. WaterMax: Breaking the LLM watermark detectability-robustness-quality trade-off. *arXiv preprint arXiv:2403.04808*, 2024.
- [26] Noah Golowich and Ankur Moitra. Edit distance robust watermarks for language models. *arXiv preprint arXiv:2406.02633*, 2024.

- [27] Veronika Gontcharuk, Sandra Landwehr, and Helmut Finner. The intermediates take it all: Asymptotics of higher criticism statistics and a powerful alternative based on equal local levels. *Biometrical Journal*, 57(1):159–180, 2015.
- [28] Emil Julius Gumbel. *Statistical theory of extreme values and some practical applications: A series of lectures*, volume 33. US Government Printing Office, 1948.
- [29] Peter Hall and Jiashun Jin. Properties of higher criticism under strong dependence. *The Annals of Statistics*, pages 381–402, 2008.
- [30] Peter Hall and Jiashun Jin. Innovated higher criticism for detecting sparse signals in correlated noise. *The Annals of Statistics*, 38(3):1686–1732, 2010.
- [31] Jean-Baptiste Hiriart-Urruty and Claude Lemaréchal. *Convex analysis and minimization algorithms I: Fundamentals*, volume 305. Springer science & business media, 1996.
- [32] Abe Hou, Jingyu Zhang, Tianxing He, Yichen Wang, Yung-Sung Chuang, Hongwei Wang, Lingfeng Shen, Benjamin Van Durme, Daniel Khashabi, and Yulia Tsvetkov. SemStamp: A semantic watermark with paraphrastic robustness for text generation. In *North American Chapter of the Association for Computational Linguistics: Human Language Technologies*, volume 1, pages 4067–4082, 2024.
- [33] Zhengmian Hu, Lichang Chen, Xidong Wu, Yihan Wu, Hongyang Zhang, and Heng Huang. Unbiased watermark for large language models. In *International Conference on Learning Representations*, 2024. URL <https://openreview.net/forum?id=uWVC5FVidc>.
- [34] Baihe Huang, Hanlin Zhu, Banghua Zhu, Kannan Ramchandran, Michael I Jordan, Jason D Lee, and Jiantao Jiao. Towards optimal statistical watermarking. *arXiv preprint arXiv:2312.07930*, 2023.
- [35] Peter J Huber. Robust estimation of a location parameter. In *Breakthroughs in statistics: Methodology and distribution*, pages 492–518. Springer, 1992.
- [36] Peter J Huber and Elvezio M Ronchetti. *Robust statistics*. John Wiley & Sons, 2011.
- [37] Yuri I Ingster. Some problems of hypothesis testing leading to infinitely divisible distributions. *Mathematical Methods of Statistics*, 6(1):47–69, 1997.
- [38] Leah Jager and Jon A Wellner. Goodness-of-fit tests via phi-divergences. *Annals of Statistics*, 35(5):2018–2053, 2007.
- [39] Eric Jang, Shixiang Gu, and Ben Poole. Categorical reparameterization with Gumbel-Softmax. In *International Conference on Learning Representations*, 2016.
- [40] Jiashun Jin and Zheng Tracy Ke. Rare and weak effects in large-scale inference: Methods and phase diagrams. *Statistica Sinica*, pages 1–34, 2016.
- [41] Jiashun Jin, Zheng Tracy Ke, and Shengming Luo. Optimal adaptivity of signed-polygon statistics for network testing. *The Annals of Statistics*, 49(6):3408–3433, 2021.

- [42] Tracy Ke, Jiashun Jin, and Jianqing Fan. Covariance assisted screening and estimation. *Annals of statistics*, 42(6):2202, 2014.
- [43] Estate V Khmaladze. Martingale approach in the theory of goodness-of-fit tests. *Theory of Probability & Its Applications*, 26(2):240–257, 1982.
- [44] John Kirchenbauer, Jonas Geiping, Yuxin Wen, Jonathan Katz, Ian Miers, and Tom Goldstein. A watermark for large language models. In *International Conference on Machine Learning*, volume 202, pages 17061–17084, 2023.
- [45] John Kirchenbauer, Jonas Geiping, Yuxin Wen, Manli Shu, Khalid Saifullah, Kezhi Kong, Kasun Fernando, Aniruddha Saha, Micah Goldblum, and Tom Goldstein. On the reliability of watermarks for large language models. In *International Conference on Learning Representations*, 2024. URL <https://openreview.net/forum?id=DEJIDCmW0z>.
- [46] Rohith Kuditipudi, John Thickstun, Tatsunori Hashimoto, and Percy Liang. Robust distortion-free watermarks for language models. *Transactions on Machine Learning Research*, 2024. ISSN 2835-8856. URL <https://openreview.net/forum?id=FpaCL1M02C>.
- [47] Jian Li and David Siegmund. Higher criticism: p-values and criticism. *The Annals of Statistics*, 43(3):1323–1350, 2015.
- [48] Xiang Li, Feng Ruan, Huiyuan Wang, Qi Long, and Weijie J. Su. A statistical framework of watermarks for large language models: Pivot, detection efficiency and optimal rules. *The Annals of Statistics (to appear)*, 2024.
- [49] Aiwei Liu, Leyi Pan, Xuming Hu, Shiao Meng, and Lijie Wen. A semantic invariant robust watermark for large language models. In *International Conference on Learning Representations*, 2024. URL <https://openreview.net/forum?id=6p8lpe4MNf>.
- [50] Yepeng Liu and Yuheng Bu. Adaptive text watermark for large language models. In *International Conference on Machine Learning*, 2024. URL <https://openreview.net/forum?id=7emOSb5UfX>.
- [51] Chris J Maddison, Daniel Tarlow, and Tom Minka. A* sampling. In *Advances in Neural Information Processing Systems*, volume 27, 2014.
- [52] Sean P Meyn and Richard L Tweedie. *Markov chains and stochastic stability*. Springer Science & Business Media, 2012.
- [53] Silvia Milano, Joshua A McGrane, and Sabina Leonelli. Large language models challenge the future of higher education. *Nature Machine Intelligence*, 5(4):333–334, 2023.
- [54] George A Miller. WordNet: A lexical database for English. *Communications of the ACM*, 38(11):39–41, 1995.
- [55] Amit Moscovich. Fast calculation of p-values for one-sided Kolmogorov-Smirnov type statistics. *Computational Statistics & Data Analysis*, 185:107769, 2023.
- [56] ÍÀkov ÍÛr’evich Nikitin. *Asymptotic efficiency of nonparametric tests*. Cambridge University Press, 1995.

- [57] Ya Yu Nikitin. Hodges-Lehmann asymptotic efficiency of the Kolmogorov and Smirnov goodness-of-fit tests. *Journal of Soviet Mathematics*, 36:517–520, 1987.
- [58] OpenAI. ChatGPT: Optimizing language models for dialogue, Jan 2023. URL <http://web.archive.org/web/20230109000707/https://openai.com/blog/chatgpt/>.
- [59] OpenAI. Understanding the source of what we see and hear online, May 2024. URL <https://https://openai.com/index/understanding-the-source-of-what-we-see-and-hear-online/>.
- [60] George Papandreou and Alan L Yuille. Perturb-and-map random fields: Using discrete optimization to learn and sample from energy models. In *International Conference on Computer Vision*, pages 193–200. IEEE, 2011.
- [61] Julien Piet, Chawin Sitawarin, Vivian Fang, Norman Mu, and David Wagner. Mark my words: Analyzing and evaluating language model watermarks. *arXiv preprint arXiv:2312.00273*, 2023.
- [62] OA Podkorytova. Large deviations and bahadur efficiency of the Khmaladze-Aki statistic. *Journal of Mathematical Sciences*, 68:560–565, 1994.
- [63] Alec Radford, Jeffrey Wu, Rewon Child, David Luan, Dario Amodei, Ilya Sutskever, et al. Language models are unsupervised multitask learners. *OpenAI blog*, 1(8):9, 2019.
- [64] Alec Radford, Jong Wook Kim, Tao Xu, Greg Brockman, Christine McLeavey, and Ilya Sutskever. Robust speech recognition via large-scale weak supervision. In *International Conference on Machine Learning*, pages 28492–28518. PMLR, 2023.
- [65] Colin Raffel, Noam Shazeer, Adam Roberts, Katherine Lee, Sharan Narang, Michael Matena, Yanqi Zhou, Wei Li, and Peter J Liu. Exploring the limits of transfer learning with a unified text-to-text transformer. *Journal of Machine Learning Research*, 21(1):5485–5551, 2020.
- [66] C Radhakrishna Rao. Efficient estimates and optimum inference procedures in large samples. *Journal of the Royal Statistical Society: Series B (Methodological)*, 24(1):46–63, 1962.
- [67] Jie Ren, Han Xu, Yiding Liu, Yingqian Cui, Shuaiqiang Wang, Dawei Yin, and Jiliang Tang. A robust semantics-based watermark for large language model against paraphrasing. In *Findings of the Association for Computational Linguistics*, pages 613–625, 2024.
- [68] Bruce Schneier. *Applied Cryptography*. John Wiley & Sons, 1996.
- [69] Ilia Shumailov, Zakhar Shumaylov, Yiren Zhao, Yarin Gal, Nicolas Papernot, and Ross Anderson. The curse of recursion: Training on generated data makes models forget. *arXiv preprint arXiv:2305.17493*, 2023.
- [70] Kate Starbird. Disinformation’s spread: Bots, trolls and all of us. *Nature*, 571(7766):449–450, 2019.
- [71] C Stokel-Walker. AI bot ChatGPT writes smart essays—Should professors worry? *Nature News*, 2022.

- [72] Hugo Touvron, Thibaut Lavril, Gautier Izacard, Xavier Martinet, Marie-Anne Lachaux, Timothée Lacroix, Baptiste Rozière, Naman Goyal, Eric Hambro, Faisal Azhar, et al. LLaMA: Open and efficient foundation language models. *arXiv preprint arXiv:2302.13971*, 2023.
- [73] Ashish Vaswani, Noam Shazeer, Niki Parmar, Jakob Uszkoreit, Llion Jones, Aidan N Gomez, Łukasz Kaiser, and Illia Polosukhin. Attention is all you need. In *Advances in Neural Information Processing Systems*, volume 30, 2017.
- [74] Laura Weidinger, John Mellor, Maribeth Rauh, Conor Griffin, Jonathan Uesato, Po-Sen Huang, Myra Cheng, Mia Glaese, Borja Balle, Atoosa Kasirzadeh, et al. Ethical and social risks of harm from language models. *arXiv preprint arXiv:2112.04359*, 2021.
- [75] Jon A Wellner and Vladimir Koltchinskii. A note on the asymptotic distribution of Berk—Jones type statistics under the null hypothesis. In *High Dimensional Probability III*, pages 321–332. Springer, 2003.
- [76] Yihan Wu, Zhengmian Hu, Hongyang Zhang, and Heng Huang. DiPmark: A stealthy, efficient and resilient watermark for large language models. *arXiv preprint arXiv:2310.07710*, 2023.
- [77] Mengzhou Xia, Tianyu Gao, Zhiyuan Zeng, and Danqi Chen. Sheared LLaMA: Accelerating language model pre-training via structured pruning. In *International Conference on Learning Representations*, 2023.
- [78] Yangxinyu Xie, Xiang Li, Tanwi Mallick, Weijie J. Su, and Ruixun Zhang. Debiasing watermarks for large language models via maximal coupling. *arXiv preprint arXiv:2411.11203*, 2024.
- [79] KiYoon Yoo, Wonhyuk Ahn, Jiho Jang, and Nojun Kwak. Robust multi-bit natural language watermarking through invariant features. In *Annual Meeting Of The Association For Computational Linguistics*, 2023.
- [80] Rowan Zellers, Ari Holtzman, Hannah Rashkin, Yonatan Bisk, Ali Farhadi, Franziska Roesner, and Yejin Choi. Defending against neural fake news. In *Advances in Neural Information Processing Systems*, volume 32, 2019.
- [81] Susan Zhang, Stephen Roller, Naman Goyal, Mikel Artetxe, Moya Chen, Shuohui Chen, Christopher Dewan, Mona Diab, Xian Li, Xi Victoria Lin, et al. OPT: Open pre-trained transformer language models. *arXiv preprint arXiv:2205.01068*, 2022.
- [82] Xuandong Zhao, Prabhanjan Vijendra Ananth, Lei Li, and Yu-Xiang Wang. Provable robust watermarking for AI-generated text. In *International Conference on Learning Representations*, 2024. URL <https://openreview.net/forum?id=SsmT8a045L>.
- [83] Xuandong Zhao, Lei Li, and Yu-Xiang Wang. Permute-and-Flip: An optimally robust and watermarkable decoder for LLMs. *arXiv preprint arXiv:2402.05864*, 2024.
- [84] Chaoyi Zhu, Jeroen Galjaard, Pin-Yu Chen, and Lydia Y Chen. Duwak: Dual watermarks in large language models. In *Findings of the Association for Computational Linguistics*, 2024.
- [85] George Kingsley Zipf. *Human behavior and the principle of least effort: An introduction to human ecology*. Ravenio books, 2016.

A Proof for Theoretical Guarantees

Notations. We establish some conventions for the proofs in the appendix. For simplicity, we denote $\mathbb{E}_{1, \mathbf{P}_t}[\cdot] = \mathbb{E}_{Y \sim \mu_{1, \mathbf{P}_t}}[\cdot]$ and $\mathbb{E}_0[\cdot] = \mathbb{E}_{Y \sim \mu_0}[\cdot]$. When using $\mathbb{E}_1[\cdot \mid \mathcal{F}_t]$, we assume Y_t follows the alternative hypothesis and take the expectation conditioned on the filtration \mathcal{F}_t . When the context is clear, we will omit subscripts—for example, we will use $\mathbb{E}[\eta_t]$ to denote its expectation (or the head probability, given that η_t is a binary variable). When the context is unclear, we will explicitly specify which variable the expectation is taken with respect to. PDF stands for probability density function, and CDF stands for cumulative distribution function. All of the following is based on the assumption that the user modifies the watermarked text following Procedure 1.

A.1 Derivation of the Alternative Distribution of $Y_t \mid (\mathbf{P}_t, \eta_t)$

Motivation for the mixture detection. First, we explain why the (conditional) distribution of Y_t is either μ_0 or μ_{1, \mathbf{P}_t} where \mathbf{P}_t is the NTP distribution for w_t . Following the framework [48], the pivotal statistic $Y_t := Y(w_t, \zeta_t)$ is a deterministic function of each (edited) token w_t and its associated pseudorandom variable $\zeta_t = \mathcal{A}(w_{(t-m):(t-1)}, \text{Key})$. Recall that the user edits the watermarked text following Procedure 1.

Case A If the human edit does not alter a consecutive segment of $(m + 1)$ tokens—specifically, if $w_{(t-m):t} = \tilde{w}_{(\tilde{t}-m):\tilde{t}}$ for some t and \tilde{t} —the value of $\tilde{Y}_{\tilde{t}} := Y(\tilde{w}_{\tilde{t}}, \tilde{\zeta}_{\tilde{t}})$ is preserved in the sequence $Y_{1:n}$ through the relation $Y_t = Y(w_t, \zeta_t) = Y(\tilde{w}_{\tilde{t}}, \tilde{\zeta}_{\tilde{t}}) = \tilde{Y}_{\tilde{t}}$. In this case, the watermark signal in $(\tilde{w}_{\tilde{t}}, \tilde{\zeta}_{\tilde{t}})$ is maintained in the tuple (w_t, ζ_t) , so that $Y_t \mid \tilde{\mathbf{P}}_t = \tilde{Y}_{\tilde{t}} \mid \tilde{\mathbf{P}}_t \sim \mu_{1, \tilde{\mathbf{P}}_t} = \mu_{1, \mathbf{P}_t}$. The last equality holds because $\mathbf{P}_t = \tilde{\mathbf{P}}_t$, which is the NTP distribution that generates $\tilde{w}_{\tilde{t}}$ or, equivalently, w_t .

On the contrary, if the human edit breaks the dependence between w_t and ζ_t such that ζ_t is no longer the correct pseudorandom variable that generated w_t , we argue that w_t and ζ_t must be statistically independent. There are two cases to consider:

Case B If the token w_t is human-generated (either via substitution or insertion), we all have $w_t = \mathcal{S}(\mathbf{P}_t^h, \zeta_t^h)$ where \mathbf{P}_t^h is the human NTP distribution that depends on $w_{1:(t-1)}$ and $\tilde{w}_{1:(\tilde{t}-1)}$, and ζ_t^h is the true randomness driving the user’s generation. In this case, since the user has no knowledge of the watermarking process, ζ_t^h is independent with ζ_t (according to the Working Hypothesis 2.2 in [48]) so that w_t and ζ_t are independent when \mathbf{P}_t^h is given.

Case C If the token w_t is watermarked, then ζ_t must have been edited. In this scenario, we must have $w_t = \mathcal{S}(\tilde{\mathbf{P}}_{\tilde{t}}, \tilde{\zeta}_{\tilde{t}})$ for some \tilde{t} , and ζ_t is a newly computed pseudorandom variable that differs from $\tilde{\zeta}_{\tilde{t}}$ (since if $\zeta_t = \tilde{\zeta}_{\tilde{t}}$, the watermark signal would be preserved). Due to the sensitive nature of pseudorandom hash functions \mathcal{A} , we know that w_t and ζ_t are independent when $\tilde{\mathbf{P}}_{\tilde{t}}$ is given.

By the definition of pivotal statistics (see Figure 15), in both cases, we have $Y_t = Y(w_t, \zeta_t) \sim \mu_0$.

In summary, if the human edit does not alter the preceding m tokens, including and before w_t , we have $w_t = \mathcal{S}(\mathbf{P}_t, \zeta_t)$ for some NTP distribution \mathbf{P}_t , and $Y_t := Y(w_t, \zeta_t) \sim \mu_{1, \mathbf{P}_t}$, following the alternative distribution. Conversely, if the human edit breaks this dependence, such that

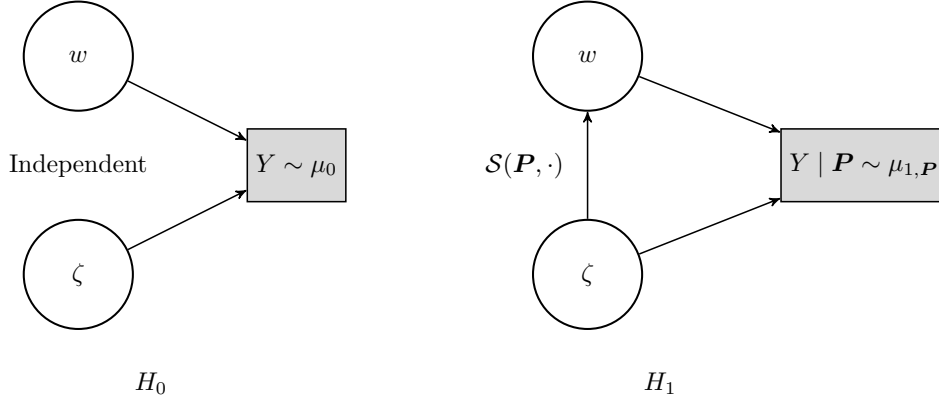


Figure 15: An illustrative diagram showcasing the distributional difference of the pivotal statistic Y . We always have $\zeta \sim \pi$. Once $w \perp \zeta$, we have $Y(w, \zeta) \sim \mu_0$, regardless of the distribution of w . For a fixed \mathbf{P} , $Y(w, \zeta) \sim \mu_{1,\mathbf{P}}$ as long as the decoder mapping $w = \mathcal{S}(\mathbf{P}, \zeta)$ holds.

$w_t \neq \mathcal{S}(\mathbf{P}_t, \zeta_t)$, then $Y_t := Y(w_t, \zeta_t) \sim \mu_0$, regardless of the distribution of w_t . Therefore, the robust watermark detection is cast as the following hypothesis testing problem:

$$H_0 : Y_t \sim \mu_0, \text{ i.i.d. } \forall 1 \leq t \leq n \quad \text{versus} \quad H_1^{\text{mix}} : Y_t | (\mathbf{P}_t, \eta_t) \sim (1 - \eta_t)\mu_0 + \eta_t\mu_{1,\mathbf{P}_t}, \quad \forall 1 \leq t \leq n, \quad (5)$$

where $\{\eta_t\}_{t=1}^n \subset \{0, 1\}$ is a binary random process indicating whether the distribution of Y_t has changed.

Equivalent form of the pivotal statistic. After introducing the binary process η_t , the pivotal statistic $Y_t = Y(w_t, \zeta_t)$ can equivalently be expressed as:

$$Y_t = \eta_t \cdot Y(\mathcal{S}(\mathbf{P}_t, \zeta_t), \zeta_t) + (1 - \eta_t) \cdot Y(\mathcal{S}(\mathbf{P}'_t, \zeta'_t), \zeta_t), \quad (13)$$

where \mathbf{P}_t represents the watermarked NTP distribution when the watermark signal is preserved (that is, $\eta_t = 1$), and $(\mathbf{P}'_t, \zeta'_t)$ is the variables that generate w_t when the watermark signal is broken (that is, $\eta_t = 0$). Based on the discussion in Section 3.1, we have $(\mathbf{P}_t, \zeta_t) = (\tilde{\mathbf{P}}_t, \tilde{\zeta}_t)$ in Case A, $(\mathbf{P}'_t, \zeta'_t) = (\mathbf{P}_t^h, \zeta_t^h)$ in Case B, and $(\tilde{\mathbf{P}}_t, \tilde{\zeta}_t)$ in Case C. Here, $Y(\mathcal{S}(\mathbf{P}_t, \zeta_t), \zeta_t)$ and $Y(\mathcal{S}(\mathbf{P}'_t, \zeta'_t), \zeta_t)$ should be interpreted as *potential outcomes*, as in practice, only one of them is realized depending on the value of η_t . The expression in (13) simplifies the theoretical analysis, as it unifies all the cases that need to be considered. In the subsequent theoretical analysis, we do not distinguish between Case A, Case B, or Case C and will proceed with the proof through variables $\zeta_t, \zeta'_t, \mathbf{P}_t, \mathbf{P}'_t$ and η_t .

Distribution analysis. Assumption 4.1 allows us to establish some intermediate results for $\zeta_t, \zeta'_t, \mathbf{P}_t, \mathbf{P}'_t$, and η_t , which helps us to derive the conditional distribution of $Y_t | (\mathbf{P}_t, \eta_t)$.

Lemma A.1. *Under Assumption 4.1, it follows that for any t ,*

- $\zeta_t \perp \zeta'_t | \{\mathcal{F}_{t-1}, \eta_t = 0\}$ and $\mathbf{P}_t, \mathbf{P}'_t \in \mathcal{F}_{t-1}$.
- $Y(\mathcal{S}(\mathbf{P}_t, \zeta_t), \zeta_t) | \{\mathcal{F}_{t-1}, \eta_t = 1\} \sim \mu_{1,\mathbf{P}_t}$ and $Y(\mathcal{S}(\mathbf{P}'_t, \zeta'_t), \zeta_t) | \{\mathcal{F}_{t-1}, \eta_t = 0\} \sim \mu_0$.

Proof of Lemma A.1. Recall that \tilde{t} is the largest value of t_0 at which Algorithm 1 remains in iteration t to select a token for w_t . Therefore, $\tilde{w}_{\tilde{t}}$ will not be deleted in the iteration t (otherwise \tilde{t} is not the largest value of t_0). If no edit is made, we have $w_t = \tilde{w}_{\tilde{t}} = \mathcal{S}(\tilde{\mathbf{P}}_{\tilde{t}}, \tilde{\zeta}_{\tilde{t}})$. By our notation, this implies $\mathbf{P}_t = \tilde{\mathbf{P}}_{\tilde{t}}$. On the other hand, if an edit occurs (either substitution or insertion), then w_t is generated by the user, meaning $w_t = \mathcal{S}(\mathbf{P}_t^h, \zeta_t^h)$ with \mathbf{P}_t^h depending on $w_{1:(t-1)}$ and $\tilde{w}_{1:(\tilde{t}-1)}$. Here we use the fact that $\tilde{t} = t_0$ must hold if we do not delete token $\tilde{w}_{\tilde{t}}$ (see Figure 5 for an example). From the discussion following (13), we know that $\{\mathbf{P}_t, \mathbf{P}'_t\} \subseteq \{\mathbf{P}_t^h, \tilde{\mathbf{P}}_{\tilde{t}}\}$ and $\zeta'_t \in \{\zeta_t^h, \tilde{\zeta}_{\tilde{t}}\}$.

For the first point, when $\eta_t = 0$, the watermark signal has been removed and thus we must have $\zeta_t \neq \tilde{\zeta}_{\tilde{t}}$, so the set $\{\tilde{\zeta}_{\tilde{t}}, \zeta_t^h, \zeta_t\}$ contains three distinct random variables. Regardless of whether $\zeta'_t \in \{\zeta_t^h, \tilde{\zeta}_{\tilde{t}}\}$, the perfect (pseudo)randomness condition ensures that ζ_t is independent of ζ'_t conditioning on $\{\mathcal{F}_{t-1}, \eta_t = 0\}$. We complete the proof by noting that $\mathbf{P}_t^h \in \sigma(w_{1:(t-1)}, \tilde{w}_{1:(\tilde{t}-1)}) \subset \mathcal{F}_{t-1}$ and $\tilde{\mathbf{P}}_{\tilde{t}} = \text{LLM}(\tilde{w}_{1:(\tilde{t}-1)}) \in \mathcal{F}_{t-1}$. For the second point, it follows by applying the first point with the definition of pivotal statistics (see Section 2). \square

Lemma A.2. *Under Assumption 4.1, it follows that*

$$Y_t \mid (\mathcal{F}_{t-1}, \eta_t) \stackrel{d}{=} Y_t \mid (\mathbf{P}_t, \eta_t) \sim (1 - \eta_t)\mu_0 + \eta_t\mu_{1, \mathbf{P}_t}.$$

Proof of Lemma A.2. For any measurable set A , it follows that

$$\begin{aligned} \mathbb{P}_1(Y_t \in A \mid \mathcal{F}_{t-1}, \eta_t) &\stackrel{(a)}{=} \eta_t \cdot \mathbb{P}_1(Y(\mathcal{S}(\mathbf{P}_t, \zeta_t), \zeta_t) \in A \mid \mathcal{F}_{t-1}, \eta_t = 1) \\ &\quad + (1 - \eta_t) \cdot \mathbb{P}_1(Y(\mathcal{S}(\mathbf{P}'_t, \zeta'_t), \zeta_t) \in A \mid \mathcal{F}_{t-1}, \eta_t = 0) \\ &\stackrel{(b)}{=} \eta_t \cdot \mathbb{P}_1(Y(\mathcal{S}(\mathbf{P}_t, \zeta_t), \zeta_t) \in A \mid \mathcal{F}_{t-1}) \\ &\quad + (1 - \eta_t) \cdot \mathbb{P}_1(Y(\mathcal{S}(\mathbf{P}'_t, \zeta'_t), \zeta_t) \in A \mid \mathcal{F}_{t-1}, \eta_t = 0) \\ &\stackrel{(c)}{=} (1 - \eta_t)\mu_0(A) + \eta_t\mu_{1, \mathbf{P}_t}(A), \end{aligned}$$

where (a) uses (13), (b) uses $\zeta_t \perp \eta_t \mid \mathcal{F}_{t-1}$, and (c) follows from Lemma A.1. Note that $\mathbb{P}_1(Y_t \in A \mid \mathcal{F}_{t-1}, \eta_t)$ is a measurable function of \mathbf{P}_t (which $\in \mathcal{F}_{t-1}$) and η_t so that $\mathbb{P}_1(Y_t \in A \mid \mathbf{P}_t, \eta_t) = \mathbb{P}_1(Y_t \in A \mid \mathcal{F}_{t-1}, \eta_t)$ which completes the proof. \square

A.2 Proof of Theorem 4.1

Detectability is essentially determined by whether the Hellinger distance between the joint distribution of $Y_{1:n}$ under H_0 and H_1^{mix} approaches 1 as n goes to infinity. It is important to note that due to the autoregressive generation structure (as shown in Figure 4), the joint distribution of $Y_{1:n}$ is not $\prod_{t=1}^n \mu_{1, \mathbf{P}_t}$, but rather $\prod_{t=1}^n \bar{\mu}_{1,t}$, where $\bar{\mu}_{1,t} = \mathbb{E}_1[\mu_{1, \mathbf{P}_t} \mid Y_1, \dots, Y_{t-1}]$ is the conditional version of μ_{1, \mathbf{P}_t} given the historical information $Y_{1:(t-1)}$. As a result, the Hellinger distance's tensorization cannot apply directly as $\bar{\mu}_{1,t}$ still depends on the history $Y_{1:(t-1)}$, so we derive a generalization in the following lemma.

Lemma A.3. *Let \mathcal{P} denote a prior set on which $\mathbf{P}_t \in \mathcal{P}$ for all $t \in [n]$. Let ρ_i denote the joint probability density distribution of (Y_1, \dots, Y_n) under the hypothesis H_i for $i \in \{0, 1\}$.*

- *If $n \cdot \sup_{\mathbf{P}_t \in \mathcal{P}} H^2(\mu_0, (1 - \varepsilon_n)\mu_0 + \varepsilon_n\mu_{1, \mathbf{P}_t}) = o(1)$, then*

$$\text{TV}(\rho_0, \rho_1) \rightarrow 0 \text{ as } n \rightarrow \infty.$$

- Let $\bar{\mu}_{1,t} = \mathbb{E}_1[\mu_{1,\mathbf{P}_t} | Y_1, \dots, Y_{t-1}]$ be the conditional version of μ_{1,\mathbf{P}_t} given the history information Y_1, \dots, Y_{t-1} . If there exists a positive non-random sequence c_n satisfying $nc_n \rightarrow \infty$ such that $\min_{t \in [n]} \inf_{\mathbf{P}_t \in \mathcal{P}} H^2(\mu_0, (1 - \varepsilon_n)\mu_0 + \varepsilon_n \bar{\mu}_{1,t}) \geq c_n$ holds almost surely for each $n \geq 1$, then

$$\text{TV}(\rho_0, \rho_1) \rightarrow 1 \text{ as } n \rightarrow \infty.$$

We use Lemma A.3 to establish the detectability and identify the optimal detection boundary. With the established Lemma A.3, we can prove Theorem 4.1.

Proof of Theorem 4.1. Recall that $f_{1,\mathbf{P}_t}(r) = \sum_{w \in \text{Voc}} r^{1/P_t, w-1}$ is the PDF of μ_{1,\mathbf{P}_t} . Note that the density ratio between μ_{1,\mathbf{P}_t} and μ_0 is still f_{1,\mathbf{P}_t} . By Lemma A.3, it suffices to show

$$n \cdot \sup_{t \in [n]} \sup_{\mathbf{P}_t} H^2(\mu_0, (1 - \varepsilon_n)\mu_0 + \varepsilon_n \mu_{1,\mathbf{P}_t}) = o(1).$$

By the definition of Hellinger distance, it is equivalent to

$$\inf_{t \in [n]} \inf_{\mathbf{P}_t} \mathbb{E}_0 \sqrt{1 - \varepsilon_n + \varepsilon_n f_{1,\mathbf{P}_t}(Y)} = 1 + o(1/n). \quad (14)$$

Using the inequality that $|\sqrt{1+x} - 1 - x/2| \leq c \cdot x^2$ for any $x \geq -1$ and plugging $x = \varepsilon_n(f_{1,\mathbf{P}_t}(Y) - 1)$ into it, we have that

$$\mathbb{E}_0 \sqrt{1 - \varepsilon_n + \varepsilon_n f_{1,\mathbf{P}_t}(Y)} \geq 1 - c \cdot \mathbb{E}_0 x^2 \geq 1 - O(|\text{Voc}|) \cdot \varepsilon_n^2.$$

The last inequality uses the result $\mathbb{E}_0(f_{1,\mathbf{P}_t}(Y) - 1)^2 = O(|\text{Voc}|)$ from Lemma A.6. Due to $p > 0.5$, we have $\varepsilon_n^2 = n^{-2p} = o(1/n)$ and thus complete the proof. \square

A.2.1 Proof of Lemma A.3

Proof of Lemma A.3. It suffices to focus on the the Hellinger distance between ρ_0 and ρ_1 due to the following inequality:

$$\frac{1}{2} H^2(\rho_0, \rho_1) \leq \text{TV}(\rho_0, \rho_1) \leq H(\rho_0, \rho_1) \sqrt{1 - \frac{1 - H^2(\rho_0, \rho_1)}{4}} \leq 1,$$

As $\rho_0 \equiv 1$, it follows by definition that

$$H^2(\rho_0, \rho_1) = 1 - \mathbb{E}_0 \sqrt{\rho_1(Y_1, \dots, Y_n)}. \quad (15)$$

where the expectation \mathbb{E}_0 means $(Y_1, \dots, Y_n) \sim \mu_0^n$. On the other hand, a crucial fact is that

$$\rho_1(Y_1, \dots, Y_{n-1}, Y_n) = \rho_1(Y_1, \dots, Y_{n-1}) \cdot [(1 - \varepsilon_n) + \varepsilon_n \bar{f}_{1,n}(Y_n)], \quad (16)$$

with

$$\bar{f}_{1,t}(y) = \mathbb{E}_1[f_{1,\mathbf{P}_t}(y) | \mathcal{G}_{t-1}],$$

where the conditional expectation is taken with respect to \mathbf{P}_t . Here $\mathcal{G}_n = \sigma(\{Y_t\}_{t=1}^n)$ is the σ -field generated by all Y_1, \dots, Y_n . We will prove this equation at the end of the proof. We define the measure introduced by the PDF $\bar{f}_{1,t}$: for any measurable set A ,

$$\bar{\mu}_{1,t}(A) = \mathbb{E}_1[\mu_{1,\mathbf{P}_t}(A) | \mathcal{G}_{t-1}] = \int_A \bar{f}_{1,t}(y) dy. \quad (17)$$

We are now ready to prove this lemma.

- By conditional Jensen's inequality, it follows that

$$\begin{aligned}
\mathbb{E}_{Y_n \sim \mu_0} \sqrt{(1 - \varepsilon_n) + \varepsilon_n \bar{f}_{1,n}(Y_n)} &\geq \mathbb{E}_{Y_n \sim \mu_0} \mathbb{E}_1 \left[\sqrt{(1 - \varepsilon_n) + \varepsilon_n f_{1, \mathbf{P}_n}(Y_n)} \middle| \mathcal{G}_{n-1} \right] \\
&\geq \inf_{\mathbf{P}_n \in \mathcal{P}} \mathbb{E}_{Y_n \sim \mu_0} \sqrt{(1 - \varepsilon_n) + \varepsilon_n f_{1, \mathbf{P}_n}(Y_n)} \\
&= 1 - \sup_{\mathbf{P}_n \in \mathcal{P}} H^2(\mu_0, (1 - \varepsilon_n)\mu_0 + \varepsilon_n \mu_{1, \mathbf{P}_n}).
\end{aligned}$$

By the last inequality, (16), and (15), it follows that

$$H^2(\rho_0, \rho_1) \leq 1 - \prod_{t=1}^n \left(1 - \sup_{\mathbf{P}_t \in \mathcal{P}} H^2(\mu_0, (1 - \varepsilon_n)\mu_0 + \varepsilon_n \mu_{1, \mathbf{P}_t}) \right).$$

We prove the first part by using the inequality that $e^{-2 \log 2 \cdot x} \leq 1 - x$ for any $x \in [0, 1/2]$.

- By the condition, it follows that

$$\mathbb{E}_{Y_n \sim \mu_0} \sqrt{(1 - \varepsilon_n) + \varepsilon_n \bar{f}_{1,n}(Y_n)} = 1 - H^2(\mu_0, (1 - \varepsilon_n)\mu_0 + \varepsilon_n \bar{\mu}_{1,n}) \leq 1 - c_n.$$

By the last inequality, (16), and (15), it follows that

$$H^2(\rho_0, \rho_1) \geq 1 - (1 - c_n)^n \geq 1 - e^{-nc_n} \rightarrow 1.$$

□

Proof of (16). To prove equation (16), we require an important lemma to understand the dependence of the pivotal statistic Y_t on all text-generating randomness. This result is presented in Lemma A.4. We will reference Lemma A.4 multiple times in the appendix.

Lemma A.4. *Let Assumption 4.1 hold with \mathcal{F}_t defined as stated therein. It follows that for any integrable function h ,*

$$\mathbb{E}_1[h(Y_t) | \mathcal{F}_{t-1}] = \mathbb{E}_1[h(Y_t) | \mathbf{P}_t] = \mathbb{E}[\eta_t] \cdot \mathbb{E}_{1, \mathbf{P}_t} h(Y) + (1 - \mathbb{E}[\eta_t]) \cdot \mathbb{E}_0 h(Y). \quad (18)$$

Proof of Lemma A.4. This follows from Lemma A.2 and $\eta_t \perp \mathcal{F}_{t-1}$. □

Recall that $\mathcal{G}_t = \sigma(\{Y_j\}_{j=1}^t)$ be the σ -field generated by all pivotal statistics before and including iteration t . Hence, $\mathcal{G}_{n-1} \subset \mathcal{F}_{n-1}$ due to $Y_t = Y(w_t, \zeta_t)$. For a given measurable A_n ,

$$\mathbb{E}_1[\mathbf{1}_{Y_n \in A_n} | \mathcal{G}_{n-1}] = \mathbb{E}_1[\mathbb{E}_1[\mathbf{1}_{Y_n \in A_n} | \mathcal{F}_{n-1}] | \mathcal{G}_{n-1}] = \mathbb{E}_1[(1 - \varepsilon_n)\mu_0(A_n) + \varepsilon_n \mu_{1, \mathbf{P}_t}(A_n) | \mathcal{G}_{n-1}],$$

where the last equation uses Lemma A.4 and $\mathbb{E}[\eta_t] = \varepsilon_n$. We emphasize that $\mathbb{E}_1[\mu_{1, \mathbf{P}_t}(A_n) | \mathcal{G}_{n-1}]$ should be regarded as a function of Y_1, \dots, Y_{n-1} due to the measurability of \mathcal{G}_{n-1} . It has a closed expression in (17) due to Fubini's theorem.

Let A_1, \dots, A_{n-1} be any measurable sets. On the one hand, it follows that

$$\mathbb{P}_1(Y_t \in A_t, \forall t \in [n]) = \int_{\prod_{t=1}^n A_t} \rho_1(Y_1, \dots, Y_n) dY_1 \dots dY_n. \quad (19)$$

On the other hand,

$$\begin{aligned}
\mathbb{P}_1(Y_t \in A_t, \forall t \in [n]) &= \mathbb{E}_1 \prod_{t=1}^n \mathbf{1}_{Y_t \in A_t} = \mathbb{E}_1 \left[\mathbb{E}_1 \left[\prod_{t=1}^n \mathbf{1}_{Y_t \in A_t} \mid \mathcal{G}_{n-1} \right] \right] \\
&= \mathbb{E}_1 \left[\prod_{t=1}^{n-1} \mathbf{1}_{Y_t \in A_t} \mathbb{E}_1 [\mathbf{1}_{Y_n \in A_n} \mid \mathcal{G}_{n-1}] \right] \\
&= \mathbb{E}_1 \left[\prod_{t=1}^{n-1} \mathbf{1}_{Y_t \in A_t} ((1 - \varepsilon_n) \mu_0(A_n) + \mathbb{E}_1[\mu_{1, \mathbf{P}_t}(A_n) \mid \mathcal{G}_{n-1}]) \right] \\
&= \int_{\prod_{t=1}^{n-1} A_t} \rho_1(Y_1, \dots, Y_{n-1}) [(1 - \varepsilon_n) \mu_0(A_n) + \mathbb{E}_1[\mu_{1, \mathbf{P}_t}(A_n) \mid \mathcal{G}_{n-1}]] dY_1 \dots dY_{n-1} \\
&= \int_{\prod_{t=1}^{n-1} A_t} \rho_1(Y_1, \dots, Y_{n-1}) dY_1 \dots dY_{n-1} \cdot \int_{A_n} [(1 - \varepsilon_n) + \varepsilon_n \bar{f}_{1,n}(Y_n)] dY_n.
\end{aligned} \tag{20}$$

By the arbitrariness of A_1, \dots, A_n in (19) and (20), we complete the proof of (16). \square

A.3 Proof of Theorem 4.2

Theorem 4.2 (Restated version of Theorem 4.2). *Under Assumption 4.1, let $0 < p \leq \frac{1}{2}$ and $\Delta_n \asymp n^{-q}$ with $0 \leq q \leq 1$.*

- *If $q + 2p > 1$ and $\mathbf{P}_{1:n} \subset \mathcal{P}_{\Delta_n}^c$, H_0 and H_1^{mix} merge asymptotically. Hence, for any test, the sum of Type I and Type II errors tends to 1 as $n \rightarrow \infty$.*
- *If $q + 2p < 1$ and $\mathbf{P}_{1:n} \subset \mathcal{P}_{\Delta_n}$, H_0 and H_1^{mix} separate asymptotically. Furthermore, for the likelihood-ratio test that rejects H_0 if the log-likelihood ratio is positive, the sum of Type I and Type II errors tends to 0 as $n \rightarrow \infty$.*

Proof of Theorem 4.2. We prove this theorem with the help of Lemma A.3. To make Lemma A.3 easier to apply, we first simplify the considered Hellinger distance to more explicit terms.

Lemma A.5. *Fix \mathbf{P}_t . It follows that*

- *Let $f_{1, \mathbf{P}_t}(r) = \sum_{w \in \text{Voc}} r^{1/P_t, w^{-1}}$ be the PDF of μ_{1, \mathbf{P}_t} . Then,*

$$H^2(\mu_0, 1 - \varepsilon_n + \varepsilon_n \mu_{1, \mathbf{P}_t}) = \Theta(1) \cdot \varepsilon_n^2 \cdot \mathbb{E}_0(f_{1, \mathbf{P}_t}(Y) - 1)^2.$$

- *Let $\mathcal{G}_n = \sigma(\{Y_t\}_{t=1}^n)$ is the σ -field generated by all Y_1, \dots, Y_n . We define the conditioned PDF and probability measure: $\bar{f}_{1,t}(y) = \mathbb{E}_1[f_{1, \mathbf{P}_t}(y) \mid \mathcal{G}_{t-1}]$ and $\bar{\mu}_{1,t} = \mathbb{E}_1[\mu_{1, \mathbf{P}_t} \mid \mathcal{G}_{t-1}]$. It follows that*

$$H^2(\mu_0, 1 - \varepsilon_n + \varepsilon_n \bar{\mu}_{1,t}) = \Theta(1) \cdot \varepsilon_n^2 \cdot \mathbb{E}_0(\bar{f}_{1,t}(Y) - 1)^2.$$

Here $\Theta(1)$ in the above denotes a universal positive constant.

Now, we are ready to prove the main theorem.

- To prove the first point, we could use a similar argument in the proof of Theorem 4.1. By Lemma A.3, it suffices to show

$$\sum_{t=1}^n \sup_{\mathbf{P}_t \in \mathcal{P}_{\Delta_n}^c} H^2(\mu_0, (1 - \varepsilon_n)\mu_0 + \varepsilon_n \mu_{1, \mathbf{P}_t}) \rightarrow 0. \quad (21)$$

Lemma A.6. Fix \mathbf{P}_t . Let $f_{1, \mathbf{P}_t}(r) = \sum_{w \in \text{Voc}} r^{1/P_{t,w}-1}$ be the PDF of μ_{1, \mathbf{P}_t} . Then,

$$\mathbb{E}_0(f_{1, \mathbf{P}_t}(Y) - 1)^2 = O(|\text{Voc}|) \cdot (1 - P_{t, \max}),$$

where $O(1)$ denotes a universal positive constant.

By Lemma A.3 and A.6, it suffices to ensure that

$$\varepsilon_n^2 \sum_{t=1}^n (1 - P_{t, \max}) \leq n \varepsilon_n^2 \Delta_n = O(n^{1-2p-q}) \rightarrow 0$$

which follows directly from the condition that $2p + q > 1$.

- To prove the second point, by Lemma A.3, we only have to show that there exists a positive non-random sequence c_n satisfying $nc_n \rightarrow \infty$ and

$$H^2(\mu_0, (1 - \varepsilon_n)\mu_0 + \varepsilon_n \bar{\mu}_{1,t}) \geq c_n \quad \text{almost surely for } \forall n \geq 1.$$

Lemma A.7. If $\mathbf{P}_t \in \mathcal{P}_{\Delta_n}$ holds almost surely and n is sufficiently large so that $\Delta_n < 0.5$, then $\mathbb{E}_0(\bar{f}_{1,t}(Y) - 1)^2 \geq \Theta(\Delta_n)$ almost surely where $\Theta(1)$ denotes a universal positive constant.

By Lemma A.5 and A.7, it suffices to show that

$$n \varepsilon_n^2 \Delta_n = \Theta(n^{1-2p-q}) \rightarrow \infty,$$

which follows directly from the condition that $2p + q < 1$.

It remains to show that the likelihood ratio test is effective if $2p + q < 1$. Since the proofs are similar, we show only that under the null hypothesis. Lemma A.8 implies that under H_0 , the log-likelihood ratio L_n goes to $-\infty$ with probability one. Hence, the likelihood ratio test that rejects H_0 if $L_n \geq 0$ has a vanishing Type I error.

Lemma A.8. Let $\ell_t(y) = \log(1 - \varepsilon_n + \varepsilon_n \bar{f}_{1,t}(y))$ and $L_n = \sum_{t=1}^n \ell_t(Y_t)$. If $\mathbf{P}_{1:n} \subset \mathcal{P}_{\Delta_n}$ and $2p + q < 1$,

$$\mathbb{E}_0 L_n \rightarrow -\infty \quad \text{and} \quad \frac{\text{Var}_0(L_n)}{[\mathbb{E}_0 L_n]^2} \rightarrow 0.$$

□

A.3.1 Missing Proofs of Lemmas

At the end of this section, we provide the missing proofs for the lemmas mentioned above.

Proof of Lemma A.5. It suffices to focus on $\mathbb{E}_0 \sqrt{1 - \varepsilon_n + \varepsilon_n f_{1, \mathbf{P}_t}(Y)}$ due to the relation that

$$H^2(\mu_0, 1 - \varepsilon_n + \varepsilon_n \mu_{1, \mathbf{P}_t}) = 1 - \mathbb{E}_0 \sqrt{1 - \varepsilon_n + \varepsilon_n f_{1, \mathbf{P}_t}(Y)}.$$

Note that as long as n is sufficiently large, we would have $\sup_{y \in [0, 1]} \varepsilon_n |f_{1, \mathbf{P}_t}(y) - 1| \leq |\text{Voc}| \cdot \varepsilon_n \leq 1$. Using the inequality that $\sqrt{1 + x} \leq 1 + \frac{x}{2} - \frac{x^2}{18}$ for any $-1 \leq x \leq 3$, we have

$$\begin{aligned} \mathbb{E}_0 \sqrt{1 - \varepsilon_n + \varepsilon_n f_{1, \mathbf{P}_t}(Y)} &\leq \mathbb{E}_0 \left[1 + \frac{\varepsilon_n}{2} (f_{1, \mathbf{P}_t}(Y) - 1) - \frac{\varepsilon_n^2}{18} (f_{1, \mathbf{P}_t}(Y) - 1)^2 \right] \\ &= 1 - \frac{\varepsilon_n^2}{18} \cdot \mathbb{E}_0 (f_{1, \mathbf{P}_t}(Y) - 1)^2. \end{aligned}$$

On the other hand, by the inequality that $\sqrt{1 + x} \geq 1 + \frac{x}{2} - \frac{x^2}{2}$ for any $x \geq -1$, we have

$$\begin{aligned} \mathbb{E}_0 \sqrt{1 - \varepsilon_n + \varepsilon_n f_{1, \mathbf{P}_t}(Y)} &\geq \mathbb{E}_0 \left[1 + \frac{\varepsilon_n}{2} (f_{1, \mathbf{P}_t}(Y) - 1) - \frac{\varepsilon_n^2}{2} (f_{1, \mathbf{P}_t}(Y) - 1)^2 \right] \\ &= 1 - \frac{\varepsilon_n^2}{2} \cdot \mathbb{E}_0 (f_{1, \mathbf{P}_t}(Y) - 1)^2. \end{aligned}$$

We then prove the first part by combining these two inequalities on $\mathbb{E}_0 \sqrt{1 - \varepsilon_n + \varepsilon_n f_{1, \mathbf{P}_t}(Y)}$.

By an almost identical argument, we can prove the second part (so we omit it). \square

Proof of Lemma A.6. We note that

$$\begin{aligned} \mathbb{E}_0 (f_{1, \mathbf{P}_t}(Y) - 1)^2 &= \mathbb{E}_0 f_{1, \mathbf{P}_t}^2(Y) - 1 = \int_0^1 \left(\sum_{w \in \text{Voc}} r^{1/P_{t,w} - 1} \right)^2 dr - 1 \\ &= \sum_{w \in \text{Voc}} \sum_{j \in \text{Voc}} \frac{1}{1/P_{t,w} + 1/P_{t,j} - 1} - 1 \\ &= \sum_{w \in \text{Voc}} \sum_{j \in \text{Voc}} P_{t,w} P_{t,j} \frac{(1 - P_{t,w})(1 - P_{t,j})}{1 - (1 - P_{t,w})(1 - P_{t,j})}. \end{aligned} \tag{22}$$

Note that $1 - (1 - P_{t,w})(1 - P_{t,j}) \geq P_{t,w} \vee P_{t,j}$. It then follows that

$$\mathbb{E}_0 (f_{1, \mathbf{P}_t}(Y) - 1)^2 \leq \sum_{1 \leq w, j \leq |\text{Voc}|} (P_{t,w} \wedge P_{t,j}) \cdot (1 - P_{t,w})(1 - P_{t,j}).$$

In the following, without loss of generality, we assume $P_{t,1} \geq P_{t,2} \geq \dots \geq P_{t,|\text{Voc}|}$. We start by analyzing the target quantity

$$\sum_{w \in \text{Voc}} \sum_{j=1}^{|\text{Voc}|} (P_{t,w} \wedge P_{t,j}) \cdot (1 - P_{t,w})(1 - P_{t,j}).$$

It follows that that quantity can be equivalently written as

$$\begin{aligned}
& \sum_{w \in \text{Voc}} \left[\sum_{j=1}^{w-1} (P_{t,w} \wedge P_{t,j}) \cdot (1 - P_{t,w})(1 - P_{t,j}) + \sum_{j=w}^{|\text{Voc}|} (P_{t,w} \wedge P_{t,j}) \cdot (1 - P_{t,w})(1 - P_{t,j}) \right] \\
& \stackrel{(a)}{=} \sum_{w \in \text{Voc}} \left[\sum_{j=1}^{w-1} (P_{t,w} \wedge P_{t,j}) \cdot (1 - P_{t,w})(1 - P_{t,j}) + \sum_{j=1}^w (P_{t,w} \wedge P_{t,j}) \cdot (1 - P_{t,w})(1 - P_{t,j}) \right] \\
& \stackrel{(b)}{=} \sum_{w \in \text{Voc}} \left[P_{t,w}(1 - P_{t,w})^2 + 2 \sum_{j=1}^{w-1} P_{t,w} \cdot (1 - P_{t,w})(1 - P_{t,j}) \right] \\
& = \sum_{w \in \text{Voc}} P_{t,w}(1 - P_{t,w}) \left[1 - P_{t,w} + 2 \sum_{j=1}^{w-1} (1 - P_{t,j}) \right] \\
& \stackrel{(c)}{\leq} 2|\text{Voc}| \sum_{w \in \text{Voc}} P_{t,w}(1 - P_{t,w}) \\
& \leq 4|\text{Voc}| \cdot (1 - P_{t,1}),
\end{aligned}$$

where (a) uses $\sum_{w=1}^{|\text{Voc}|} \sum_{j=w}^{|\text{Voc}|} = \sum_{j=1}^{|\text{Voc}|} \sum_{w=1}^j$ first and then switches the notation of w and j , (b) simplifies the expression by using the fact that $P_{t,j} \geq P_{t,w}$ if $j \leq w$, and (c) uses the relation that $1 - P_{t,w} + 2 \sum_{j=1}^{w-1} (1 - P_{t,j}) = 2w - 1 - (P_{t,w} + 2 \sum_{j=1}^{w-1} P_{t,j}) \leq 2w - 1 \leq 2|\text{Voc}|$ for any $w \in \text{Voc}$. \square

Proof of Lemma A.7. We denote the distribution of \mathbf{P}_t conditional on \mathcal{G}_{t-1} by ρ for notation simplicity. Then our target quantity can be written as

$$\begin{aligned}
\mathbb{E}_0(\bar{f}_{1,t}(Y) - 1)^2 &= \mathbb{E}_{Y \sim \mu_0} (\mathbb{E}_{\mathbf{P}_t \sim \rho} f_{1,\mathbf{P}_t}(Y) - 1)^2 \\
&= \mathbb{E}_{Y \sim \mu_0} (\mathbb{E}_{\mathbf{P}_t \sim \rho} f_{1,\mathbf{P}_t}(Y))^2 - 1 \\
&= \mathbb{E}_{Y \sim \mu_0} \mathbb{E}_{\mathbf{P}_1 \sim \rho} \mathbb{E}_{\mathbf{P}_2 \sim \rho} f_{1,\mathbf{P}_1}(Y) f_{1,\mathbf{P}_2}(Y) - 1 \\
&= \mathbb{E}_{\mathbf{P}_1 \sim \rho} \mathbb{E}_{\mathbf{P}_2 \sim \rho} [\mathbb{E}_{Y \sim \mu_0} f_{1,\mathbf{P}_1}(Y) f_{1,\mathbf{P}_2}(Y) - 1]
\end{aligned}$$

Note that the following inequality holds (which one can prove by a similar analysis in (22)):

$$\begin{aligned}
\mathbb{E}_{Y \sim \mu_0} f_{1,\mathbf{P}_1}(Y) f_{1,\mathbf{P}_2}(Y) - 1 &= \sum_{w \in \text{Voc}} \sum_{j \in \text{Voc}} P_{1,w} P_{2,j} \cdot \frac{(1 - P_{1,w})(1 - P_{2,j})}{1 - (1 - P_{1,w})(1 - P_{2,j})} \\
& \stackrel{(a)}{\geq} \sum_{w \in \text{Voc}} \sum_{j \in \text{Voc}} P_{1,w} P_{2,j} \cdot \frac{(1 - P_{1,w})(1 - P_{2,j})}{P_{1,w} + P_{2,j}} \\
& \stackrel{(b)}{\geq} \frac{1}{2} \sum_{w \in \text{Voc}} \sum_{j \in \text{Voc}} (P_{1,w} \wedge P_{2,j}) \cdot (1 - P_{1,w})(1 - P_{2,j}) \\
& \stackrel{(c)}{\geq} \frac{1}{2} \Delta_n (1 - \Delta_n)^2 = \Theta(\Delta_n),
\end{aligned}$$

where (a) uses $1 - (1 - P_{1,w})(1 - P_{2,j}) \leq P_{1,w} + P_{2,j}$, (b) uses $\frac{2P_{1,w}P_{2,j}}{P_{1,w} + P_{2,j}} \geq P_{1,w} \wedge P_{2,j}$, and (c) follows from Lemma A.9 by requiring $\Delta_n < 0.5$.

Lemma A.9. *If $\mathbf{P}_1, \mathbf{P}_2 \in \mathcal{P}_\Delta$ where $\Delta < 0.5$, then it follows that*

$$\sum_{w \in \text{Voc}} \sum_{j \in \text{Voc}} (P_{1,w} \wedge P_{2,j}) \cdot (1 - P_{1,w})(1 - P_{2,j}) \geq \Delta(1 - \Delta)^2 + 3\Delta^2(1 - \Delta).$$

□

We provide the proof of Lemma A.9 at the end of the proof.

Proof of Lemma A.9. For simplicity, we define $L(\mathbf{P}_1, \mathbf{P}_2) = \sum_{w \in \text{Voc}} \sum_{j \in \text{Voc}} (P_{1,w} \wedge P_{2,j}) \cdot (1 - P_{1,w})(1 - P_{2,j})$. Let Π denote any permutation on Voc . For any fixed \mathbf{P}_2 , we define an auxiliary function $h_{\mathbf{P}_2}(\mathbf{P}_1) : \mathbf{P}_1 \mapsto L(\mathbf{P}_1, \mathbf{P}_2)$. It is easy to see that the function $h_{\mathbf{P}_2}(\mathbf{P}_1)$ is concave in \mathbf{P}_1 for any fixed \mathbf{P}_2 . By a classic result in convex analysis [31], the infimum of any concave function over a compact convex set in a Euclidean space is necessarily attained at an extreme point of the convex set. We note that by Lemma 3.4 in [48], the set of extreme points of \mathcal{P}_Δ is given by $\{\pi(\mathbf{P}_\Delta^*) : \pi \in \Pi\}$, where $\mathbf{P}_\Delta^* = (1 - \Delta, \Delta, 0, \dots, 0)$ (due to the fact that $\Delta < 0.5$). On the other hand, we find that for any permutation $\pi \in \Pi$, $h_{\mathbf{P}_2}(\cdot)$ is π -invariant in the sense that $h_{\mathbf{P}_2}(\mathbf{P}_1) = h_{\mathbf{P}_2}(\pi(\mathbf{P}_1))$ for any \mathbf{P}_1 . Here $\pi(\mathbf{P}_1)$ denotes the permuted distribution $(P_{\pi(1)}, \dots, P_{\pi(n)})$. As a result, it follows that

$$h_{\mathbf{P}_2}(\mathbf{P}_1) \geq \inf_{\mathbf{P}_1 \in \mathcal{P}_\Delta} h_{\mathbf{P}_2}(\mathbf{P}_1) = \inf_{\pi \in \Pi} h_{\mathbf{P}_2}(\pi(\mathbf{P}_\Delta^*)) = h_{\mathbf{P}_2}(\mathbf{P}_\Delta^*).$$

Note that $L(\mathbf{P}_1, \mathbf{P}_2) = L(\mathbf{P}_2, \mathbf{P}_1)$. Repeating the above argument would yield that

$$L(\mathbf{P}_1, \mathbf{P}_2) \geq h_{\mathbf{P}_2}(\mathbf{P}_\Delta^*) = L(\mathbf{P}_2, \mathbf{P}_\Delta^*) \geq h_{\mathbf{P}_\Delta^*}(\mathbf{P}_\Delta^*) = L(\mathbf{P}_\Delta^*, \mathbf{P}_\Delta^*) = \Delta(1 - \Delta)^2 + 3\Delta^2(1 - \Delta).$$

□

Proof of Lemma A.8. Assume that n is sufficiently large so that $|\text{Voc}| \varepsilon_n \leq 1$. As a result, it follows that for any $t \in [n]$, $\varepsilon_n \bar{f}_{1,t}(Y_t) \leq 1$. Using the inequality that $\log(1 + x) \leq x - x^2/4$ for $x \in (-1, 1]$, we have that

$$\mathbb{E}_0 \ell_t(Y_t) \leq \mathbb{E}_0 \varepsilon_n (\bar{f}_{1,t}(Y_t) - 1) - \frac{\varepsilon_n^2}{4} \mathbb{E}_0 (\bar{f}_{1,t}(Y_t) - 1)^2 = -\frac{\varepsilon_n^2}{4} \mathbb{E}_0 (\bar{f}_{1,t}(Y_t) - 1)^2. \quad (23)$$

By Lemma A.7, when $P_{t,\max} \leq 1 - \Delta_n$, we have $\mathbb{E}_0 (\bar{f}_{1,t}(Y_t) - 1)^2 \geq \Theta(1) \cdot \Delta_n$. Hence, $\mathbb{E}_0 L_n = \sum_{t=1}^n \mathbb{E}_0 \ell_t(Y_t) \leq -\Theta(1) \cdot n \varepsilon_n^2 \Delta_n = -\Theta(1) \cdot n^{1-2p-q} \rightarrow -\infty$ if $2p + q < 1$.

To prove the other statement, it suffices to show $\text{Var}_0(L_n) \leq C \cdot \mathbb{E}_0 L_n$ for some constant $C > 0$. To that end, we will show $\mathbb{E}_0 \ell_t(Y_t)^2 \leq C \cdot |\mathbb{E}_0 \ell_t(Y_t)|$. Using the inequality that $\log^2(1 + x) \leq 2 \cdot x^2$ for $x \in [-0.5, 1]$, as long as $\varepsilon_n \leq 0.5$, we have that

$$\mathbb{E}_0 \ell_t(Y_t)^2 \leq 2\varepsilon_n^2 \cdot \mathbb{E}_0 (\bar{f}_{1,t}(Y_t) - 1)^2 \leq 8 \cdot |\mathbb{E}_0 \ell_t(Y_t)|,$$

where the last inequality uses (23) which implies $\varepsilon_n^2 \cdot \mathbb{E}_0 (\bar{f}_{1,t}(Y_t) - 1)^2 \leq 4 \cdot |\mathbb{E}_0 \ell_t(Y_t)|$. □

A.4 Higher Criticism and Its Optimal Adaptivity

We first introduce Higher Criticism and then show that it achieves optimal adaptivity introduced in Section 4.4.

Higher Criticism. In literature, Higher Criticism (HC), as a non-parametric procedure, has shown success in the sparse detection problem [19, 10, 9]. It is an instance of the above Tr-GoF test when $s = 2$. We introduce it in more detail in the following. Given the observed pivotal statistics $\{Y_t\}_{t=1}^n$, HC contains three steps:

1. For each $t \in [n]$, we obtain a p-value by $p_t := \mathbb{P}_0(Y \geq Y_t | Y_t) = 1 - Y_t$.
2. Sort the p-values to $p_{(1)} < p_{(2)} < \dots < p_{(n)}$. We make a convention that $p_{(n+1)} = 1$.
3. Define the HC statistic as

$$\text{HC}_n^+ = \sup_{t: p_{(t+1)} \geq c_n^+} \text{HC}_{n,t}, \quad \text{HC}_{n,t} = \sqrt{n} \frac{t/n - p_{(t)}}{\sqrt{p_{(t)}(1 - p_{(t)})}}. \quad (24)$$

For any given $\delta > 0$, we would reject H_0 if

$$\text{HC}_n^+ \geq \sqrt{2(1 + \delta) \log \log n}. \quad (25)$$

Remark A.1. We mention that except for the expression in (24), there are other variants or generalizations of HC statistics. See [38, 4, 20] for further discussions.

One can check that $S_n^+(2)$ is connected to HC_n^+ via the following relationship [38]:

$$n \cdot S_n^+(2) = \sup_{r \in [p^+, 1)} \frac{n (\mathbb{F}_n(r) - r)^2}{2 r(1 - r)} \mathbf{1}_{\mathbb{F}_n(r) \geq r} = \frac{1}{2} (\text{HC}_n^+)^2. \quad (11)$$

Heavy Tail of HC. The observations by Donoho and Jin [19, 20] suggest that the statistic $\text{HC}_{n,t}$ behaves poorly for very small values of t , such as 1 or 2, often leading to extremely large outlier values. To mitigate this issue, the constraint $p_{(t+1)} \geq c_n^+$ (with c_n^+ a small positive constant) is introduced in the definition of HC_n^+ . This constraint effectively prevents calculating these extreme values without altering the statistic's asymptotic properties (see Appendix B.3 for numerical support). When $c_n^+ = 0$, the constraint disappears and we refer to this special case as HC_n^* .

Optimal adaptivity of HC. Theorem A.1 will be crucial in proving the optimal adaptivity of Tr-GoF.

Theorem A.1 (Optimal adaptivity of HC). *Assume Assumption 4.1 holds and $\mathbf{P}_{1:n} \subset \mathcal{P}_{\Delta_n}$ almost surely with $\Delta_n \asymp n^{-q}$. If $q + 2p < 1$, for the HC test in (25) with any $0 \leq c_n^+ \leq \Delta_n$, the sum of Type I and Type II errors tends to 0 as $n \rightarrow \infty$.*

In Theorem A.1, we demonstrate that HC remains effective for robustly detecting employing Gumbel-max watermarks. As a result, it achieves complete optimal adaptivity as the likelihood ratio test but does not necessitate any knowledge of the sampling token distribution \mathbf{P}_t .

We explain the intuition of why HC works. Under H_0 , p_t 's are i.i.d. copies of $U(0, 1)$ so that $\text{HC}_{n,t} \approx \mathcal{N}(0, 1)$. Using results from empirical processes, we can show that $\mathbb{P}_0(\text{HC}_n^+ \leq \sqrt{2 \log \log n}) \rightarrow 1$. Hence, HC_n^+ would grow to the infinity very slowly. In contrast, under H_1^{mix} , as long as each μ_{1, \mathbf{P}_t} differs from μ_0 moderately, we will have $\text{HC}_n^+ = \Omega_{\mathbb{P}}(n^{\frac{1}{2} - p - \frac{q}{2}})$. In fact, HC_n^+ would grow to the infinity in a rate faster than $\sqrt{\log \log n}$ as long as $\frac{1}{2} - p - \frac{q}{2} > 0$. As a result, the HC test can eventually separate two hypotheses.

Proof of Theorem A.1. For simplicity, we use $\mathbb{P}_0(\cdot)$ and $\mathbb{P}_1(\cdot)$ to denote the probability measure under H_0 and H_1^{mix} respectively. It suffices to show that as $n \rightarrow \infty$,

$$\mathbb{P}_0 \left(\text{HC}_n^+ \geq \sqrt{(2 + \delta) \log \log n} \right) \rightarrow 0 \quad (26a)$$

$$\text{and } \mathbb{P}_1 \left(\text{HC}_n^+ < \sqrt{(2 + \delta) \log \log n} \right) \rightarrow 0. \quad (26b)$$

Recall that the p-value is given by $p_t = 1 - Y_t$. Let $\bar{\mathbb{F}}_n$ be the empirical CDF of p_t 's so that $\bar{\mathbb{F}}_n(r) = \frac{1}{n} \sum_{t=1}^n \mathbf{1}_{p_t \leq r}$ for any $r \in [0, 1]$. Let U denote the CDF of $U(0, 1)$ so that $\mathbb{F}_0(r) = r$. We let $W_n(r)$ be the standardized form of $\bar{\mathbb{F}}_n(r) - r$,

$$W_n(r) = \sqrt{n} \cdot \frac{\bar{\mathbb{F}}_n(r) - r}{\sqrt{r(1-r)}} = \frac{1}{\sqrt{n}} \sum_{t=1}^n \frac{\mathbf{1}_{p_t \leq r} - r}{\sqrt{r(1-r)}}. \quad (27)$$

For a given $t \in [n]$, note that exactly t p-values are less than or equal to $p_{(t)}$ so that $\bar{\mathbb{F}}_n(p_{(t)}) = \frac{t}{n}$ which implies that

$$W_n(p_{(t)}) = \sqrt{n} \cdot \frac{t/n - p_{(t)}}{\sqrt{p_{(t)}(1-p_{(t)})}}.$$

Note that for any $r \in [p_{(n)}, 1]$, $W_n(r) = \sqrt{n} \cdot \sqrt{\frac{1-r}{r}} \geq 0$, which implies that $W_n(r)$ is non-negative and $\sup_{r \in [p_{(n)}, 1]} W_n(r) = W_n(p_{(n)})$. Furthermore, it is easy to see that for any $r \in [p_{(t)}, p_{(t+1)}]$, $W_n(r)$

is decreasing in r so that $\sup_{r \in [p_{(t)}, p_{(t+1)}]} W_n(r) = W_n(p_{(t)})$. Varying the value of r in (27) and letting

$p^+ = \sup\{p_{(t)} : p_{(t)} \leq c_n^+\}$ be the smallest p-value that is no smaller than c_n^+ , we have that

$$\text{HC}_n^+ = \sup_{t: p_t \geq c_n^+} W_n(p_{t-1}) = \sup_{r \in [p^+, 1]} W_n(r).$$

We introduce another sequence

$$\text{HC}_n^* := \sup_{t \in [n]} W_n(p_t) = \sup_{r \in [p_{(1)}, 1]} W_n(r).$$

Under H_0 , HC_n^* equals in distribution the extreme value of a normalized uniform empirical process (see Theorem 1.1 of [19] for a reason) and thus in probability

$$\frac{\text{HC}_n^*}{\sqrt{2 \log \log n}} \rightarrow 1 \quad \text{and} \quad \mathbb{P}_0 \left(\text{HC}_n^* \geq \sqrt{(2 + \delta) \log \log n} \right) \rightarrow 0.$$

On the other hand, we have $\text{HC}_n^* \geq \text{HC}_n^+$ almost surely. Hence, for any $\delta > 0$, (26a) follows directly.

We now consider to prove (26b). Define the σ -field \mathcal{F}_t in the same way as in Lemma A.4. By Lemma A.4, it follows that

$$\mathbb{E}[\mathbf{1}_{Y_i \geq 1-r} \mid \mathcal{F}_{t-1}] = \mathbb{E}_{1, \mathbf{P}_t} \mathbf{1}_{Y_i \geq 1-r} = (1 - \varepsilon_n)r + \varepsilon_n[1 - F_{1, \mathbf{P}_t}(1-r)].$$

Using the notation of conditional expectation, we introduce another sequence $\bar{W}_n(r)$ following the spirit of $W_n(r)$:

$$\bar{W}_n(r) = \frac{1}{\sqrt{n}} \sum_{t=1}^n \frac{\mathbb{E}[\mathbf{1}_{Y_i \geq 1-r} \mid \mathcal{F}_{t-1}] - r}{\sqrt{r(1-r)}} = \frac{\varepsilon_n}{\sqrt{n}} \sum_{t=1}^n \frac{1 - F_{1, \mathbf{P}_t}(1-r) - r}{\sqrt{r(1-r)}}.$$

An observation is that for any fixed r , $W_n(r) - \overline{W}_n(r)$ is a martingale difference sequence adapted to the filtration \mathcal{F}_n .

For simplicity, we introduce $x_n = 1 - \Delta_n$ and denote $a_n \asymp (\lesssim) b_n$ if $\lim_{n \rightarrow \infty} \frac{a_n}{b_n} \geq (\leq) c$ for an absolute positive constant. Direct calculations show that

$$\begin{aligned}
\overline{W}_n(\Delta_n) &= \frac{\varepsilon_n}{\sqrt{n}} \sum_{t=1}^n \frac{x_n - F_{1, \mathbf{P}_t}(x_n)}{\sqrt{x_n(1-x_n)}} \\
&\stackrel{(a)}{\asymp} \sqrt{n} \varepsilon_n \cdot \frac{(1-x_n)}{\sqrt{x_n(1-x_n)}} \\
&= \sqrt{n} \varepsilon_n \cdot \sqrt{\frac{1-x_n}{x_n}} \\
&= \Theta(1) \cdot \sqrt{n} \varepsilon_n \cdot \sqrt{\Delta_n} \\
&\stackrel{(b)}{=} \Theta(1) \cdot n^{\frac{1}{2}-p-\frac{q}{2}}
\end{aligned} \tag{28}$$

where (a) uses the following Lemma A.10 and (b) uses the definition of ε_n and Δ_n .

Lemma A.10. *Recall that $x_n = 1 - \Delta_n$ with $\Delta_n \asymp n^{-q}$ and $F_{1, \mathbf{P}_t}(r) = \sum_{w \in \text{Voc}} P_{t,w} r^{1/P_{t,w}}$. If $q \in [0, 1)$, then as long as $\mathbf{P}_t \in \mathcal{P}_{\Delta_n}$,*

$$1 + e^{-1} \asymp x_n^{\frac{\Delta_n}{1-\Delta_n}} + x_n^{\frac{1-\Delta_n}{\Delta_n}} \leq \frac{1 - F_{1, \mathbf{P}_t}(x_n)}{1 - x_n} \leq |\text{supp}(\mathbf{P}_t)|, \tag{29}$$

where $\text{supp}(\mathbf{P}_t) = \{w : P_{t,w} \neq 0\}$ collects non-zero entries in the NTP distribution \mathbf{P}_t .

Proof of Lemma A.10. Note that by the mean value theorem, it follows that

$$\frac{1 - F_{1, \mathbf{P}_t}(x_n)}{1 - x_n} = f_{1, \mathbf{P}_t}(\theta_n), \tag{30}$$

where $f_{1, \mathbf{P}}$ is the PDF of $F_{1, \mathbf{P}}$ and $\theta_n \in [x_n, 1]$.

The upper bound follows from the fact that $f_{1, \mathbf{P}_t}(\theta_n) \leq f_{1, \mathbf{P}_t}(1) \leq |\text{supp}(\mathbf{P}_t)|$. We then turn to the lower bound. By Lemma A.17, for any $\mathbf{P}_t \in \mathcal{P}_{\Delta_n}$, it follows that for

$$F_{1, \mathbf{P}_t}(x_n) \leq \sup_{\mathbf{P} \in \mathcal{P}_{\Delta_n}} F_{1, \mathbf{P}}(x_n) = F_{1, \mathbf{P}_{\Delta_n}^*}(x_n)$$

where

$$\mathbf{P}_{\Delta}^* = \left(\underbrace{1 - \Delta, \dots, 1 - \Delta}_{\lfloor \frac{1}{1-\Delta} \rfloor \text{ times}}, 1 - (1 - \Delta) \cdot \left\lfloor \frac{1}{1-\Delta} \right\rfloor, 0, \dots \right).$$

Hence, once n is sufficiently large so that $\Delta_n < 0.5$, it follows that

$$(30) \geq \frac{1 - F_{1, \mathbf{P}_{\Delta_n}^*}(x_n)}{1 - x_n} \geq f_{1, \mathbf{P}_{\Delta_n}^*}(x_n) = x_n^{\frac{\Delta_n}{1-\Delta_n}} + x_n^{\frac{1-\Delta_n}{\Delta_n}} \asymp 1 + e^{-1}$$

where the last \asymp is because $\lim_{x \rightarrow 0} (1-x)^{\frac{x}{1-x}} = 1$ and $\lim_{x \rightarrow 0} (1-x)^{\frac{1-x}{x}} = e^{-1}$. \square

By (28), as long as $2p+q < 1$, we would have $\overline{W}_n(\Delta_n) \geq C \cdot n^{\frac{1}{2}-p-\frac{q}{2}} \geq \sqrt{(2+\delta) \log \log n}$ for some constant $C > 0$. On the other hand, the quadratic variation of the martingale $\{W_t(\Delta_n) - \overline{W}_t(\Delta_n)\}_{t=1}^n$ is given by

$$\frac{\sum_{t=1}^n \text{Var}_1[\mathbf{1}_{Y_t \geq 1-\Delta_n} | \mathcal{F}_{t-1}]}{nx_n(1-x_n)} = \frac{1}{n} \sum_{t=1}^n \frac{(1-\varepsilon_n)x_n + \varepsilon_n F_{1, \mathcal{P}_t}(x_n)}{x_n} \cdot \frac{1 - (1-\varepsilon_n)x_n - \varepsilon_n F_{1, \mathcal{P}_t}(x_n)}{1-x_n} \leq |\text{Voc}|. \quad (31)$$

Here we use the inequality $F_{1, \mathcal{P}}(r) \leq r$ for any $r \in [0, 1]$ and the upper bound in Lemma A.10. As a result, by the properties of square integrable martingales,

$$\mathbb{E}_1 |W_n(\Delta_n) - \overline{W}_n(\Delta_n)|^2 \leq \mathbb{E}_1 \text{its quadratic variation} \leq |\text{Voc}|.$$

Combining these pieces, it follows from Doob's martingale inequality that

$$\begin{aligned} \mathbb{P}_1(W_n(\Delta_n) < 0.5C \cdot n^{\frac{1}{2}-p-\frac{q}{2}}) &\leq \mathbb{P}_1(|W_n(\Delta_n) - \overline{W}_n(\Delta_n)| \geq 0.5 \cdot \overline{W}_n(x_n)) \\ &\leq \mathbb{P}_1(|W_n(\Delta_n) - \overline{W}_n(\Delta_n)| \geq 0.5C \cdot n^{\frac{1}{2}-p-\frac{q}{2}}) \\ &\leq \frac{4}{C^2} \cdot \frac{\mathbb{E}_1 |W_n(\Delta_n) - \overline{W}_n(\Delta_n)|^2}{n^{1-2p-q}} \\ &= O(n^{-(1-2p-q)}). \end{aligned} \quad (32)$$

As long as $2p+q < 1$, it follows that as $n \rightarrow \infty$,

$$\mathbb{P}_1(W_n(\Delta_n) < \sqrt{(2+\delta) \log \log n}) \leq \mathbb{P}_1(W_n(\Delta_n) < 0.5C \cdot n^{\frac{1}{2}-p-\frac{q}{2}}) \rightarrow 0.$$

We complete the proof by noting that $\Delta_n \geq p^+$ (otherwise we would have $\Delta_n < p^+ \leq c_n^+$ which is contradictory with the condition that $c_n^+ \leq \Delta_n$) and thus

$$\mathbb{P}_1\left(\text{HC}_n^+ < \sqrt{(2+\delta) \log \log n}\right) \leq \mathbb{P}_1(W_n(\Delta_n) < \sqrt{(2+\delta) \log \log n}) \rightarrow 0.$$

□

Remark A.2. In the proof of Theorem A.1, we also proved that

$$\mathbb{P}_0\left(\text{HC}_n^* \geq \sqrt{(2+\delta) \log \log n}\right) \rightarrow 0 \quad \text{and} \quad \mathbb{P}_1\left(\text{HC}_n^* < \sqrt{(2+\delta) \log \log n}\right) \rightarrow 0$$

Hence, the additional constraint $p_{(t)} \geq c_n^+$ in the definition of HC_n^+ does not affect the asymptotic behaviors of HC_n^* .

A.5 Rationale for Truncation

In this subsection, we expand on the discussion in Remark 3.3. Our definition of S_n^+ introduces two truncations relative to the previous S_n . As indicated by the relationship in (11), the untruncated $S_n(s)$ has a heavy-tail issue, as noted in Remark 3.3 and formally stated in Lemma A.11. Consequently, we impose a constraint in Tr-GoF (6) (for a similar rationale, see Appendix A.4), distinguishing it from the original approach in [38]. In numerical experiments, excluding these small p-values substantially reduces the heavy-tail effect, as demonstrated by comparing Figure 7 with Figure 16.

Lemma A.11. For any $n \geq 2$, $\mathbb{P}_0(n \cdot S_n(2) \geq z) \geq \frac{1}{2z}$ for sufficiently large $z > 0$.

Proof of Lemma A.11. It follows that

$$\begin{aligned} \mathbb{P}_0(n \cdot S_n(2) \geq z) &= \mathbb{P}_0(n \cdot K_2(1/n, p_{(1)}) \geq z) \\ &\stackrel{(a)}{=} \mathbb{P}_0(\text{HC}_{n,1}^2 \geq 2z) \\ &\stackrel{(b)}{\asymp} \mathbb{P}_0\left(\left|\frac{1}{\sqrt{E}} - \sqrt{E}\right| \geq \sqrt{2z}\right) \\ &\stackrel{(c)}{\asymp} \frac{1}{2z}, \end{aligned}$$

where (a) uses the definition of $\text{HC}_{n,1}$ from (24) and (b) follows from the result that $\text{HC}_{n,1} \xrightarrow{d} \frac{1}{\sqrt{E}} - \sqrt{E}$ where E is exponentially distributed with mean 1. This is due to the fact that $np_{(1)} \xrightarrow{d} E$ if p_1, \dots, p_n are i.i.d. from $U(0, 1)$. Finally, (c) uses the fact that for large $z > 0$,

$$\begin{aligned} \mathbb{P}_0\left(\frac{1}{\sqrt{E}} - \sqrt{E} \geq \sqrt{2z}\right) &= \mathbb{P}_0\left(\sqrt{E} \leq \sqrt{\frac{z}{2} + 1} - \sqrt{\frac{z}{2}}\right) \asymp \frac{1}{2z}, \\ \mathbb{P}_0\left(\frac{1}{\sqrt{E}} - \sqrt{E} \leq -\sqrt{2z}\right) &= \mathbb{P}_0\left(\sqrt{E} \geq \sqrt{\frac{z}{2} + 1} + \sqrt{\frac{z}{2}}\right) \asymp \exp(-2z). \end{aligned}$$

□

Another truncation involves using K_s^+ (see Definition (7)) instead of K_s in defining our statistic S_n^+ . This modification not only facilitates the theoretical analysis in Theorem 4.5 but also allows HC to become an exact special case of S_n^+ through the relation (11). Generally, truncating K_s to K_s^+ has mild impact, as for any small $\delta > 0$, $p_{(t)} \leq \frac{t}{n} + \delta$ holds for all $t \in [n]$ with probability approaching one, as demonstrated in the following lemma.

Lemma A.12. Assume p_1, \dots, p_n are i.i.d. copies from $U(0, 1)$ and let $p_{(1)} \leq \dots \leq p_{(n)}$ denote the ordered values. It follows that for any $\delta > 0$,

$$\lim_{n \rightarrow \infty} \mathbb{P}_0(p_{(t)} \leq t/n + \delta, \forall t \in [n]) = 1.$$

Proof of Lemma A.12. To prove this lemma, it suffices to show that for any $\delta > 0$,

$$\lim_{n \rightarrow \infty} \mathbb{P}_0\left(\exists t \in [n] \text{ such that } p_{(t)} \geq \frac{t}{n} + \delta\right) = 0.$$

Fix t, n , and δ . First, consider the case when $\frac{t}{n} + \delta \geq 1$. In this situation, we have $\mathbb{P}_0(p_{(t)} \geq \frac{t}{n} + \delta) = 0$ because $p_{(t)} \in [0, 1]$. Now, consider the case when $\frac{t}{n} + \delta < 1$. By Hoeffding's inequality, we have:

$$\begin{aligned} \mathbb{P}_0\left(p_{(t)} \geq \frac{t}{n} + \delta\right) &= \mathbb{P}_0\left(\sum_{i=1}^n \mathbf{1}_{p_i \geq \frac{t}{n} + \delta} \geq n + 1 - t\right) \\ &\leq \exp\left(-2n \left[1 - \frac{t-1}{n} - \left(1 - \frac{t}{n} - \delta\right)\right]^2\right) \leq \exp(-2n\delta^2). \end{aligned}$$

Combining these two cases, we always have $\mathbb{P}_0\left(p_{(t)} \geq \frac{t}{n} + \delta\right) \leq \exp(-2n\delta^2)$ for any t, n and δ . Using the union bound, it follows that as $n \rightarrow \infty$,

$$\mathbb{P}_0\left(\exists t \in [n] \text{ such that } p_{(t)} \geq \frac{t}{n} + \delta\right) \leq \sum_{t=1}^n \mathbb{P}_0\left(p_{(t)} \geq \frac{t}{n} + \delta\right) \leq n \exp(-2n\delta^2) \rightarrow 0.$$

□

A.6 Proof of Theorem 4.3

Theorem 4.3 (Restated version of Theorem 4.3). *Assume Assumption 4.1 holds and $\mathbf{P}_{1:n} \subset \mathcal{P}_{\Delta_n}$ almost surely with $\Delta_n \asymp n^{-q}$. If $q + 2p < 1$, for Tr-GoF with any $0 \leq c_n^+ \leq \Delta_n$ and $s \in [-1, 2]$, the sum of Type I and Type II errors tends to 0 as $n \rightarrow \infty$.*

To prove Theorem 4.3, we start by introducing two key lemmas. The first lemma shows how $K_s^+(u, v)$ and $K_2^+(u, v)$ are connected numerically for different values of s . Our main focus is to estimate the lower bound of $K_s^+(u, v)$ using $K_2^+(u, v)$. However, it's also possible to establish an upper bound similarly, as shown in Lemma 7.2 of [38], which is left for interested readers.

Lemma A.13. • *For any $s \leq 2$ and $s \neq 1$, it follows that*

$$K_s^+(u, v) \geq K_2^+(u, v) \cdot \left[1 - (1 - v) \left(1 - \left(\frac{v}{u}\right)^{2-s}\right)\right].$$

• *For $s = 1$, it follows that*

$$K_1^+(u, v) \geq K_2^+(u, v) \cdot \frac{v}{u}.$$

Proof of Lemma A.13. If $u < v$, $K_s^+(u, v) = 0$; thus, all the inequalities follow directly. We then assume $0 < v \leq u < 1$. Note that by definition, $K_2(u, v) = \frac{1}{2} \frac{(u-v)^2}{v(1-v)}$ is always non-negative.

• If $s \neq 1$, from the proof of Lemma 7.2 (ii) in [38], it follows that

$$K_s(u, v) = K_2(u, v) [1 + v(1 - v)D_s(u^*, v) - 1],$$

where $u^* \in [v, u]$ is determined by the mean value theorem and $D_s(u^*, v)$ is given by

$$D_s(u, v) = \left(\frac{v}{u}\right)^{2-s} \frac{1}{v} + \left(\frac{1-v}{1-u}\right)^{2-s} \frac{1}{1-v}. \quad (33)$$

Given $v \leq u$ and $s \leq 2$, it follows that

$$-(1 - v) \left[1 - \left(\frac{v}{u}\right)^{2-s}\right] \leq v(1 - v)D_s(u^*, v) - 1 \leq v \left[\left(\frac{1 - v}{1 - u}\right)^{2-s} - 1\right].$$

We then complete the proof by noting that $K_s^+(u, v) = K_s(u, v)$ if $v \leq u$.

- If $s = 1$, from the proof of Theorem 1.1 in [75], we similarly have

$$K_1(u, v) = K_2(u, v) [1 + v(1 - v)D_1(u^*, v) - 1],$$

where $u^* \in [v, u]$ is determined by the mean value theorem and the quantity $D_1(u^*, v)$, according to (33), is given by

$$D_1(u^*, v) = \frac{1}{u^*(1 - u^*)}$$

By the inequality $u^* \in [v, u]$, it follows

$$\frac{v}{u} - 1 \leq v(1 - v)D_1(u^*, v) - 1 \leq \frac{1 - v}{1 - u} - 1.$$

We then complete the proof by noting that $K_s^+(u, v) = K_s(u, v)$ if $v \leq u$.

□

The second lemma establishes constant probabilistic upper and lower bounds for $\frac{\Delta_n}{\mathbb{F}_n(\Delta_n)}$.

Lemma A.14. *Let Assumption 4.1 hold. If $q < 1$, there exists a universal constant $0 < c < C \leq 1$ such that*

$$\lim_{n \rightarrow \infty} \mathbb{P}_1 \left(c \leq \frac{\Delta_n}{\mathbb{F}_n(\Delta_n)} \leq C \right) = 1.$$

Proof of Lemma A.14. We define the σ -field \mathcal{F}_t in the same way as in Lemma A.4. Recall that each p-value is given by $p_t = 1 - Y_t$ and its empirical CDF is equivalently written as

$$\mathbb{F}_n(r) = \frac{1}{n} \sum_{t=1}^n \mathbf{1}_{p_t \leq r} = \frac{1}{n} \sum_{t=1}^n \mathbf{1}_{Y_t \geq 1-r}.$$

We introduce an auxiliary CDF:

$$\bar{\mathbb{F}}_n(r) = \frac{1}{n} \sum_{t=1}^n \mathbb{E}_1[\mathbf{1}_{Y_t \geq 1-r} \mid \mathcal{F}_{t-1}] = \frac{1}{n} \sum_{t=1}^n [(1 - \varepsilon_n)r + \varepsilon_n(1 - F_{1, \mathbf{P}_t}(1 - r))],$$

where the last equation uses Lemma A.4 and $\mathbb{E}[\eta_t] = \varepsilon_n$. Therefore, it follows that

$$\begin{aligned} \frac{\Delta_n}{\bar{\mathbb{F}}_n(\Delta_n)} &= \frac{1}{1 - \varepsilon_n + \frac{\varepsilon_n}{n\Delta_n} \sum_{t=1}^n (1 - F_{1, \mathbf{P}_t}(1 - \Delta_n))} \\ &\stackrel{(a)}{=} \frac{1}{1 - \varepsilon_n + \frac{\varepsilon_n}{n} \sum_{t=1}^n \frac{1 - F_{1, \mathbf{P}_t}(x_n)}{1 - x_n}} \\ &\stackrel{(b)}{\in} (c, C), \end{aligned}$$

where (a) uses the notation $x_n = 1 - \Delta_n$ and (b) follows from Lemma A.10 which shows $\frac{1 - F_{1, \mathbf{P}_t}(x_n)}{1 - x_n}$ is bounded above and below by positive constants c and C for sufficiently large n .

To finish the proof, it suffices to focus on the concentration of $\frac{\mathbb{F}_n(\Delta_n)}{\bar{\mathbb{F}}_n(\Delta_n)} - 1$. On the one hand, it follows from (31) that

$$\mathbb{E}_1 |\mathbb{F}_n(\Delta_n) - \bar{\mathbb{F}}_n(\Delta_n)|^2 = \frac{1}{n^2} \mathbb{E}_1 \sum_{t=1}^n \text{Var}_1[\mathbf{1}_{Y_t \geq 1 - \Delta_n} \mid \mathcal{F}_{t-1}] \leq \frac{|\text{Voc}| \cdot \Delta_n}{n},$$

where the last inequality uses Lemma A.10. On the other hand, it follows almost surely that

$$\bar{\mathbb{F}}_n(\Delta_n) \geq (1 - \varepsilon_n) \Delta_n.$$

As a result, it follows that

$$\mathbb{E}_1 \left| \frac{\mathbb{F}_n(\Delta_n)}{\bar{\mathbb{F}}_n(\Delta_n)} - 1 \right|^2 \leq \frac{|\text{Voc}|}{n(1 - \varepsilon_n)^2 \Delta_n} \rightarrow 0,$$

where we use the fact that $q < 1$ so that $n\Delta_n \rightarrow \infty$ as $n \rightarrow \infty$. It implies that $\frac{\mathbb{F}_n(\Delta_n)}{\bar{\mathbb{F}}_n(\Delta_n)}$ converges to 1 in probability, as a result of which, we complete the proof by using Slutsky's Theorem. \square

Now we have the tools in place to prove Theorem 4.3.

Proof of Theorem 4.3. We start by analyzing the Type I error. Under H_0 , Y_t 's are i.i.d. $U(0, 1)$ so that $\mathbb{F}_n(r)$ is the empirical CDF of n i.i.d. $U(0, 1)$ random variables. We first note that S_n^+ can be equivalently written as

$$S_n^+(s) := \begin{cases} \sup_{r \in [\mathfrak{p}^+, 1]} K_s^+(\mathbb{F}_n(r), \mathbb{F}_0(r)), & \text{if } s \geq 1, \\ \sup_{r \in [\mathfrak{p}_{(1)}, \mathfrak{p}_{(n)}] \cap [\mathfrak{p}^+, 1]} K_s^+(\mathbb{F}_n(r), \mathbb{F}_0(r)), & \text{if } s < 1. \end{cases}$$

where c_n^+ is the custom threshold for stability concern and $\mathfrak{p}_{(t)}$ is the t th smallest p-value. The equivalence follows because we have the following equities when $s < 1$ by definition:

$$\begin{aligned} \sup_{r \in (0, \mathfrak{p}_{(1)})} K_s^+(\mathbb{F}_n(r), \mathbb{F}_0(r)) &= 0, \\ \sup_{r \in (\mathfrak{p}_{(n)}, 1)} K_s^+(\mathbb{F}_n(r), \mathbb{F}_0(r)) &= K_s^+(1, \mathfrak{p}_{(n)}) = K_s^+(\mathbb{F}_n(\mathfrak{p}_{(n)}), \mathbb{F}_0(\mathfrak{p}_{(n)})). \end{aligned}$$

Under H_0 , [38] analyzes the null distribution of another related statistic $S_n(s)$, which is defined by

$$S_n(s) := \begin{cases} \sup_{r \in (0, 1)} K_s(\mathbb{F}_n(r), \mathbb{F}_0(r)), & \text{if } s \geq 1, \\ \sup_{r \in [\mathfrak{p}_{(1)}, \mathfrak{p}_{(n)}]} K_s(\mathbb{F}_n(r), \mathbb{F}_0(r)), & \text{if } s < 1. \end{cases}$$

Theorem 3.1 in [38] shows that for any $s \in [-1, 2]$, as $n \rightarrow \infty$, the following weak convergence holds:

$$nS_n(s) - b_n \xrightarrow{d} Z, \tag{34}$$

where $b_n = \log \log n + \frac{1}{2} \log \log \log n - \frac{1}{2} \log(4\pi)$ and $\mathbb{P}(Z \leq r) = e^{-4e^{-r}}$ for any $r \in \mathbb{R}$. Note that $S_n(s) \geq S_n^+(s)$ and $\frac{r_n}{\log \log n} \rightarrow 1$. It then follows that for any $\delta > 0$, as $n \rightarrow \infty$,

$$\mathbb{P}_0(nS_n^+(s) \geq (1 + \delta) \log \log n) \leq \mathbb{P}_0(nS_n(s) \geq (1 + \delta) \log \log n) \rightarrow 0.$$

We then focus on the Type II error. By the condition $\Delta_n \geq p^+$, it follows that

$$nS_n^+(s) = \sup_{r \in [p^+, 1]} nK_s^+(\mathbb{F}_n(r), \mathbb{F}_0(r)) \geq nK_s^+(\mathbb{F}_n(\Delta_n), \Delta_n).$$

If $s \in [-1, 2]$ and $s \neq 1$, it follows that

$$\begin{aligned} nK_s^+(\mathbb{F}_n(\Delta_n), \Delta_n) &\stackrel{(a)}{\geq} nK_2^+(\mathbb{F}_n(\Delta_n), \Delta_n) \cdot \left[1 - (1 - \Delta_n) \left(1 - \left(\frac{\Delta_n}{\mathbb{F}_n(\Delta_n)} \right)^{2-s} \right) \right] \\ &\stackrel{(b)}{\geq} nK_2^+(\mathbb{F}_n(\Delta_n), \Delta_n) \cdot \Omega_{\mathbb{P}}(1) \\ &\stackrel{(c)}{\geq} \Omega_{\mathbb{P}}(n^{1-2p-q}), \end{aligned}$$

where (a) uses Lemma A.13, (b) uses Lemma A.14 with $\Omega_{\mathbb{P}}(1)$ denoting a random variable which is bounded below with probability one, and (c) uses the relation that $nK_2^+(\mathbb{F}_n(\Delta_n), \Delta_n) = \frac{1}{2} W_n^2(\Delta_n)$ with W_n defined in (27) and the lower bound for $W_n(\Delta_n)$ in (32).

From the last inequality, we know that with probability one, $nK_s^+(\mathbb{F}_n(\Delta_n), \Delta_n) \rightarrow \infty$ as long as $q + 2p < 1$. The analysis for the case where $s = 1$ is almost the same and thus omitted. \square

A.7 Proof of Theorem 4.4

In this section, we will prove Theorem 4.4. To that end, we need first to figure out the expectation gaps of different score functions.

A.7.1 Expectation Gap

Let $T_n^{\text{ars}} = \sum_{t=1}^n h_{\text{ars}}(Y_t)$ denote the sum of scores. Aaronson [1] argued that if $w_{1:n}$ is LLM-generated, then

$$\mathbb{E}_1 T_n^{\text{ars}} \geq n + \left(\frac{\pi^2}{6} - 1 \right) \sum_{t=1}^n \mathbb{E}_1 \text{Ent}(\mathbf{P}_t), \quad (35)$$

where $\text{Ent}(\mathbf{P}_t)$ is the Shannon entropy defined by $\text{Ent}(\mathbf{P}_t) := - \sum_{w \in \text{Voc}} P_{t,w} \log P_{t,w}$. Here the expectation $\mathbb{E}_1(\cdot)$ is taken with respect to the token distributions $\mathbf{P}_1, \dots, \mathbf{P}_n$. In his talk [1], he did not furnish a proof for it. We prove the lower bound and establish a new upper bound in the following proposition. We note that while Fernandez et al. [23] attempts to offer a proof for (35), the inequality they demonstrate differs from that specified in (35) because they use a different notion of entropy.

Proposition A.1.

$$n + \sum_{t=1}^n \mathbb{E}_1 \text{Ent}(\mathbf{P}_t) \geq \mathbb{E}_1 T_n^{\text{ars}} \geq n + \left(\frac{\pi^2}{6} - 1 \right) \sum_{t=1}^n \mathbb{E}_1 \text{Ent}(\mathbf{P}_t).$$

Proof of Proposition A.1. We first evaluate the following integral

$$\begin{aligned}
-\frac{1}{p} \int_0^1 r^{1/p-1} \log(1-r) dr &\stackrel{(a)}{=} \int_0^1 \frac{1-r^{1/p}}{1-r} dr \\
&\stackrel{(b)}{=} \sum_{j=1}^{\infty} \left(\frac{1}{j} - \frac{1}{j+1/p} \right) \\
&\stackrel{(c)}{=} p + \psi(1/p) - \psi(1) \\
&\stackrel{(d)}{=} \psi(1+1/p) - \psi(1)
\end{aligned}$$

where (a) uses integration by parts, (b) applies Taylor's expansion to $(1-r)^{-1}$, (c) uses the definition of the digamma function that is $\psi(x) := -\gamma + \sum_{j=0}^{\infty} \left(\frac{1}{j+1} - \frac{1}{j+x} \right)$ for any $x > 0$ with γ the Euler–Mascheroni constant, and (d) uses the property that $\psi(1+x) = \psi(x) + \frac{1}{x}$ for any $x > 0$.

Recall that an important property of the digamma function from Theorem 2 (a) in [22] is that for any $x \geq 1$,⁸

$$\frac{1}{x + \frac{1}{\frac{\pi^2}{6} - 1} - 1} \leq \psi'(1+x) \leq \frac{1}{x + \frac{1}{2}},$$

which implies that for any $x \geq 1$,

$$\left(\frac{\pi^2}{6} - 1 \right) \log x \leq \psi(1+x) - \psi(2) \leq \log x.$$

By setting $x = 1/P_{t,w}$ and summing over $w \in \text{Voc}$, we have

$$\begin{aligned}
-\mathbb{E}_{1, \mathbf{P}_t} \log(1 - U_{t,w_t}) dr - 1 &= - \int_0^1 \sum_{w \in \text{Voc}} r^{1/P_{t,w}-1} \log(1-r) dr - 1 \\
&= \sum_{w \in \text{Voc}} P_{t,w} \left[\psi \left(1 + \frac{1}{P_{t,w}} \right) - \psi(2) \right] \\
&\in \left[\left(\frac{\pi^2}{6} - 1 \right) \text{Ent}(\mathbf{P}_t), \text{Ent}(\mathbf{P}_t) \right],
\end{aligned}$$

where $\text{Ent}(\mathbf{P}_t) = \sum_{w \in \text{Voc}} P_{t,w} \log \left(\frac{1}{P_{t,w}} \right)$ is the Shannon entropy of $\mathbf{P}_t = (P_{t,1}, \dots, P_{t,|\text{Voc}|})$. \square

Proposition A.1 essentially provides a tight bound for the expectation gap of h_{ars} , that is,

$$\mathbb{E}_{1, \mathbf{P}} h_{\text{ars}}(Y) - \mathbb{E}_0 h_{\text{ars}}(Y) = \Theta(1) \cdot \text{Ent}(\mathbf{P})$$

where $\Theta(1)$ denotes a universal constant. In the following, we provide tight bounds (up to constant factors) of the expectation gaps for other score functions.

⁸This inequality deviates slightly from the original version (see Theorem 2 (a) in [22]). It can be established using the same methodology they employed, with the alteration being the adjustment of the domain from $u \geq 1$ to $u \geq 2$, where x is defined according to their context. In this way, their inequality (20) becomes $2 - \frac{1}{\psi'(2)} \leq (\psi')^{-1}(1/t) - t < 1/2$ where $t = 1/\psi'(u)$ and $u \geq 2$.

Proposition A.2. Let $\Delta = 1 - P_{\max}$ be the gap between 1 and the largest probability in \mathbf{P} . Once Δ is smaller than a universal constant $c \in (0, 1)$, it follows that

- For h_{ars} , $\mathbb{E}_{1, \mathbf{P}} h_{\text{ars}}(Y) - \mathbb{E}_0 h_{\text{ars}}(Y) = \Theta(1) \cdot \text{Ent}(\mathbf{P}) = \Theta(\Delta \log \frac{1}{\Delta})$.
- For h_{\log} , $\mathbb{E}_{1, \mathbf{P}} h_{\log}(Y) - \mathbb{E}_0 h_{\log}(Y) = 1 - \sum_{w \in \text{Voc}} P_w^2 = \Theta(\Delta)$.
- For $h_{\text{ind}, \delta}$ with $\delta \in (0, 1)$, $\mathbb{E}_{1, \mathbf{P}} h_{\text{ind}, \delta}(Y) - \mathbb{E}_0 h_{\text{ind}, \delta}(Y) = \delta - F_{\mathbf{P}}(\delta) = \Theta(\Delta)$.
- For h_{opt, Δ_0} with $\Delta_0 \in (0, 1)$, $\mathbb{E}_{1, \mathbf{P}} h_{\text{opt}, \Delta_0}(Y) - \mathbb{E}_0 h_{\text{opt}, \Delta_0}(Y) = \Theta(\Delta)$.

Here $\Theta(1)$ denotes a positive constant that depends on c , the log factor $\log |\text{Voc}|$ if we consider h_{ars} , δ if we consider $h_{\text{ind}, \delta}$, and Δ_0 if we consider h_{opt, Δ_0} .

In fact, we have the following general result for the expectation gap of increasing score functions.

Lemma A.15. We say a score function h is parameter-free if for any $y \in [0, 1]$, $h(y)$ does not depend on Δ and ε . Let $\Delta = 1 - P_{\max}$ be the gap between 1 and the largest probability in \mathbf{P} . For any parameter-free score function $h : [0, 1] \rightarrow \mathbb{R}$, as long as it is increasing and satisfies $\int_0^1 y \log \frac{1}{y} dh(y) > 0$ and $h(1) - h(0) < \infty$, it follows that for sufficiently small Δ ,

$$\mathbb{E}_{1, \mathbf{P}} h(Y) - \mathbb{E}_0 h(Y) = \Theta(\Delta).$$

Remark A.3. Since $h_{\text{ars}}(1) = \infty$, h_{ars} does not satisfy the condition in Lemma A.15, resulting in an expectation gap of $\Theta(\Delta \log \frac{1}{\Delta})$ rather than $\Theta(\Delta)$.

Remark A.4. If h is non-decreasing, non-constant, and does not have discontinuities at both 0 and 1, then we have both (i) $h(1) - h(0) < \infty$ and (ii) $\int_0^1 y \log \frac{1}{y} dh(y) > 0$. We prove (ii) as follows.

As a non-decreasing function, h introduces a measure on $[0, 1]$, which we denote by μ_h . Since 0 and 1 are not discontinuous points of h , μ_h assigns all of its probability mass on $(0, 1)$. Therefore, there must exist an interval (a, b) satisfying $0 < a < b < 1$ and $\mu_h(a, b) = h(b) - h(a-) > 0$. Thus, we have:

$$\int_0^1 y \log \frac{1}{y} dh(y) \geq \min_{y \in [a, b]} y \log \frac{1}{y} \cdot \mu_h(a, b) > 0.$$

Proof of Lemma A.15. Using the integration by parts, we have that

$$\mathbb{E}_{1, \mathbf{P}} h(Y) - \mathbb{E}_0 h(Y) = \int_0^1 [y - F_{1, \mathbf{P}}(y)] dh(y)$$

where $F_{1, \mathbf{P}}$ is the conditional CDF of watermarked Y given \mathbf{P} . Let P_{\max} denote the largest probability in \mathbf{P} . We then have that (see the third bullet point in Proposition A.2):

$$y - y^{1/P_{\max}} \leq y - F_{1, \mathbf{P}}(y) \leq y - P_{\max} y^{1/P_{\max}} \leq \Delta + P_{\max}(y - y^{1/P_{\max}}).$$

It then suffices to show

$$\int_0^1 (y - y^{1/P_{\max}}) dh(y) = \Theta(\Delta).$$

We introduce an auxiliary function $J : [0, 1] \rightarrow \mathbb{R}$ defined by

$$J(p) := \int_0^1 (y - y^{1/p}) dh(y).$$

We note that $J(1) = 0$ and $J'(1) = -\int_0^1 y \log \frac{1}{y} dh(y)$. Because the score function h is parameter-free, we conclude that $J'(1)$ depends on neither Δ nor ε . Furthermore, by assumption, $J'(1) < 0$. Hence, it follows from Taylor's expansion that

$$J(P_{\max}) = J(1) + J'(1)(P_{\max} - 1) + O(1) \cdot (1 - P_{\max})^2 = (-J'(1)) \cdot \Delta + o(\Delta)$$

As long as Δ is sufficiently small, we would have $J(P_{\max}) = \Theta(\Delta)$. \square

Finally, we provide the proof of Proposition A.2 below.

Proof of Proposition A.2. This proposition mainly follows from the following inequalities.

- We first note that

$$\begin{aligned} \text{Ent}(\mathbf{P}) &= P_{\max} \log \frac{1}{P_{\max}} + (1 - P_{\max}) \log \frac{1}{1 - P_{\max}} \\ &\quad + (1 - P_{\max}) \sum_{w: P_w \neq P_{\max}} \frac{P_w}{1 - P_{\max}} \log \frac{1 - P_{\max}}{P_w}. \end{aligned}$$

It is easy to find the lower bound holds: $\text{Ent}(\mathbf{P}) \geq (1 - P_{\max}) \log \frac{1}{1 - P_{\max}} = \Delta \log \frac{1}{\Delta}$. For the upper bound, we note that if $P_{\max} \geq 1 - c$ (due to $\Delta \leq c$),

$$\text{Ent}(\mathbf{P}) \leq \frac{\Delta}{c} + \Delta \log \frac{1}{\Delta} + \Delta \log(|\text{Voc}| - 1) = \Theta\left(\Delta \log \frac{1}{\Delta}\right).$$

- It follows that $1 - P_{\max} \leq 1 - \sum_{w \in \text{Voc}} P_w^2 \leq 1 - P_{\max}^2 \leq 2(1 - P_{\max})$.
- Due to $P_{\max} \delta^{1/P_{\max}} \leq F_{\mathbf{P}}(\delta) \leq \delta^{1/P_{\max}}$, once we set $g(x) = \delta^x$, the mean value theorem implies that

$$g(1) - g\left(\frac{1}{P_w}\right) = g'(\theta) \left(1 - \frac{1}{P_w}\right) \stackrel{(*)}{=} \Theta(1 - P_{\max})$$

where $\theta \in [1, 1/P_{\max}]$. Given P_{\max} is smaller than a constant, say c , we have that $-g'(\theta)$ is a positive constant that depends only on δ and c , which implies the above equation (*).

- We first consider the simplest case where $\Delta_0 \in (0, 0.5)$,

$$h_{\text{opt}, \Delta_0}(y) = \log \left(y^{\frac{\Delta_0}{1 - \Delta_0}} + y^{\frac{1}{\Delta_0} - 1} \right) = \frac{\Delta_0}{1 - \Delta_0} \log y + \log \left(1 + y^{\frac{1 - \Delta_0}{\Delta_0} - \frac{\Delta_0}{1 - \Delta_0}} \right).$$

We note that by integration by parts, it follows that

$$\begin{aligned} \mathbb{E}_{1, \mathbf{P}} h_{\text{opt}, \Delta_0}(Y) - \mathbb{E}_0 h_{\text{opt}, \Delta_0}(Y) &= \frac{\Delta_0}{1 - \Delta_0} [\mathbb{E}_{1, \mathbf{P}} h_{\log}(Y) - \mathbb{E}_0 h_{\log}(Y)] \\ &\quad + \int_0^1 \frac{y - F_{\mathbf{P}}(y)}{1 + y^{\frac{1 - \Delta_0}{\Delta_0} - \frac{\Delta_0}{1 - \Delta_0}}} dy^{\frac{1 - \Delta_0}{\Delta_0} - \frac{\Delta_0}{1 - \Delta_0}} \\ &= \frac{\Delta_0}{1 - \Delta_0} \cdot \Theta(\Delta) + \Theta(\Delta). \end{aligned}$$

where the second equation uses the result in the second bullet point and the inequality that $0 \leq y - F_{\mathbf{P}}(y) \leq \Theta(\Delta) \cdot \ln \frac{1}{y}$ (which is already proved in the third bullet point).

We complete the proof by noting that the above argument can be extended to the general case where $\Delta_0 \in (0, 1)$. \square

A.7.2 Failure of Existing Sum-based Detection Rules

Theorem 4.4 (Restated version of Theorem 4.4). *Let Assumption 4.1 hold. Consider the detection rule specified by h : $T_h(Y_{1:n}) = 1$ if $\sum_{t=1}^n h(Y_t) \geq n \cdot \mathbb{E}_0 h(Y) + \Theta(1) \cdot n^{\frac{1}{2}} a_n$, otherwise it equals 0, where $a_n \rightarrow \infty$ and $\frac{a_n}{n^\gamma} \rightarrow 0$ for any $\gamma > 0$. For any score function that is (i) non-decreasing, (ii) non-constant, (iii) parameter-free, and (iv) does not have discontinuities at both 0 and 1, the following results hold for T_h :*

- If $q + p < \frac{1}{2}$ and $\mathbf{P}_{1:n} \subset \mathcal{P}_{\Delta_n}$, the sum of Type I and Type II errors tends to 0.
- If $q + p > \frac{1}{2}$ and $\mathbf{P}_{1:n} \subset \mathcal{P}_{\Delta_n}^c$, the sum of Type I and Type II errors tends to 1.

Proof of Theorem 4.4. Recall that the considered detection rule has the following form:

$$T_h(Y_{1:n}) = \begin{cases} 1 & \text{if } \sum_{t=1}^n h(Y_t) \geq n \cdot \mathbb{E}_0 h(Y) + C \cdot n^{\frac{1}{2}} a_n, \\ 0 & \text{if } \sum_{t=1}^n h(Y_t) < n \cdot \mathbb{E}_0 h(Y) + C \cdot n^{\frac{1}{2}} a_n, \end{cases}$$

where $\{a_n\}$ is a positive sequence satisfying $a_n \rightarrow \infty$ and $\frac{a_n}{n^\gamma} \rightarrow 0$.

By the choice of the sequence $\{a_n\}$, the Markov inequality implies that the Type I error converges to zero as $n \rightarrow \infty$,

$$\mathbb{P}_0(T_h(Y_{1:n}) = 1) = \mathbb{P}_0 \left(\sum_{t=1}^n [h(Y_t) - \mathbb{E}_0 h(Y)] \geq C \cdot n^{\frac{1}{2}} a_n \right) \leq \frac{\text{Var}_0(h(Y))}{C^2 a_n^2} \rightarrow 0.$$

We then focus on the Type II error. By Lemma A.4, we have that

$$\mathbb{E}_1[h(Y_t) \mid \mathcal{F}_{t-1}] = (1 - \varepsilon_n) \mathbb{E}_0 h(Y_t) + \varepsilon_n \mathbb{E}_{1, \mathbf{P}_t} h(Y_t).$$

Therefore, the Type II error can be equivalently written as

$$\mathbb{P}_1(T_h(Y_{1:n}) = 0) = \mathbb{P}_1 \left(\frac{X_n}{\sqrt{n}} \leq \frac{\bar{X}_n}{\sqrt{n}} + C a_n \right),$$

where we denote by

$$X_n = \sum_{t=1}^n (h(Y_t) - \mathbb{E}_1[h(Y_t) \mid \mathcal{F}_{t-1}]) \quad \text{and} \quad \bar{X}_n = \sum_{t=1}^n (\mathbb{E}_0 h(Y_t) - \mathbb{E}_1[h(Y_t) \mid \mathcal{F}_{t-1}]).$$

By the construction of an embedded watermark, we know that X_n is a square-integrable martingale under H_1^{mix} . For the considered score functions, given that the alternative CDF of $h(Y_t)$ is continuous in \mathbf{P} , we know its conditional variance is also continuous in \mathbf{P} such that it is bounded uniformly over $\mathbf{P} \in \text{Simp}(\text{Voc})$. It implies that there exists some $C > 0$ so that for any $n \geq 1$,

$$\mathbb{E}_1 |X_n|^2 \leq C \cdot n.$$

On the other hand, by Lemma A.15, it follows that

$$\bar{X}_n = -\Theta \left(\varepsilon_n \sum_{t=1}^n (1 - P_{t, \max}) \right).$$

- If $p + q < \frac{1}{2}$ and $\mathbf{P}_{1:n} \subset \mathcal{P}_{\Delta_n}$, we then have that

$$\bar{X}_n \leq -\Theta(n \cdot \varepsilon_n \cdot \Delta_n).$$

By condition $\frac{a_n}{n^{1/2-p-q}} \rightarrow 0$, we have $\frac{\bar{X}_n}{\sqrt{n}} \rightarrow -\infty$ as $n \rightarrow \infty$. Hence, by Chebyshev's inequality, it follows that as long as n is sufficiently large,

$$\mathbb{P}_1(T_h(Y_{1:n}) = 0) \leq \mathbb{P}_1\left(\left|\frac{X_n}{\sqrt{n}}\right| \geq \left|\frac{\bar{X}_n}{\sqrt{n}}\right| - Ca_n\right) \leq \frac{O(1)}{n^{\frac{1}{2}-p-q}} \rightarrow 0.$$

- If $p + q > \frac{1}{2}$ and $\mathbf{P}_{1:n} \subset \mathcal{P}_{\Delta_n}^c$, we then have that

$$0 \geq \bar{X}_n \geq -\Theta(n \cdot \varepsilon_n \cdot \Delta_n),$$

which implies that $\frac{\bar{X}_n}{\sqrt{n}} \rightarrow 0$ as $n \rightarrow \infty$. Hence, by Chebyshev's inequality, it follows that as long as n is sufficiently large,

$$\mathbb{P}_1(T_h(Y_{1:n}) = 1) \leq \mathbb{P}_1\left(\left|\frac{X_n}{\sqrt{n}}\right| \geq Ca_n - \left|\frac{\bar{X}_n}{\sqrt{n}}\right|\right) \leq \frac{O(1)}{a_n^2} \rightarrow 0.$$

The case for h_{ars} where $\bar{X}_n = -\Theta\left(\sum_{t=1}^n \varepsilon_n(1 - P_{t,\max}) \log \frac{1}{1 - P_{t,\max}}\right)$ can be analyzed similarly and thus omitted. \square

A.8 Proof of Theorem 4.5

Proof of Theorem 4.5. By the definition of the \mathcal{P}_{Δ} -efficiency (in Definition 4.1), we should analyze the rate of the exponential decrease of the Type II error $\mathbb{P}_1(S_n^+(s) \leq \gamma_{n,\alpha})$ where $\gamma_{n,\alpha}$ is the critical value satisfying $\mathbb{P}_0(S_n^+(s) \geq \gamma_{n,\alpha}) = \alpha$. By Theorem 4.3, it follows that $\gamma_{n,\alpha} = O\left(\frac{\log \log n}{n}\right)$. It implies that for any small $\varepsilon_0 > 0$, as long as n is sufficiently large, we have

$$\mathbb{P}_1(S_n^+(s) \leq \gamma_{n,\alpha}) \leq \mathbb{P}_1(S_n^+(s) \leq \varepsilon_0). \quad (36)$$

Subsequently, we focus on the probability $\mathbb{P}_1(S_n^+(s) \leq \varepsilon_0)$. To this end, we need two auxiliary lemmas. The first one, Lemma A.16, bounds the event $\{S_n^+(s) \leq \varepsilon_0\}$ with a more manageable one.

Lemma A.16. *Let $s \in (0, 1)$ and $c_n^+ = 0$. For any $\varepsilon_0 \rightarrow 0$, there exists $\delta_0 \rightarrow 0$ so that the following event inclusion holds:*

$$\{S_n^+(s) \leq \varepsilon_0\} \subseteq \{\mathbb{F}_n(r) \leq r + \delta_0, \forall r \in [0, 1]\}$$

where $\mathbb{F}_n(r) = \frac{1}{n} \sum_{t=1}^n \mathbf{1}_{p_t \leq r}$ is the empirical CDF of observed p-values (where $p_t = 1 - Y_t$).

Proof of Lemma A.16. When $s \in (0, 1)$, $K_s(u, v)$ is jointly continuous in the closed domain $[0, 1]^2$, so it is uniformly continuous. By defining an auxiliary function J by $J(x) = \sup_{v \in [0, 1]} K_s(v + x, v)$, we have that J is a continuous function.

On the other hand, $K_s(u, u) = 0$ and $\frac{\partial}{\partial u} K_s(u, v) = \frac{1}{1-s} \left[\left(\frac{1-v}{1-u}\right)^{1-s} - \left(\frac{v}{u}\right)^{1-s} \right] \geq 0$ if $u \geq v$. It's easy to see that $K_s(\cdot, v)$ is strictly increasing on $[v, 1]$. As a result, J is an increased function on $[0, 1]$. As $J(0) = 0$, for any $\varepsilon_0 \rightarrow 0$, there exists $\delta_0 \rightarrow 0$ so that $\{x \geq 0 : J(x) \leq \varepsilon_0\} = \{x \geq 0 : x \leq \delta_0\}$. In fact, we should have $\delta_0 = J(\varepsilon_0)$.

We aim to analyze the event $\{S_n^+(s) \leq \varepsilon_0\}$ for a given ε_0 . As $c_n^+ = 0$, we have that $S_n^+(s) = \sup_{r \in [0,1]} K_s^+(\mathbb{F}_n(r), r) = \sup_{r \in [0,1]} K_s(\mathbb{F}_n(r), r) \mathbf{1}_{\mathbb{F}_n(r) \geq r}$. It then follows that $\{S_n^+(s) \leq \varepsilon_0\} \subseteq \{\mathbb{F}_n(r) - r \leq \delta_0, \forall r \in [0, 1]\}$. \square

The second lemma examines the superiority of \mathbf{P}_t over \mathcal{P}_Δ in terms of the CDF value.

Lemma A.17. *Let $F_{1,\mathbf{P}}(r) = \mu_{1,\mathbf{P}}(Y \leq r) = \sum_{w \in \text{Voc}} P_w r^{1/P_w}$. It then follows that for any $r \in [0, 1]$,*

$$\sup_{\mathbf{P} \in \mathcal{P}_\Delta} F_{1,\mathbf{P}}(r) = F_{1,\mathbf{P}_\Delta^*}(r)$$

where \mathbf{P}_Δ^* is defined in (12).

Proof of Lemma A.17. Note that $F_{1,\mathbf{P}}(r)$ is convex in \mathbf{P} in any $r \in [0, 1]$. A similar argument of Lemma 3.3 in [48] can prove this lemma. \square

Recall that $p_t = 1 - Y_t$. By Lemma A.4, we know that the CDF of p_t conditioned on \mathcal{F}_{t-1} depends only on \mathbf{P}_t . We denote the CDF of p_t conditioned on \mathcal{F}_t by $G_{\mathbf{P}_t}$. It then follows from Lemma A.4 that for any $r \in [0, 1]$,

$$G_{\mathbf{P}_t}(r) = \mathbb{P}_1(Y_t \geq 1 - r | \mathbf{P}_t) = (1 - \varepsilon)r + \varepsilon[1 - F_{1,\mathbf{P}_t}(1 - r)].$$

By Lemma A.17, it follows that $G_{\mathbf{P}_t}(r) \geq G_{\mathbf{P}_\Delta^*}(r)$ for any $r \in [0, 1]$ and $t \geq 1$ (since $\mathbf{P}_t \in \mathcal{P}_\Delta$ by the definition of \mathcal{P}_Δ -efficiency). Note that each $G_{\mathbf{P}}$ is strictly increasing and continuous, then its inverse exists uniquely which we denote by $G_{\mathbf{P}}^{-1}$. It follows that for any $r \in [0, 1]$,

$$G_{\mathbf{P}_t}^{-1}(r) \leq G_{\mathbf{P}_\Delta^*}^{-1}(r). \quad (37)$$

Now, we are ready to prove this theorem.

$$\begin{aligned} \mathbb{P}_1(S_n^+(s) \leq \gamma_{n,\alpha}) &\stackrel{(a)}{\leq} \mathbb{P}_1(S_n^+(s) \leq \varepsilon_0) \\ &\stackrel{(b)}{\leq} \mathbb{P}_1(\mathbb{F}_n(r) \leq r + \delta_0, \forall r \in [0, 1]) \\ &= \mathbb{P}_1\left(\mathbb{F}_n\left(G_{\mathbf{P}_\Delta^*}^{-1}(r)\right) \leq G_{\mathbf{P}_\Delta^*}^{-1}(r) + \delta_0, \forall r \in [0, 1]\right) \\ &\stackrel{(c)}{\leq} \mathbb{P}_1\left(\frac{1}{n} \sum_{t=1}^n \mathbf{1}_{p_t \leq G_{\mathbf{P}_t}^{-1}(r)} \leq G_{\mathbf{P}_\Delta^*}^{-1}(r) + \delta_0, \forall r \in [0, 1]\right) \\ &\stackrel{(d)}{=} \mathbb{P}_1\left(\frac{1}{n} \mathbf{N}(nr) \leq G_{\mathbf{P}_\Delta^*}^{-1}(r) + \delta_0, \forall r \in [0, 1]\right), \end{aligned}$$

where (a) uses (36), (b) uses Lemma A.16, (c) uses (37), and (d) uses the fact that $G_{\mathbf{P}_t}(p_t) \stackrel{i.i.d.}{\sim} U(0, 1)$, as a result of which, $\frac{1}{n} \sum_{t=1}^n \mathbf{1}_{p_t \leq G_{\mathbf{P}_t}^{-1}(r)} = \frac{1}{n} \sum_{t=1}^n \mathbf{1}_{G_{\mathbf{P}_t}(p_t) \leq r}$ has the same distribution of $\frac{1}{n} \mathbf{N}(nr)$ where $\mathbf{N}(t)$ is a Poisson process with parameter 1 under the condition that $\mathbf{N}(n) = n$. We emphasize that the right-hand side of (d) does not depend on the NTP distributions \mathbf{P}_t 's.

We will apply Theorem 2 in [57] to bound the right-hand side of (d). To do this, we need to verify that $G_{\mathbf{P}_\Delta^*}^{-1}(r)$ is a convex function of r , which is a prerequisite of that Theorem 2. This follows

easily from the fact that $F_{1, \mathbf{P}_\Delta^*}(r)$ is a convex function of r . Therefore, by Theorem 2 in [57], it follows that

$$\begin{aligned} \lim_{\varepsilon_0 \rightarrow 0} \lim_{n \rightarrow \infty} \frac{1}{n} \log \mathbb{P}_1 \left(\frac{1}{n} \mathbf{N}(nr) \leq G_{\mathbf{P}_\Delta^*}^{-1}(r) + \delta_0, \forall r \in [0, 1] \right) &\leq - \int_0^1 [G_{\mathbf{P}_\Delta^*}^{-1}]'(r) \log [G_{\mathbf{P}_\Delta^*}^{-1}]'(r) dr \\ &= -D_{\text{KL}}(\mu_0, (1 - \varepsilon)\mu_0 + \varepsilon\mu_{1, \mathbf{P}_\Delta^*}), \end{aligned}$$

where $[G_{\mathbf{P}_\Delta^*}^{-1}]'$ is the derivative of $G_{\mathbf{P}_\Delta^*}^{-1}$. The proof technique used therein is mainly adapted from the classic works [7, 6] that study large deviations in boundary-value problems. As a result, we prove the upper bound:

$$\limsup_{n \rightarrow \infty} \sup_{\mathbf{P}_t \in \mathcal{P}_\Delta} \frac{1}{n} \log \mathbb{P}_1(S_n^+(s) \leq \gamma_{n, \alpha}) \leq -D_{\text{KL}}(\mu_0, (1 - \varepsilon)\mu_0 + \varepsilon\mu_{1, \mathbf{P}_\Delta^*}).$$

For the lower bound, it essentially follows from the worst nature:

$$\begin{aligned} \liminf_{n \rightarrow \infty} \sup_{\mathbf{P}_t \in \mathcal{P}_\Delta} \frac{1}{n} \log \mathbb{P}_1(S_n^+(s) \leq \gamma_{n, \alpha}) &\geq \liminf_{n \rightarrow \infty} \sup_{\mathbf{P}_t \in \{\mathbf{P}_\Delta^*\}} \frac{1}{n} \log \mathbb{P}_1(S_n^+(s) \leq \gamma_{n, \alpha}) \\ &\stackrel{(*)}{\geq} -D_{\text{KL}}(\mu_0, (1 - \varepsilon)\mu_0 + \varepsilon\mu_{1, \mathbf{P}_\Delta^*}). \end{aligned}$$

We explain the last inequality (*) as follows. When $\mathbf{P}_t \equiv \mathbf{P}_\Delta^*$, we are essentially dealing with an i.i.d. case where the alternative CDF of each Y_t is $G_{\mathbf{P}_\Delta^*}$. The inequality (*) represents the lower bound for i.i.d. case efficiency, where our \mathcal{P}_Δ -efficiency reduces to the Hodges-Lehmann efficiency [57]. This inequality (*) follows from the existing lower bound found in [66].

Combining these two parts, we complete the proof. \square

B Details of Simulation Studies

B.1 Additional Histogram of Tr-GoF Statistics

In Figure 16, we present the density histograms and powers of $\log(nS_n^+(s))$ for different values of s with $c_n^+ = 0$ and $(p, q) = (0.2, 0.5)$, following the same setting introduced in Section 5.1. We observe that even with c_n^+ set to 0, the patterns identified in Figure 7 are still maintained, except that the support under H_1^{mix} is considerably larger due to the heavy-tailed behavior of $p_{(1)}$.

B.2 Histograms of HC

Though HC_n^+ is connected to $S_n^+(s)$ via the square relation in (11), their distribution might have slightly different shapes and ranges. We perform an empirical study of the distribution of HC_n^+ and HC_n^* in this subsection. Recall that HC_n^* is the special instance of HC_n^+ where $c_n^+ = 0$. We set $\Delta_n = n^{-q}$ and $\varepsilon_n = n^{-p}$, and use the following procedure to create samples from null and alternative.

1. Draw $n = 10^4$ samples from $U(0, 1)$ to represent H_0 and then calculate HC_n^+ or HC_n^* .
2. Replace $\lceil n\varepsilon_n \rceil$ of the previous samples by the same number of samples from F_{1, \mathbf{P}_t} where \mathbf{P}_t is generated according to the M3 method in which the top probability is forced to be $1 - \Delta_n$.
3. Repeat Steps 1 and 2 over $N = 10^3$ times and make histograms of the simulated HC_n^+ or HC_n^* .

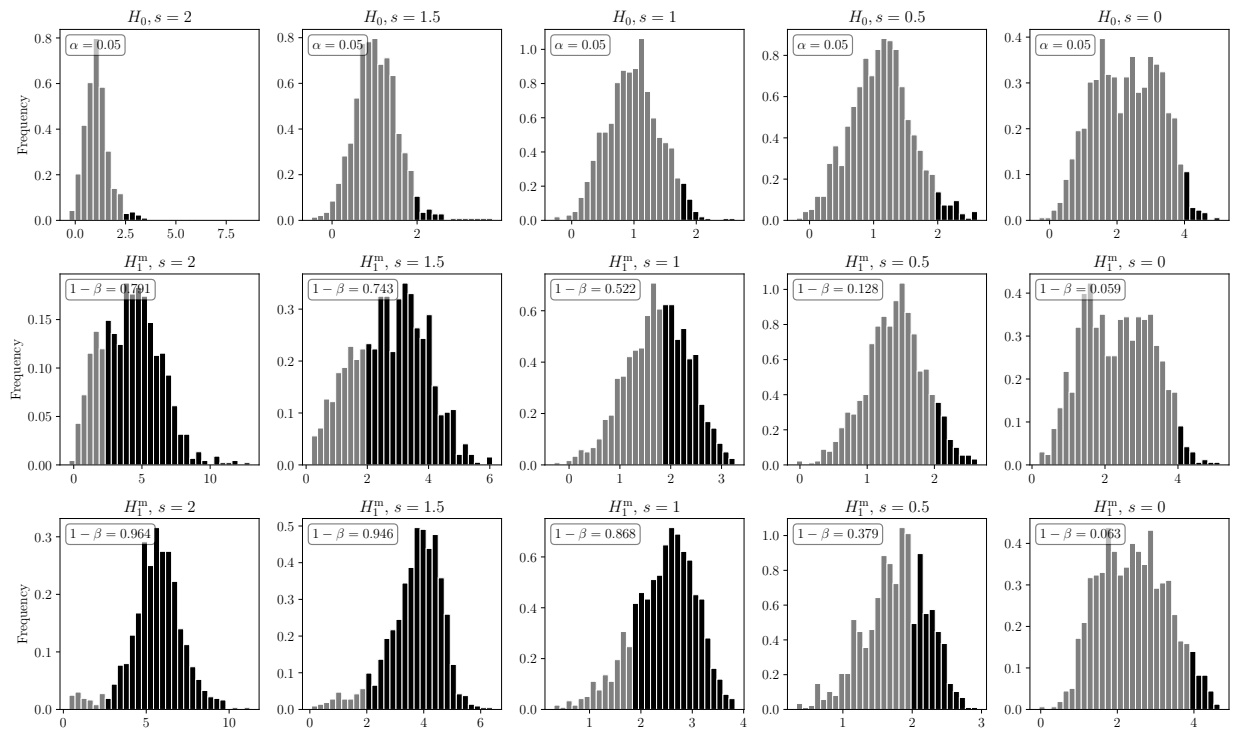


Figure 16: Density histograms and powers of $\log(nS_n^+(s))$ for different values of s with $c_n^+ = 0$ and $(p, q) = (0.2, 0.5)$. The first row presents results under H_0 , while the second and third rows display results under H_1^{mix} , corresponding to the M1 and M2 settings respectively. The dark area indicates the portion of the distribution that rejects H_0 which is the Type I error α under the null hypothesis H_0 and the power $1 - \beta$ under the alternative hypothesis H_1^{mix} .

See Figure 17 for the distribution of HC_n^+ (top) and HC_n^* (bottom) under interesting (p, q) pairs. Let's first focus on the top row. Under H_0 , the distribution of HC_n^+ values is primarily concentrated around 2. As suggested by Cai et al. [10], we pick the $(1 - \alpha)$ -quantile of the empirical distribution of HC_n^+ as the critical value, which is usually much more accurate than $\sqrt{(2 + \delta) \log \log n}$. This rejection region is marked in black in Figure 17, which corresponds to a Type I error rate of α under H_0 and a power of $1 - \beta$ under H_1^{mix} . Recall that our experiment setup confirms that $P_{t, \max} = 1 - \Delta_n$ for all $t \in [n]$. Under H_1^{mix} with $(p, q) = (0.5, 0.5)$, the distribution nudges slightly right, with a power of $1 - \beta = 0.087$. This slight shift aligns with Theorem 4.2, where the statistical indistinguishability of H_1^{mix} from H_0 results in a similar distribution of HC_n^+ if $q + 2p > 1$. Conversely, if $q + 2p < 1$, the distributions of HC_n^+ under H_1^{mix} and H_0 diverge. As a result, under H_1^{mix} with $(p, q) = (0.2, 0.5)$, HC_n^+ centers around 8 instead and achieves a higher power of $1 - \beta = 0.965$.

The bottom row of Figure 17 shows that HC_n^* tends to exhibit significantly large values particularly when $2p + q < 1$. This extreme value could potentially lead to the outlier issue. To illustrate, under H_0 , the largest value observed for HC_n^+ typically hovers around 4, whereas for HC_n^* , it can exceed 15. This observation aligns with the theoretical analysis in Section 3 [19] that shows HC_n^* has "heavy tails" under H_0 . This heavy-tail issue is more severe under H_1^{mix} : the largest value of HC_n^* could exceed 180, while the counterpart of HC_n^+ is merely around 18. This disparity raises a concern:

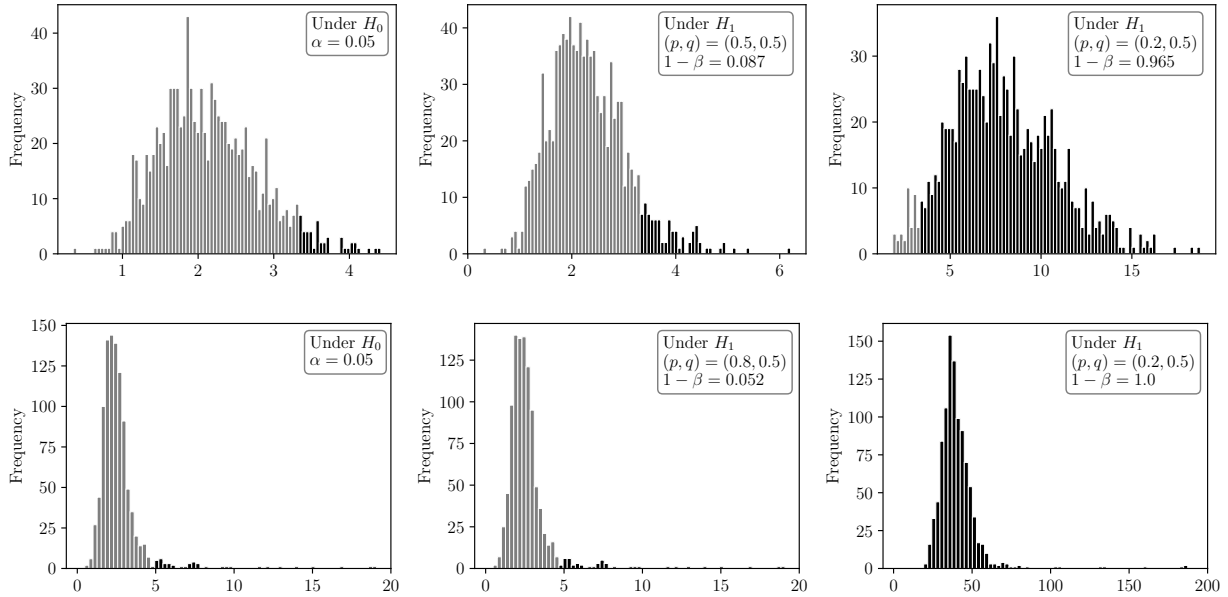


Figure 17: Frequency histograms for HC_n^+ with $c_n^+ = \frac{1}{n}$ (top) and HC_n^* (bottom). The dark area indicates the portion of the distribution that rejects H_0 which is the Type I error α under the null hypothesis H_0 and the power $1 - \beta$ under the alternative hypothesis H_1^{mix} .

it becomes challenging to determine whether a large value of HC_n^* is attributable to its tendency towards extreme values (due to the heavy-tail issue), or a strong indication of embedded watermarks. HC_n^+ is proposed to mitigate this issue and exhibits less heavy-tailed performance.

B.3 Detection Boundaries for HC

Generally, the decision boundary for HC methods should align with that of $nS_n^+(2)$ due to the relation in (11). For completeness, we will include numerical illustrations for HC methods after presenting the corresponding results for $nS_n^+(s)$ in the main text.

We aim to verify the correctness of Theorem A.1. This theory implies that HC_n^+ is of $O_{\mathbb{P}}(\sqrt{\log \log n})$ under H_0 and is of $\Omega_{\mathbb{P}}(n^{\frac{1}{2}-p-\frac{q}{2}})$ under H_1^{mix} . Hence, detectability requires increasingly large samples as one approaches the detection boundary $q + 2p = 1$. We investigate the detection boundary by checking the smallest sum of Type I and Type II errors in the following. Following the approach in [10], we tune the parameter δ as the optimal value in the set $\{0, 0.2, 0.4, \dots, 3.8, 4\}$ that results in the smallest sum of Type I and Type II errors. We use the same setup introduced in Section 5.1 where the vocabulary size is $|\text{Voc}| = 10^3$ and each NTP distribution \mathbf{P}_t is \mathbf{Q}_{Δ_n} which is a uniform distribution, after ensuring that the highest probability is $1 - \Delta_n$. Again, we replace pseudorandomness with true randomness for illustration purposes.

The results are displayed in Figure 18. All observations noted in Figure 8 remain applicable here as well. These results not only substantiate the accuracy of our theory but also provide empirical evidence supporting the claim: HC_n^+ has the same asymptotic behavior as HC_n^* , making them an identical detection boundary. As discussed in Remark A.2, Theorem A.1 remains true even if we replace HC_n^+ with HC_n^* .

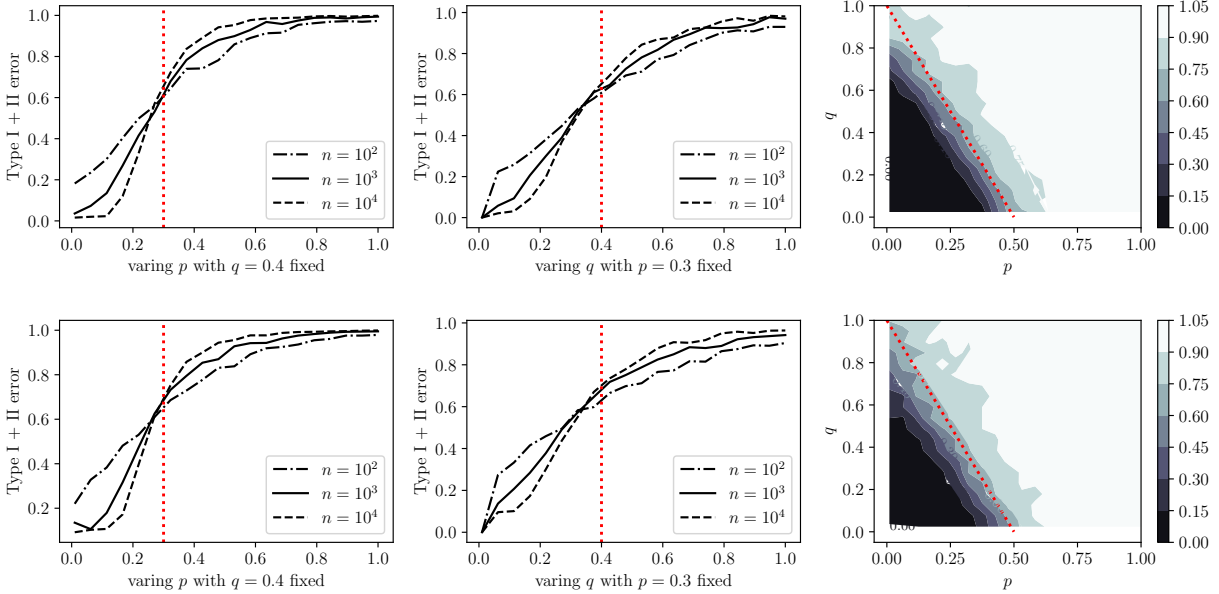


Figure 18: The smallest sum of Type I and Type II errors of HC_n^+ with $c_n^+ = \frac{1}{n}$ (top) and HC_n^* (bottom). The red dotted line indicates the theoretical boundary. Each point is obtained by averaging $N = 10^3$ independent experiments.

C Details of Language Model Experiments

C.1 Details of Experiment Setup

We employ a context window of size $m = 5$, allowing the randomness variable $\zeta_t = \mathcal{A}(s_{(t-m):(t-1)}, \text{Key})$ to depend on the previous m tokens. We utilize the hash function \mathcal{A} , as used in [83], for generating this randomness. We set different values of c_n^+ for the Tr-GoF test in different experiments. For the experiments in Section 6.2, we use $c_n^+ = \frac{1}{n}$. The specific values of c_n^+ for other experiments will be provided in the following implementation details. In all experiments, we apply a watermark to a token only if the current text window is unique within the generation history, aiming to prevent repetitive generation [33, 76, 16]. When no watermark is applied, we use multinomial sampling from the NTP distribution with the temperature set to 0.7.

How to generate prompts. The experimental setup we employed is largely based on the methodology described in Appendix D.1 of [46]. In our approach, each generation is conditioned on a prompt which is obtained by sampling documents from the news-oriented segment of the C4 dataset [65]. We enforce a minimum prompt size of 50 tokens in all experiments and skip over any document that is not long enough. Note that retokenization may not precisely match the original tokens. Therefore, to guarantee that the verifier consistently receives at least n tokens, we augment its input with special padding tokens, which vary according to the tokenizer of each model. Additionally, to mitigate the need for padding, we initially generate many buffer tokens beyond n . We set the number of buffer tokens to be 20 in every experiment. This additional buffer typically makes padding unnecessary.

Computation of critical values. Critical values are used to control the Type I error. For sum-based detection rules, we estimate the critical value by

$$\hat{\gamma}_{n,\alpha} = n \cdot \mathbb{E}_0 h(Y) + \Phi^{-1}(1 - \alpha) \cdot \sqrt{n \cdot \text{Var}_0(h(Y))}.$$

It is easy to see that $\mathbb{P}_0(\sum_{t=1}^n h(Y_t) \geq \hat{\gamma}_{n,\alpha}) \rightarrow \alpha$ due to the central limit theorem. To determine the critical value for HC and Tr-GoF, we resort to simulation. For a given text length n and $s \in [-1, 2]$, we generate n i.i.d. copies of Y_t from $U(0, 1)$ and calculate the corresponding statistic $\log(nS_n^+(s))$. This procedure is replicated 10^4 times, using the empirical $1 - \alpha$ quantile of these 10^4 samples as an initial estimate. To enhance the precision of this estimate, we repeat the process 10 times and average these 10 initial estimates to establish the final critical value.

Details of the random edits. In general, we set the text length to $n = 400$ to fully utilize the observed data. However, when the detection problem becomes easier, $n = 400$ may be excessive, leading to near-zero Type II errors for most detection methods. In such cases, we reduce the length for better visualization. In the substitution and insertion experiments, n is set to 400 for temperatures of 0.1 and 0.3, and reduced to 200 for temperatures of 0.7 and 1. For the deletion experiment, we initially generate more than n watermarked tokens to ensure that, even after deleting a fraction, at least n tokens remain. In this case, n is set to 200. For the Tr-GoF test, we select the best stability parameter c_n^+ from the set $\{0, 10^{-3}, \frac{1}{n}\}$ (with n varying accordingly).

Details of Figures 2 and 3 In Figures 2 and 3, for the paraphrase edit, we use random synonym substitution to edit watermarked texts and evaluate Type II error as a function of text length, with a temperature parameter of 0.3. We select 1000 prompts from the C4 news-like dataset as before and randomly replace 5% of words. For each selected word, synonyms with multiple alternatives are retrieved from WordNet [54] to ensure meaningful substitutions. The modified text is then reconstructed with each target word replaced by a randomly chosen synonym.

In the adversarial edit, we first compute the pivotal statistics for all tokens, then identify the top 5% with the largest values, replacing these tokens with uniformly selected alternatives. This type of edit assumes that the human editor has knowledge of the hash function \mathcal{A} and the secret key Key , which generally results in the removal of more watermark signals.

For the Tr-GoF test, we set $s = 1.5$ and $c_n^+ = \frac{1}{n}$. For h_{opt,Δ_0} , we set $\Delta_0 = 0.1$.

Details of the edit tolerance limit. We prompt ChatGPT-4o to generate 100 popular poems along with their authors and ask the target model (either OPT-1.3B or Sheared-LLaMA-2.7B) to perform either the poem recitation or poem generation task. Taking the poem Adonais by Percy Bysshe Shelley as an example, the prompt for poem recitation is: Please recite the poem: Adonais by Percy Bysshe Shelley. For poem generation, the prompt is: Please write a new poem in the style of this one: Adonais by Percy Bysshe Shelley. The temperature is set to 1 for both the poem recitation and generation tasks.

We use binary search (Algorithm 1) to determine the edit tolerance limit. We set the initial length to $n_0 = 400$. We pass only the first n tokens in the edited text to our verifier. For random substitution and insertion, the test length is $n = 200$, while for random deletion, $n = 100$. All critical values are computed with a Type I error rate of $\alpha = 0.01$. For simplicity, the stability parameter c_n^+ in the Tr-GoF test is set to 10^{-3} .

Algorithm 1 Binary search to compute the edit tolerance limit

1: **Input:** A watermarked sentence $\tilde{w}_{1:n_0}$ and a specified edit.
2: **Initial:** Set $l = 1$, $u = n_0$, and generate a random permutation π_0 over the vocabulary Voc.
3: **while** $u - l \geq 2$ **do**
4: Compute the middle point $m = \lfloor \frac{u+l}{2} \rfloor$.
5: Apply the considered edit type to corrupt the watermarked tokens $\tilde{w}_{\pi(1)}, \dots, \tilde{w}_{\pi(m)}$.
6: Denote the resulting edited text by $w_{1:n_1}^{(m)}$.
7: Pass the first n tokens of $w_{1:n_1}^{(m)}$ to the detection method.
8: **if** the detection method rejects the null hypothesis H_0 **then**
9: Set $l \leftarrow m$
10: **else**
11: Set $u \leftarrow m$
12: **end if**
13: **end while**
14: **Output:** The edit tolerance limit is $\frac{m}{n_0} \times 100\%$.

Details of the roundtrip translation. The roundtrip translation, as described in Appendix D.2 of [46], involves translating text from English to French and back to English using the OPUS-MT series of translation models. These models are available on Huggingface Hub.⁹ The specific models used for this attack are:

- Helsinki-NLP/opus-mt-tc-big-en-fr for English to French translation,
- Helsinki-NLP/opus-mt-tc-big-fr-en for French to English translation.

This method leverages the subtle nuances of translation to detect inconsistencies or vulnerabilities in language models. Since the text length may change after roundtrip translation, we use the last 200 tokens from each (edited) sentence as the input to our verifier. If a sentence is shorter than 200 tokens, we pad it with zeros at the beginning to ensure a consistent length of 200. We set $c_n^+ = \frac{1}{n}$ for the Tr-GoF test.

⁹<https://huggingface.co/>.

C.2 Additional Results on Statistical Power

Figure 19 presents results analogous to those shown in Figure 11, but with the use of a larger model, Sheared-LLaMA-2.7B [77]. All observations noted in Section 6.2 remain valid: Tr-GoF performs exceptionally well at low temperatures and achieve performance comparable to the practical h_{ars} at high temperatures.

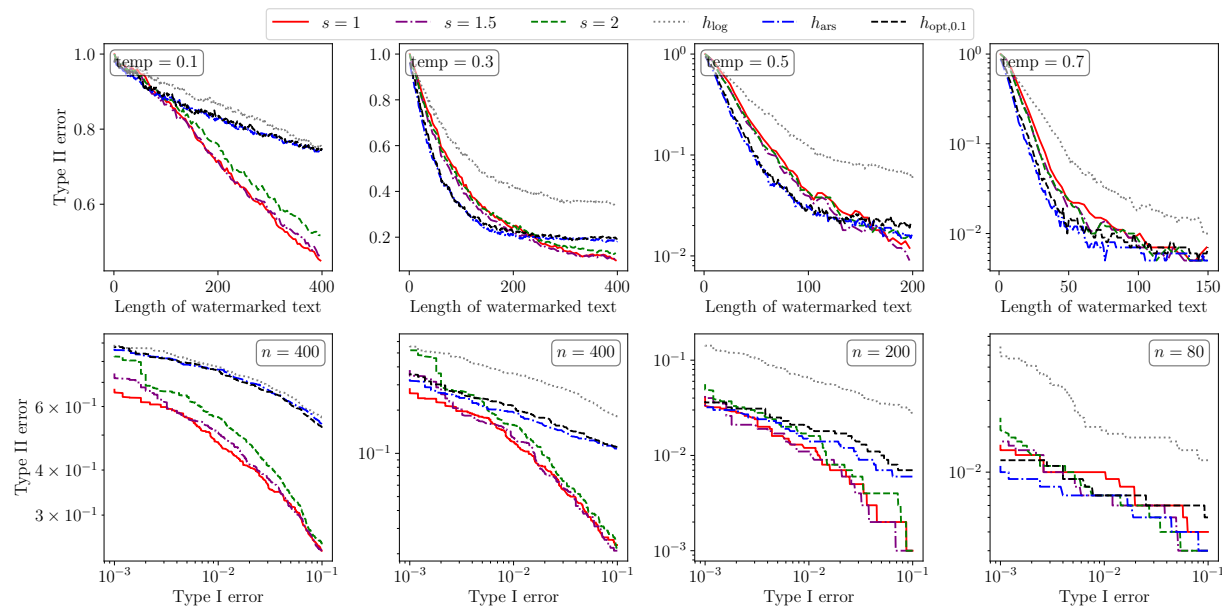


Figure 19: Empirical Type II errors (top row) on the C4 dataset across different detection rules applied to the Gumbel-max watermark. Here we use Sheared-LLaMA-2.7B [77]. The bottom row illustrates the trade-off function for a specific text length n . The temperatures used, from left to right columns, are 0.1, 0.3, 0.5, and 0.7, respectively.

C.3 Additional Results on Robustness

Figure 20 presents results analogous to those shown in Figure 12, but with the use of a larger model, Sheared-LLaMA-2.7B [77]. Similarly, Figure 21 presents results analogous to those shown in Figure 14, and Table 2 presents results analogous to those shown in Table 1 with this larger model. Figure 22 provides the complete results of adversarial edits on OPT-1.3B, expanding on Figure 13. Corresponding results for the Sheared-LLaMA-2.7B model are shown in Figure 23.

All observations from Section 6.3 remain consistent: (i) Tr-GoF performs exceptionally well at low temperatures and shows comparable performance to the practical h_{ars} at higher temperatures, and (ii) they exhibit the largest edit tolerance limit in most cases among all the detection methods considered.

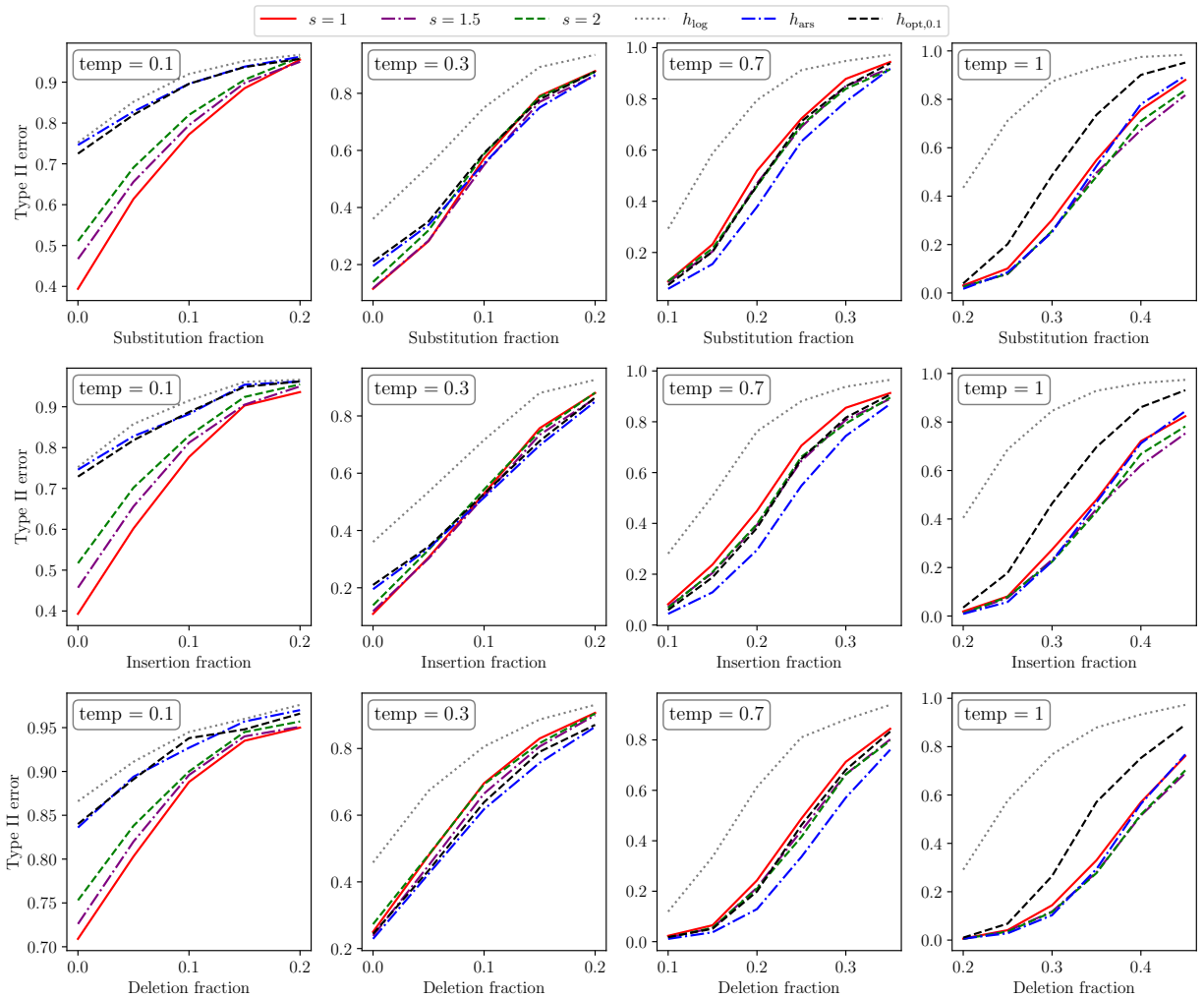


Figure 20: Effect of three random edits on Type II error across different temperatures at $\alpha = 0.01$ on the Sheared-LLaMA-2.7B model. The top, middle, and bottom plots correspond to random substitution, insertion, and deletion, respectively.

Task	Edit types	$s = 1$	$s = 1.5$	$s = 2$	h_{\log}	h_{ars}	$h_{\text{opt},0.3}$	$h_{\text{opt},0.2}$	$h_{\text{opt},0.1}$
Poem Recitation	Substitution	36.22	38.49	38.76	22.39	37.08	26.1	28.43	32.03
	Insertion	38.49	40.77	40.83	24.93	40.45	28.92	31.79	36.01
	Deletion	35.85	38.66	39.43	22.66	37.73	25.2	28.38	32.34
Poem Generation	Substitution	36.06	38.15	38.81	22.0	36.88	26.07	28.85	31.94
	Insertion	38.7	40.86	41.75	24.94	40.22	28.35	31.47	35.03
	Deletion	39.7	42.12	41.83	21.93	41.08	26.6	30.8	35.23

Table 2: The edit tolerance limits (%) on the Sheared-LLaMA-2.7B model.

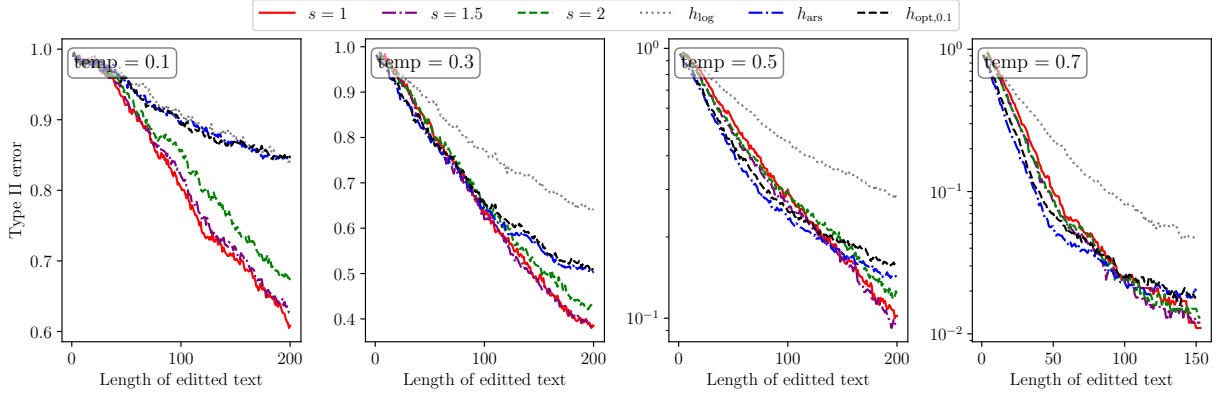


Figure 21: Empirical Type II errors on Sheared-LLaMA-2.7B across different lengths of edited texts at different temperature parameters with a fixed Type I error of $\alpha = 0.01$.

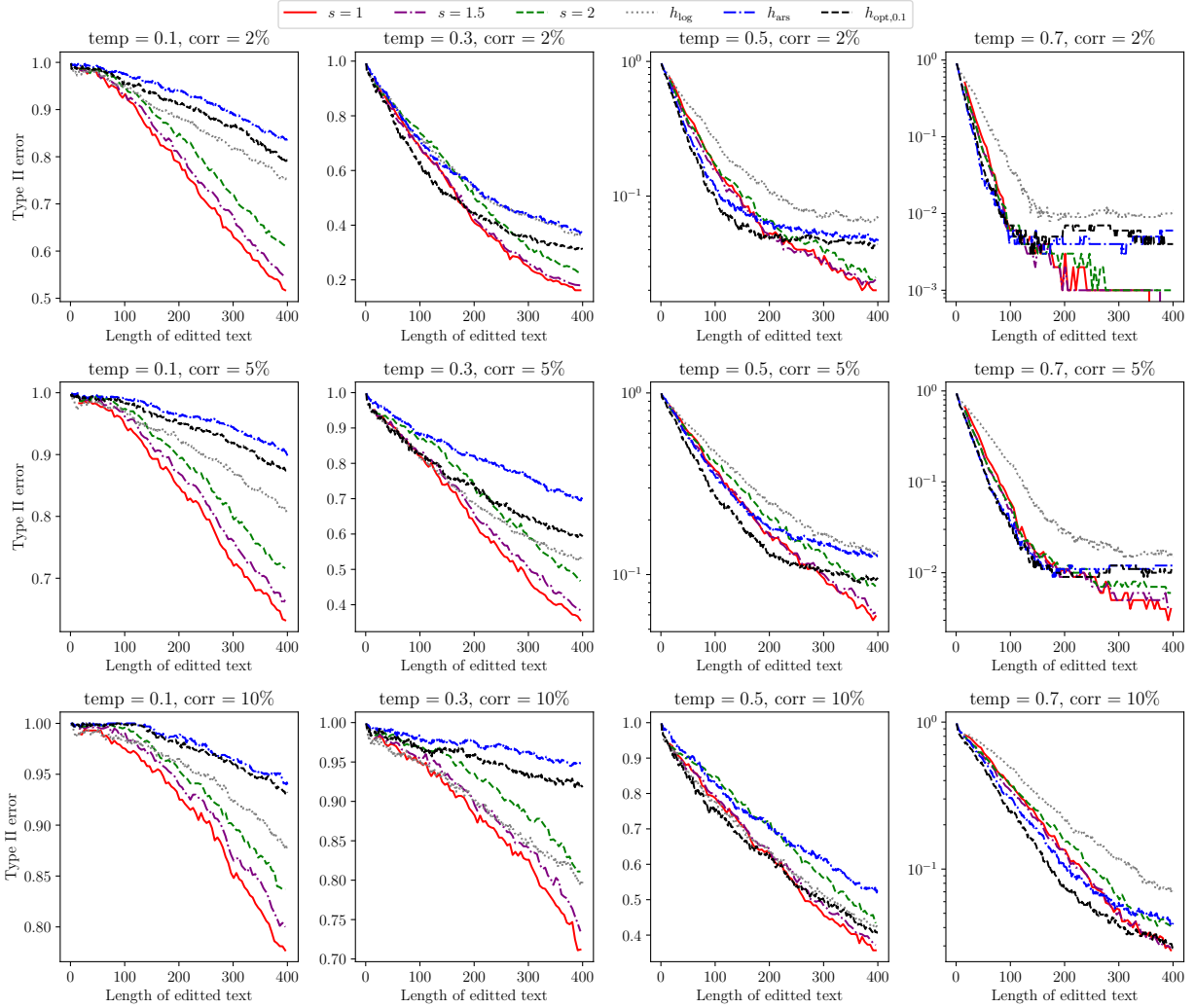


Figure 22: Complete results of Type II error under adversarial edits across various temperatures and edit fractions at $\alpha = 0.01$ on the OPT-1.3B model. Columns represent four temperatures: $\{0.1, 0.3, 0.5, 0.7\}$, and rows correspond to four edit fractions: $\{2\%, 5\%, 10\%, 20\%\}$.

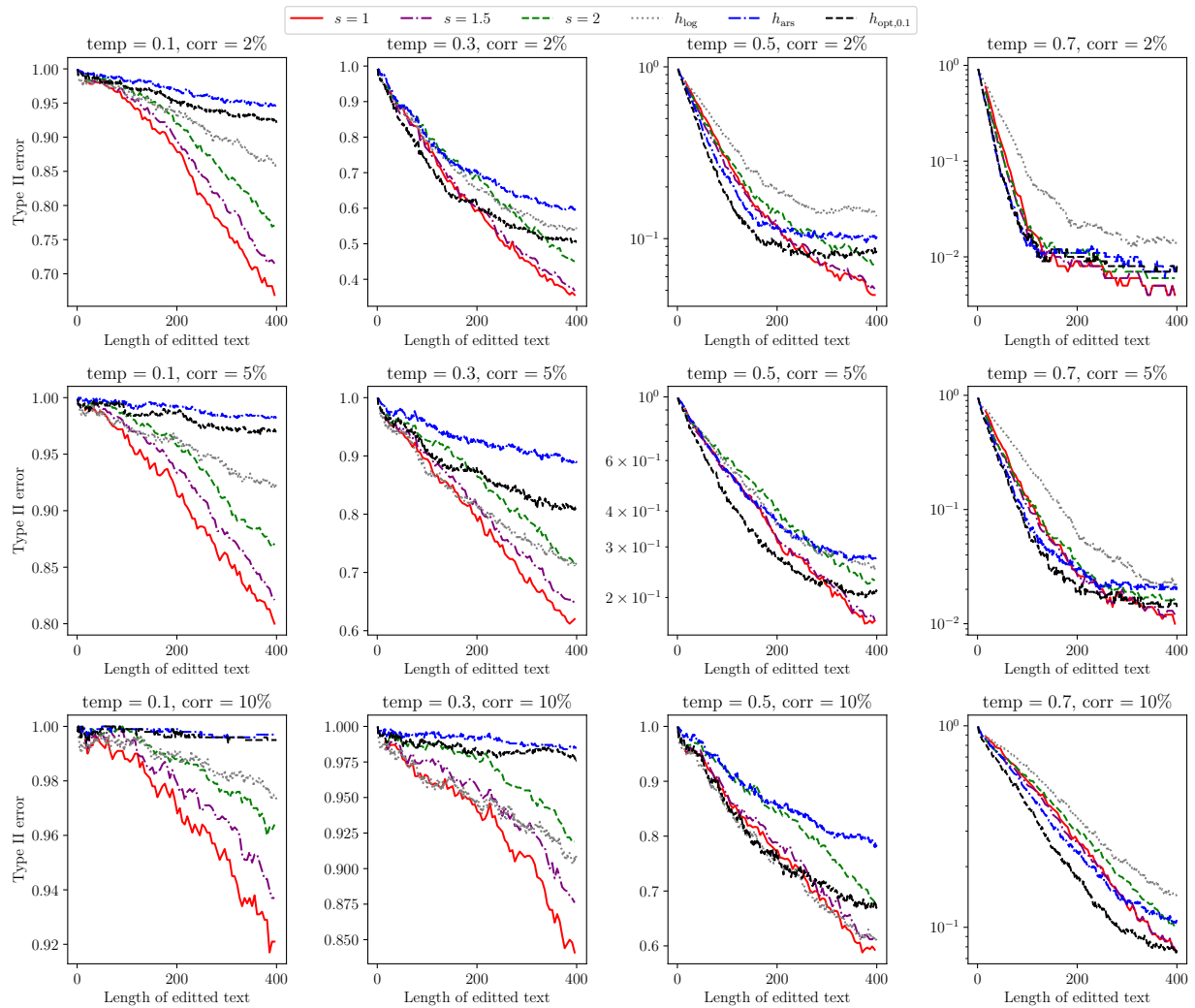


Figure 23: Complete results of Type II error under adversarial edits across various temperatures and edit fractions at $\alpha = 0.01$ on the Sheared-LLaMA-2.7B model. Columns represent four temperatures: $\{0.1, 0.3, 0.5, 0.7\}$, and rows correspond to four edit fractions: $\{2\%, 5\%, 10\%, 20\%\}$.